



LIBRARY Michigan State University

This is to certify that the

thesis entitled

Non-linear Time - Dependent Loss Analysi's of Transformers presented by

Tufan Batan

has been accepted towards fulfillment of the requirements for +4c

Masters degree in Electrical Engineering

Elis 65tra-gy

Date 25Jan 1990

PLACE IN RETURN BOX to remove this checkout from your record. TO AVOID FINES return on or before date due.

DATE DUE	DATE DUE	DATE DUE

MSU is An Affirmative Action/Equal Opportunity Institution chaintedus.pm3-p.1

# Non-Linear Time-Dependent Loss Analysis of Transformers

Ву

Tufan Batan

### A THESIS

Submitted to
Michigan State University
in partial fulfillment of the requirements
for the degree of

MASTER OF SCIENCE

Department of Electrical Engineering Michigan State University East Lansing, MI 48824

#### **ABSTRACT**

# Non-linear Time-Dependent Loss-Analysis of Transformers

By

### Tufan Batan

In this thesis the copper and the iron losses in a single-phase small-size transformer are analyzed taking all the harmonics of the current in the windings and the magnetizing flux in the iron core into consideration. The analysis is started by separating the iron losses into hysteresis and eddy-current losses because of the fact that the hysteresis loss is only a function of maximum flux density. In the analysis of the current and the flux density, which are the variables needed to calculate the copper and iron losses, two different method are used. The first is to combine the two-dimensional non-linear time-dependent field equation, describing the magnetic vector potential in everywhere in the transformer, with the circuit equations, including the external loads and sources, and solve them by the finite element method. The second method is to solve a set of non-linear first-order differential equations derived from lumped-parameter model and describing the transformer. The results of the current and flux analysis of two methods are presented and compared. The copper losses is calculated by the joule loss formula considering all current harmonics and the changes in the winding resistances for higher harmonics due to skin effect. Finally, the eddy current losses are calculated by analyzing of the flux density in harmonics in iron core, whereas the calculation of the hysteresis losses is performed using a non-recursive formula.

## **ACKNOWLEDGEMENT**

I wish to express my sincere appreciation to my major advisor, Dr. Elias G. Strangas, for his guidance and encourgement in the course of this research.

Also, I would like to thank my committee members Dr. Timothy Grothjohn and Dr. R.A. Schlueter for their suggestions.

Finally, I owe a special thanks to my parents for their encourgement and support.

# TABLE OF CONTENTS

CHAPTER			PAGE
I.	INTR	ODUCTION	1
	1.1	Iron Losses in Magnetic Cores	1
	1.2	Copper Losses	2
II.		LOSSES AND DERIVATION OF ITS RELATED METERS	5
	2.1	Introduction	5
	2.2	Hysteresis Loss and its Parameters	5
	2.3	The Eddy-Current Losses and Its Parameters	12
	2.4	Total Core Loss	21
	2.5	Separation of the Hysteresis and Eddy Current Losses	26
III.		YTICAL CALCULATION OF THE (ADDITIONAL) SFORMER LOSSES DUE TO HARMONICS	28
	3.1	Introduction	28
	3.2	Equivalent Circuit	29
	3.3	Calculation of the Ohmic Losses Due to Harmonics	31
	3.4	Calculation of the Iron Losses Due to Harmonics	31
	3.5	Sample Calculation	33
VI.		LINEAR TIME DEPENDENT FINITE ELEMENT OD ANALYSIS OF TRANSFORMERS	37
	4.1	Introduction	37
	4.2	Analysis	38

	4.3	Time Dependence and Solution Method	. 44
	4.4	Calculation of Iron Losses	.44
	4.4.1	Calculation of Eddy-Current Losses	.44
	4.4.2	Calculation of Hysteresis Losses	.45
v.	APPLIC	ATIONS	.46
	5.1 I	ntroduction	.46
	5.2 T	he Model	.47
	5.3 T	ransient Field Analysis	.49
		he Results of Non-Linear Time-Dependent urrent, Flux Density and Voltage Analysis	.52
	5.4.1	Case 1: Sinusoidal Input and Resistive Load	.53
	5.4.1.	1 The Results of FEM for Case 1	.53
	5.4.1.	2 The Results of ACSL for Case 1	.61
	5.4.2	Case 2: Sinusoidal Input and Inductive Load	.65
	5.4.2.	1 The Results of FEM for Case 2	.65
	5.4.2.	2 The Results of ACSL for Case 2	.73
	5.4.3	Case 3: Sinusoidal Input and Resistive Load with a one-way rectifier circuit	.77
	5.4.3.	1 The Results of FEM for Case 3	.77
	5.4.3.	2 The Results of ACSL for Case 3	.85
		Case 4: Sinusoidal Input and Inductive Load with a one-way rectifier circuit	.89
	5.4.4.	1 The Results of FEM for Case 4	.89
	5.4.4	2 The Results of ACSI for Case 4	97

	5.4.5 Case 5: Six-step Voltage Input (Inverter) and Inductive Load	101
	5.4.5.1 The Results of FEM for Case 5	101
VI.	CONCLUSIONS	109
	TICT OF DEFEDENCES	111

## LIST OF FIGURES

F:	IGURE		PAGE
	1	Hysteresis loop	.7
	2	Cross-section of lamination showing a current path	.13
	3	Unit element of lamination for calculation of eddy current loss	.15
	4	Equivalent circuit of a transformer for the harmonics	.29
	5	Approximate equivalent circuit of a transformer	.30
	6	Six-step applied voltage	.36
	7	Reference directions and the circuit for a coil	.41
	8	Cross-section of the transformer model	.47
	9	A simple grid of the model for the FEM	.48
	10	Equipotential lines of the model at 1 msec to sinusoidal input	.50
	11	Equipotential lines of the model at 50 msec to sinusoidal input	.51
	12	Equivalent circuit of the model	.52
	13	Applied voltage for the first case	.54
	14	Primary current of the model connected to resistive load	.55
	15	Secondary current of the model connected to resistive load	.56
	16	Flux density of the 166th element for case 1	.57
	17	Induced voltage in the primary windings for case 1	5.8

18	Induced voltage in the secondary windings for case 1
19	The reluctivity of the 166th element for case 160
20	Applied voltage61
21	Primary current of the model connected to resistive load
22	Secondary current of the model connected to resistive load
23	Flux density of the model for case 164
24	Applied voltage for the second case66
25	Primary current of the model connected to inductive load
26	Secondary current of the model connected to inductive load
27	Flux density of the 166th element for case 269
28	Induced voltage in the primary windings for case 2
29	Induced voltage in the secondary windings for case 271
30	The reluctivity of the 166th element for case 272
31	Applied voltage for case 273
32	Primary current of the model connected to inductive load
33	Secondary current of the model connected to inductive load
34	Flux density of the model for case 276
35	Applied voltage for the third case

36	Primary current of the model connected to a one-way rectifier circuit together with resistive load
37	Secondary current of the model connected to a one-way rectifier circuit together with resistive load80
38	Flux density of the 166th element for case 381
39	Induced voltage in the primary windings for case 382
40	Induced voltage in the secondary windings for case 383
41	The reluctivity of the 166th element for case 384
42.	Applied voltage for case 385
43	Primary current of the model connected to a one-way rectifier circuit together with resistive load86
44	Secondary current of the model connected to a one-way rectifier circuit together with resistive load
45	Flux density of the model for case 388
46	Applied voltage for the fouth case90
47	Primary current of the model connected to a one-way rectifier circuit together with inductive load91
48	Secondary current of the model connected to a one-way rectifier circuit together with inductive load92
49	Flux density of the 166th element for case 493
50	Induced voltage in the primary windings for case 494

51	Induced voltage in the secondary windings for case 495
53	Applied voltage for case 497
54	Primary current of the model connected to a one-way rectifier circuit together with inductive load98
55	Secondary current of the model connected to a one-way rectifier circuit together with inductive load99
56	Flux density of the model for case 4100
57	Applied voltage for case 5102
58	Primary current of the model connected to inductive load and fed by six-step voltage
59	Secondary current of the model connected to inductive load and fed by six-step voltage
60	Flux density of the model for case 5105
61	Induced voltage in the primary windings for case 5
62	Induced voltage in the secondary windings for case 5
63	The reluctivity of the 166th element for case 5108

## CHAPTER I

#### INTRODUCTION

The advantages of the electronic-power-switching circuits lead to a rapid increase of the use of electrical drives such as inverters equipped with such circuits. Because of the non-linear characteristics of these devices, harmonics are introduced to the power systems. The effects of these harmonics on the transformers connected to such power systems cause an increase both in the copper losses, due to the current harmonics in the windings, and in the iron losses, due to the harmonics in the magnetizing flux.

In this thesis, the copper and the iron losses analysis is presented for a single phase small size transformer connected to a power system which has current and voltage harmonics.

Losses in transformers may originate in the windings, in the magnetic core or in the dielectric. For practical purposes at power frequencies the dielectric losses are small and usually included in the iron-losses. For convenience in calculations and testing, it is common to divide losses into core losses, which are independent of the load, and into copper losses, which increase with the load. It is, at the same time, common to study of two groups loosely as iron and copper losses.

## 1.1 IRON LOSSES IN MAGNETIC CORES

In magnetic devices operating with constant flux, no heating occurs in the core materials. A direct-current lifting magnet or a direct current relay, for example, has almost no energy loss in its magnetic circuit unless it is energized and

de-energized very frequently. But power and audio frequency transformers and devices actuated by alternating currents have alternating fluxes in their magnetic circuits, and these fluxes give rise to currents which produce heat in the iron core.

The losses that occur in the material arise from two causes: (a) the tendency of material to retain magnetism or to oppose a change in magnetism, often referred to as magnetic hysteresis; and (b) the  $I^{2}R$  heating which appears in the material as a result of the voltages and consequent circulatory currents induced in it by the time variation of flux. The first of these contributions to the energy dissipation is known as hysteresis loss and the second as eddy-current loss. The hysteresis loss is the result of the tendency for the saturation characteristic (B(H)) of the material to involve a loop when the material is subjected to a cyclic magnetizing force. The distinction between hysteresis and hysteresis loss is important. The phenomenon known as hysteresis is the result of the material's property of retaining magnetism or opposing a change in magnetic state. The hysteresis loss is the energy converted into heat because of the hysteresis phenomenon and, as usually interpreted, is associated only with a cyclic variation of magnetomotive force. This interpretation is the result of the extensive engineering use of the material under cyclic magnetizing forces, and the relatively large importance of loss data representative of this manner of use. The eddy-current loss is produced by the currents in the magnetic material, and these currents are caused by electromotive forces set up by the varying fluxes. The sum of the hysteresis and eddy-current losses is called the total core loss.

## 1.2 COPPER LOSSES

It is evident from well-known principles that the primary copper loss in a given transformer is proportional to the square of the primary current. The secondary current or load current can be referred to the primary, so that the secondary copper loss will also vary with the same way. The effect of the no-load component on the total copper loss is small in transformers of any size, but in small transformers for a few hundred watts or less it may be appreciable. In those cases where account is taken of this loss, it must of course be reckoned as a no-load loss, but to do so complicates the picture because the loss depends upon the power factor of the secondary load. The subject will therefore be dealt with on the assumption that the copper loss increases in proportional to the output current.

Another loss which varies with the load current is that arising from eddycurrents in the conductors due to the fields produced by alternating currents flowing in them. These losses are also proportional to the square of the current and can be conveniently added to those due to the normal copper loss. If this is done, the total copper loss is equivalent to that which would occur if the winding were assumed to have a higher resistance than its true value, and it is very often convenient to regard the effect in this light. From this point of view the winding is said to have a higher resistance to alternating current than to direct current. This effect is known as skin effect and much more pronounced at the higher frequencies. The ratio of a.c. resistance to d.c. resistance is greater for large section conductors than for thin ones and it is also greater in coils than straight conductors; consequently it is appreciable even at power-frequencies in the very large conductors used in the low voltage windings of large transformer. The skin effect can be reduced by using a number of separately insulated small section conductors instead of a solid bar.

•

Although the eddy-current losses in the copper can be grouped with the resistance losses due to an apparent increase in resistance to A.C., it should not be forgotten that they are really distinct. One instance of when this should be borne in mind is in considering the effect of the temperature on the resistance. The true ohmic resistance of copper conductors increase with temperature at the rate of 0.38 per cent per 1 °C. Whereas the eddy current loss decreases at the same rate with rising temperature, because the magnitude of the circulating current is reduced by the higher resistance of the path around which it flows. Therefore the loss, being proportional to the square of the current, decreases more rapidly on this account than it increases on account of high resistance of the path. The ratio of a.c. resistance to d.c. resistance, thus, decreases at higher temperatures because of the lower contribution of eddy current losses to the total copper loss, and apparent temperature coefficient of a.c. resistance is lower than the normal figure. The extent of this reduction is, of course, dependent on the proportion of the eddy-current to the true ohmic loss.

The current harmonics in the primary and secondary windings introduce additional copper losses to the total copper losses as well. These additional losses will be analyzed in chapter III.

 $(\mathbf{r}_{i},$ 

#### CHAPTER II

#### IRON LOSSES AND DERIVATION OF ITS RELATED PARAMETERS

#### 2.1 INTRODUCTION

As earlier mentioned, the iron losses can be divided into two groups which are the hysteresis loss and the eddy-current losses. The focus of this chapter will be on the derivation of some parameters to calculate these losses and the separation of the given iron losses into the hysteresis and the eddy current losses.

#### 2.2 HYSTERISIS LOSS AND ITS PARAMETERS

The occurrence of hysteresis loss is a matter intimately associated with the phenomenon whereby energy is absorbed by a region which is permeated by a magnetic field. If the region is other than vacuum, only a portion of the energy taken from the electric circuit is stored and wholly recoverable from the region when magnetizing force is removed. The rest of the energy is converted into heat as a result of work done on the material in the medium when it responds to the magnetization. When the flux density in a region is increased from a value  $B_1$  to a value  $B_2$ , energy is absorbed by the region. The magnitude of the energy absorbed by per unit volume can be given by:

$$w = \int_{B_1}^{B_2} H dB \tag{1}$$

The integral of Eq. 1 is proportional to the area bounded by the B(H) curve for the region, the B axis, and the lines parallel to the H axis representing constant  $B_1$  and  $B_2$  respectively. Hence, its magnitude depends on the values  $B_1$  and  $B_2$ 

and the shape of the curve between  $B_1$  and  $B_2$ . If the flux density is decreased from any specified value to a smaller value, the algebraic sign of w is negative and energy is given up by the material.

When the region considered consists of ferromagnetic material, the magnetization curve between any two values  $B_1$  and  $B_2$ , corresponding to a decreasing value of H, is different from the curve corresponding to an increasing value of H. The values of flux density in a ferromagnetic material are larger for a given magnetizing force H when H is decreasing than when H is increasing, even though, for a cyclic variation in H, the extreme values of B are the same for each cycle when the material reaches its steady-state condition. On account of the difference in two curves, which for cyclic condition actually form the two sides of a closed loop, the energy absorbed by the material when the flux density is increased from  $B_1$  to  $B_2$  is larger than the energy returned when the flux density is decreased from  $B_2$  to  $B_1$ . The difference in these energies is the magnitude of the hysteresis loss. By the evaluation of the integral Eq. 1 over a complete cycle of magnetization, the energy loss per cycle caused by magnetic hysteresis can be determined.

As an illustration of the integration process, the energy stored per cycle, a magnetic core having an exciting coil carrying an alternating current is to be considered. In this case, the magnetizing force is reversing cyclically between the limits  $+H_1$  and  $-H_1$ . The relation between B and H is as shown Fig 1. During the part of the cycle ab, the magnetic energy absorbed by the core per unit volume is

$$w_1 = \int_{-B_-}^{B_{\text{max}}} H \ dB = (area \ abea \ shaded \ in \ Fig. \ 1a)$$
 (2)

the second

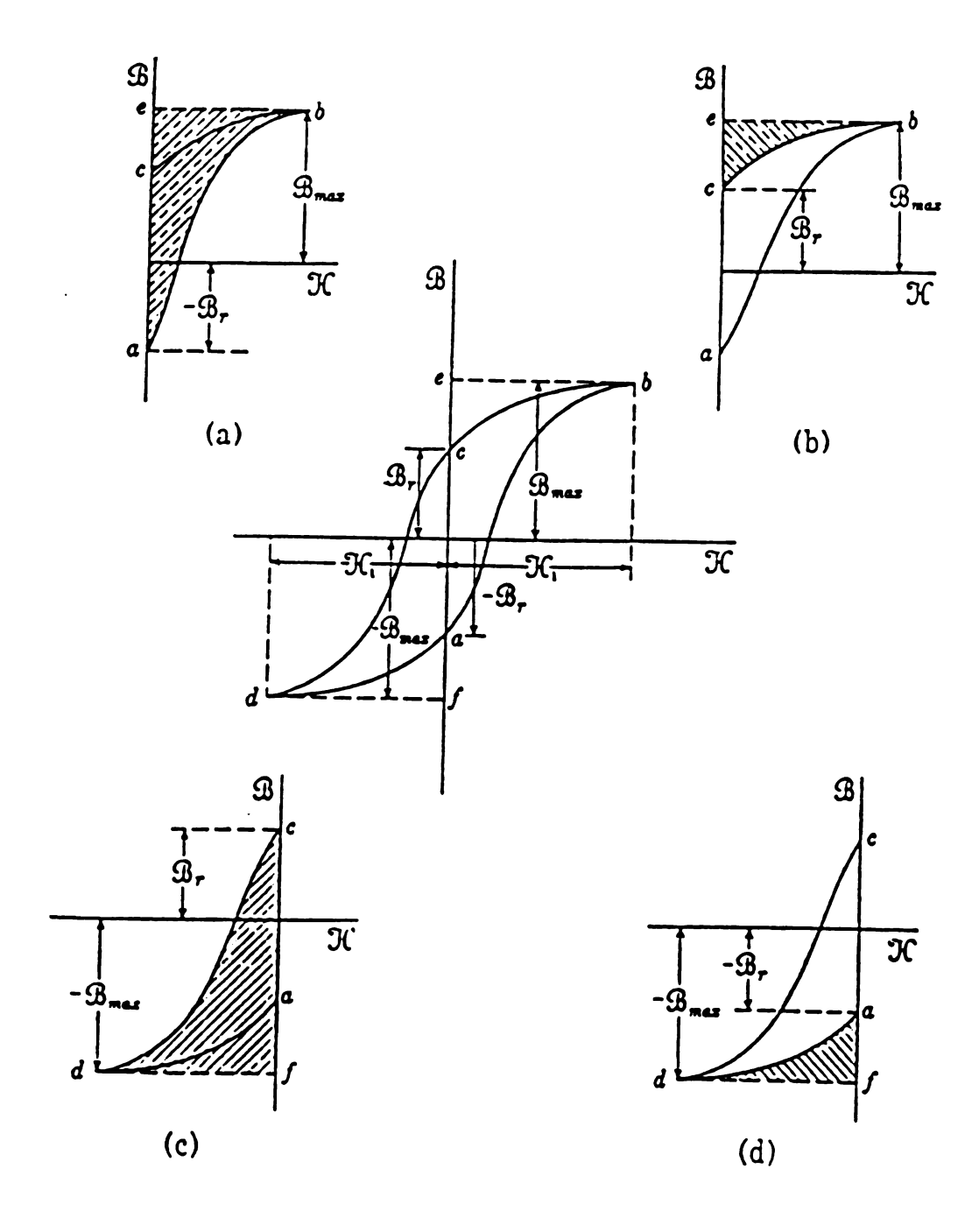


Figure 1. Hysteresis loop. Shaded areas in (a) and (c) show energy absorbed; in (b) and (d) energy returned by steel. [2]

The area would be determined either by numerical integration or through counting squares by the use of a planimeter.

During the part of the cycle bc the energy absorbed magnetically per unit of volume is, by Eq. 1,

$$w_2 = \int_{B_{\text{max}}}^{B_r} H \ dB = -(\text{area bceb shaded in Fig. 1.b}). \tag{3}$$

Since  $B_r < B_{\text{max}}$  and H is positive, this integral is negative; that is, energy is being given up by the magnetic field and returned to the exciting circuit.

Similarly, during the part of the cycle cd, the energy absorbed magnetically is equal to

$$w_3 = \int_{B_c}^{-B_{\text{max}}} H \ dB = (area \ cdfc \ shaded \ in \ Fig. \ 1c). \tag{4}$$

During the part of the cycle da energy is given up by magnetic field and returned to the electric circuit. The absorbed energy is therefore negative and given by

$$w_4 = \int_{-B_{max}}^{-B_r} H \ dB = -(area \ dafd \ shaded \ in \ Fig. \ 1d). \tag{5}$$

The net energy  $w_h$  absorbed by the magnetic field per unit of volume for one complete cycle is

$$w_h = w_1 + w_2 + w_3 + w_4 . ag{6}$$

...

This energy is dissipated as heat in the material each cycle. The dissipation is called the hysteresis loss. Its occurrence has an important effect in the efficiency, the temperature rise, and hence the rating of electromagnetic devices such as transformers.

Although the area of a closed hysteresis loop indicates how much energy is dissipated in the core per unit volume per unit cycle because of hysteresis, it does not indicate at what part of the cycle the dissipation occurs. For example, during the part of the cycle ab, an amount of energy  $w_1$ , Eq. 2, is absorbed by unit volume of the core. However, this analysis does not indicate how much of this absorbed energy is dissipated as heat later during the part of the cycle bc.

If the volume V of the magnetic material, throughout which the flux distribution is uniform and for which the hysteresis loop is known, is subjected to a cyclic change at a frequency of f cycle per second, the rate at which energy is dissipated because of hysteresis (hysteresis power loss) is

$$P_h = V f w = V f$$
 (area of the loop) (7)

The hysteresis power loss per cycle can be calculated by means of the foregoing relations if the hysteresis loop for given maximum flux density  $B_{\rm max}$  is known, but the manner in which this loss varies as a function of  $B_{\rm max}$  can be determined only through repeating the calculations for the hysteresis loops having various values of  $B_{\rm max}$ . Empirically, Steinmetz[2] found from the results of a large number of measurements that the area of the normal hysteresis loop of specimens of various irons and steels commonly used in the construction of electromagnetic apparatus of his time was approximately proportional to the 1.6th power of the maximum flux density throughout the range of flux densities from about 0.1 to 1.2 T. As a result of research on ferromagnetic materials, numerous magnetic steels

having widely varying properties have been made available since Steinmentz performed his measurements. The exponent 1.6 fails nowadays to give the area of the loops with a sufficient degree of accuracy to be useful. The empirical expression for the energy loss per unit volume per cycle is more properly given as:

$$w_h = \sigma B_{\text{max}}^n$$
,  $(W / kg \ cycle)$  (8)

where n,  $\sigma$  are the constants which depend on the magnetic material. Equation 8 should be used with caution since the value for n, which may vary between 1.5 and 2.5 for present-day materials, may not be constant for a given material. For some material, an expression of the form of Eq.8 is not sufficiently accurate to be generally useful. Hence, these constants should be evaluated for a certain range of  $B_{\text{max}}$  and then subsequently used for values of  $B_{\text{max}}$  only within this range.

If Eq.8 is written in its logarithmic form,

$$\log w_h = n \log B_{\max} + \log \sigma \tag{9}$$

a straight-line relationship between  $logw_h$  and  $logB_{max}$  is indicated. From test data, several values of  $logw_h$  can be plotted as ordinates corresponding to the different values of  $logB_{max}$  as abscissas. These points should lie along a straight line having a slope equal to the exponent n and having an intercept on the vertical axis equal to  $log\sigma$ . Obviously two points would be sufficient to determine the values of n and  $\sigma$ , but, if several points are used, the straightness of the curve joining them indicates how well the resulting Eq.8 fits the data in the range underconsideration. If the points do not lie along a straight line, the constant-exponent type of equation is not appropriate[3].

Any convenient system of units can be used for  $w_h$  and  $B_{max}$  in Eq.8 of the corresponding value if the coefficient  $\sigma$  is used. The total hysteresis loss in a

volume V in which the flux density is everywhere uniform and carrying cyclically at a frequency f second can then be expressed empirically as:

$$P_h = \sigma f B_{\text{max}}^n V \tag{10}$$

The equations given here can only be used for the symmetrical hysteresis loop in which B ranges between equal positive and negative values and in which there are no re-entrant loops.

#### 2.3 THE EDDY-CURRENT LOSS AND ITS PARAMETERS

Whenever the magnetic flux in a medium is changing, an electric field appears within the medium as a result of the time variation of the flux. The line integral of this electric field E taken around any closed path that bounds the flux is given by Faraday induction law as

$$\int_{abcda} \mathbf{E} \ d\mathbf{l} = -\frac{d}{dt} \int \mathbf{B} \mathbf{n} \ ds \tag{11}$$

where abcda is the path bounding the area crossed by the flux  $\Phi$  or  $\int \mathbf{B} \, \mathbf{n} \, ds$ . When the medium is conducting, a current is set up around this path by the induced electromotive force e resulting from the line integral of the electric field. These currents are called *eddy currents*. Their presence results in an energy loss in the material proportional to  $i^2R$ , called *eddy-current loss*, the energy being absorbed from the circuit that sets up the field and being dissipated as heat in the medium.

Since the flux density in ferromagnetic materials is usually relatively large, and since the resistivity of the materials is not extremely large, the induced electromotive forces, the eddy currents and the eddy-current loss may become appreciable if means to minimize them are not taken. This loss is of considerable importance in determining the efficiency, the temperature rise, and the rating, of electromagnetic apparatus in which the flux density varies.

To illustrate the conditions typical of those that occur in an iron core, the thin metal slab shown in Fig. 2 is considered to be permeated by an alternating flux  $\Phi$ . From Eq. 11, the electromotive force e induced around a boundary abcda of the area through which a flux is changing is given by:

$$e = -\frac{d\Phi}{dt}. (12)$$

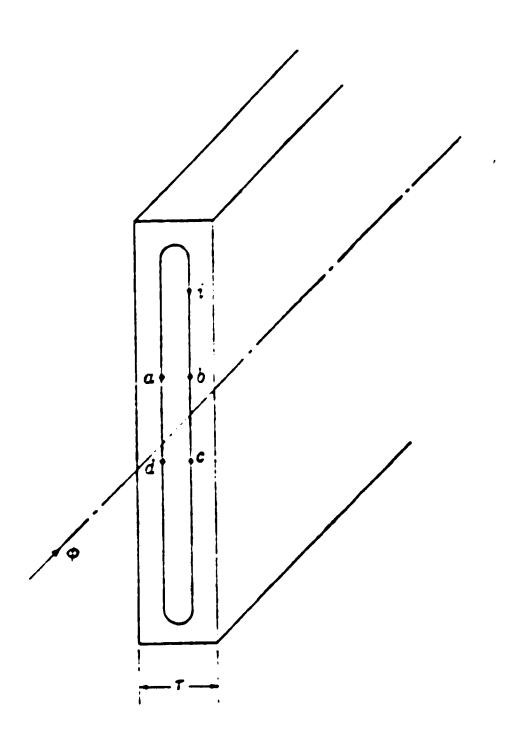


Figure 2. Cross section of lamination showing a current path. [4]

This voltage acting around the circuit abcda causes a current i to circulate around the boundary and to set up a magnetomotive force in such a direction as to oppose any change in  $\Phi$ . The effect of such currents is to screen or to shield the material from the flux, and to bring about a smaller flux density near the center of the slab than at

the surface for a specified total flux varying periodically, the maximum flux density at the center is smaller than the value obtained from dividing the total maximum flux by the area. Another way to describe this effect is to say that the total flux tends to be crowded toward the surface of the slab. This phenomenon is known as skin effect. A similar skin-effect phenomenon occurs in an electric conductor that has a varying current, even when it is composed of materials having unit relative permeability. In such conductor, the electric current density is larger at the surface. Since magnetic and electric skin effects are similar in nature, they are subject to the same type of analysis.

An analysis of eddy-current loss that arbitrarily ignores skin effect is useful and relatively simple, and gives results that are sufficiently accurate for many applications, especially in devices having laminated cores.

The analysis is developed for a thin plane slab of electrically conducting material having a thickness  $\tau$  as shown in Fig. 2. In this slab, it is assumed a uniformly distributed magnetic field whose magnitude is varying with time and whose direction is everywhere parallel to the arrow. The assumption of uniform magnetic-field distribution means that the magnetomotive forces of the eddy currents have negligible effect on the flux distribution, and that the current paths such as abcda are symmetrical about the center line through zero as shown. Also, because of the great height as compared with the thickness, the voltage gradient is practically uniform along the vertical current paths except near the top and bottom of the slab. For this reason, any horizontal slice of unit height very close to the top or the bottom has practically the same configuration of voltage gradients and current densities as any other horizontal slice. The portion of the slab considered is shown in Fig 3; It is a rectangular parallelepiped which has unit height, unit weight, and thickness  $\tau$  and is

1

and the second of the second o

symmetrical about the OY axis which passes though the center of the slab. The narrow face containing points a, b, c, and d is normal to direction of the flux. The decrease in the magnitude of the flux density with time through the area abcd in the direction shown induces a voltage around the path in the direction abcd.

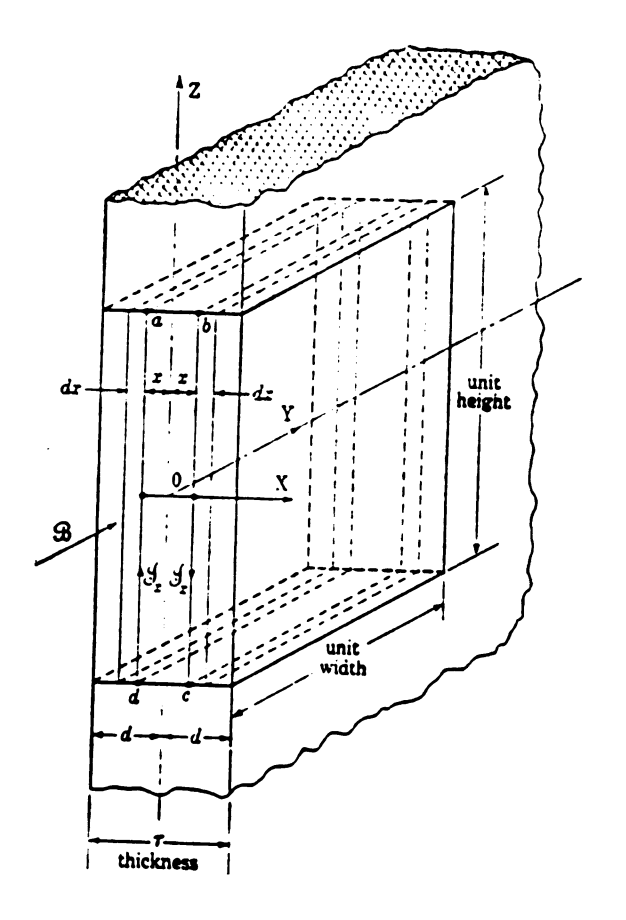


Figure 3. Unit element of lamination for calculation of eddy-curreent loss.

The application of the Faraday's induction law to the path abcda in the XZ plane normal to the direction of B gives

$$\int_{abtda} \mathbf{E}_{\mathbf{x}} \cdot d\mathbf{1} = -\frac{d}{dt} \int \mathbf{B} \, \mathbf{n} \, ds \quad , \tag{13}$$

where  $\mathbf{E}_x$  is the vertical voltage gradient at a horizontal distance x from the XY plane. In accordance with the above argument, the value of the line integral  $\int_{abcda} \mathbf{E}_x \cdot dl$  taken around the closed loop is  $2E_x$ , since the parallelepiped is of unit height. The surface integral  $\int_{abcda} \mathbf{B} \cdot \mathbf{n} ds$ , evaluated over the plane abcd, is 2x B; hence Eq.13 can be written

$$2E_x = -\frac{d}{dt}(2B \ x) \tag{14}$$

If the conducting material has a volume resistivity  $\rho$ , the current density  $J_x$  along bc or da is

$$J_{x} = \frac{E_{x}}{\rho} = -\frac{1}{\rho} \frac{d}{dt} (B \ x)$$

$$= (-\frac{x}{\rho}) \frac{dB}{dt}$$
(15)

since x is not a function of t. Along the two planes parallel to the extended faces and containing lines bc and da respectively the instantaneous power per unit volume is

$$J_x^2 \rho = \frac{x^2}{\rho} \left( \frac{dB}{dt} \right)^2. \tag{16}$$

This power loss occurs at the distance x from the central YZ plane of the slab. The instantaneous power loss in the differential slab dx thick is

$$J_x^2 \rho \, dx = \frac{1}{\rho} \left( \frac{dB}{dt} \right)^2 x^2 \, dx \ . \tag{17}$$

•

The instantaneous loss in the volume of slab having unit width and unit height and thickness  $\tau = 2d$  is

$$2\int_{0}^{d} J_{x}^{2} \rho \, dx = \frac{2}{\rho} \left[ \frac{dB}{dt} \right]^{2} \int_{0}^{d} x^{2} \, dx = \frac{2}{3} \frac{d^{3}}{\rho} \left[ \frac{dB}{dt} \right]^{2}. \tag{18}$$

A unit cube of the laminated material made up of similar slab contains  $\frac{1}{2d}$  such volumes; hence the instantaneous eddy-current loss per unit cube of laminated material with perfect insulation between the slab so that no current exists across the lamination is

$$\frac{1}{2d} \left[ \frac{2}{3} \frac{d^3}{\rho} \left( \frac{dB}{dt} \right)^2 \right] = \frac{d^2}{3\rho} \left( \frac{dB}{dt} \right)^2. \tag{19}$$

Equation 19 gives the instantaneous power loss caused by the time variation of B. In the alternating-current-machinery practice, the variation of B is usually sinusoidal. If b is its instantaneous value,

$$b = B_{\max} \cos \omega t, \tag{20}$$

from which

$$\frac{db}{dt} = -\omega B_{\text{max}} \sin \omega t, \qquad (21)$$

$$\left(\frac{db}{dt}\right)^2 = \omega^2 B_{\max}^2 \sin^2 \omega r, \qquad (22)$$

and therefore the instantaneous power loss is

$$\frac{d^2 \omega^2 B_{\max}^2}{3 \rho} \sin^2 \omega r. \tag{23}$$

Since the average value of a sine-squared function over any integral number of cycles, or over any long-time interval is one-half the maximum, the average eddy-current power loss per unit volume when the flux density is varying sinusoidally at a frequency f is

$$p_e = \frac{d^2 2 \pi^2 f^2 B_{\text{max}}^2}{3 \rho} = \frac{\pi^2 f^2 \tau^2 B_{\text{max}}^2}{6 \rho}, \qquad (24)$$

where  $\tau$  is the thickness of the individual slab, or lamination.

In the magnetic circuit containing a volume V of laminated core material subjected to the same magnetic condition as the foregoing unit volume, the average eddy-current power loss is

$$P_e = V_{P_e} = \frac{\pi^2 f^2 \tau^2 B_{\text{max}}^2}{6\rho} V . \tag{25}$$

when V is expressed in cubic meters, f in cycles per second,  $\tau$  in meters,  $B_{\text{max}}$  in webers per square meter, and  $\rho$  in ohms per meter cube,  $P_e$  is expressed in watts in Eq. 25.

The loss for any specific material is preferably written as:

$$p_e = k_e f^2 \tau^2 B_{\text{max}}^2 \tag{26}$$

and, although theoretically

$$k_e = \frac{\pi^2}{6\rho} , \qquad (27)$$

the effect of finite volume of material, low resistance between laminations, and air gaps within the core make the eddy-current calculation more accurate if  $k_e$  is determined from power measurements performed on a sample of the material and used for

Eq. 26.

In above eddy-current loss analysis, the magnetic flux is considered as sinusoidal, however in some applications the magnetic flux would not be sinusoidal. In this case, the magnetic flux can be expressed as:

$$b = \sum_{n=1}^{k} B_{n, \max} \cos n \, \omega t \tag{28}$$

then,

$$\frac{db}{dt} = \sum_{n=1}^{k} (-n\omega) B_{n,\text{max}} \sin n\omega t$$
 (29)

and the instantaneous power loss per volume becomes,

$$\frac{d^2}{3\rho} \left[ \sum_{n=1}^k n^2 \, \omega^2 \, B_{n,\text{max}}^2 \, \sin^2 n \, \omega \epsilon \right]. \tag{30}$$

from which, the average power loss is

$$p_{e} = \frac{d^{2}}{3\rho} \left\{ \frac{1}{2\pi} \int_{n=1}^{2\pi} \sum_{n=1}^{k} n^{2} \omega^{2} B_{n,\max}^{2} \sin^{2}n \omega t \ d(\omega t) \right\}$$

$$= \frac{d^{2}}{3\rho} \left\{ \frac{1}{2\pi} \sum_{n=1}^{k} n^{2} \omega^{2} B_{n,\max}^{2} \int_{0}^{2\pi} \sin^{2}n \omega t \ d(\omega t) \right\}$$

$$= \frac{d^{2}}{3\rho} \left\{ \frac{1}{2} \sum_{n=1}^{k} n^{2} \omega^{2} B_{n,\max}^{2} \right\}.$$
(31)

Where  $w=2\pi f$  and the average eddy-current loss for non-sinusoidal flux density can be given as:

$$p_e = \frac{2\pi^2}{3} \frac{f^2 d^2}{\rho} \sum_{n=1}^{k} n^2 B_{n,\text{max}}^2 . \tag{32}$$

## 2.4 TOTAL CORE LOSS

The total power loss occurring in iron cores subjected to an alternating magnetizing force is the sum of the hysteresis and the eddy-current losses. From Eq. 1 the total area of the hysteresis loop and Eq. 24, the total power loss  $p_c$  per unit volume is expressed by

$$p_c = p_h + p_e$$

OF

$$p_c = f \int_{\omega_{00}} B \ dH + \frac{\pi^2 f^2 \tau^2 B_{\text{max}}^2}{6 \rho}$$
 (33)

where the symbols have the significance previously given. If the core material is such that the hysteresis loss follows the empirical relation given by Eq. 8, this loss can be written as

$$p_c = \sigma f \ B_{\max}^n + \frac{\pi^2 f^2 \tau^2 B_{\max}^2}{6\rho} \ . \tag{34}$$

If the average flux density is the same throughout the volume V of core, the total loss  $P_c$  in this volume is

$$P_c = V p_c. ag{35}$$

Devices in which ferromagnetic materials carry alternating fluxes practically always have associated electric circuits which interlink the magnetic circuits. Transformers for example, have laminated ferromagnetic cores around which are

wound the turns of one or more coils of wire. The core losses are related to the electromotive force induced in such a coil by the changing flux. The maximum flux  $\Phi_{\text{max}}$  in terms of the effective value of the induced electromotive force E in a coil of N turns is

$$\Phi = \frac{E}{4.44 f N} \ . \tag{36}$$

when the flux and consequently the electromotive force vary sinusoidally. If the flux density is uniform over the cross-sectional area A of the core,

$$B_{\max} = \frac{\Phi}{A} = \frac{E}{4.44 f N A} \ . \tag{37}$$

For a given transformer the number of turns and the core area are fixed by the design. Then,

$$B_{\text{max}} = K \frac{E}{f} \tag{38}$$

by substituting into Eq. 34, gives

$$p_c = \sigma f \left( \frac{K E}{f} \right)^n + \frac{\pi^2 f^2 \tau^2 K^2 E^2}{6 \rho f^2}$$

$$=K_{1}\frac{E^{n}}{f^{n-1}}+K_{2}E^{2}. (39)$$

Equation 39 applies only when the waveform is sinusoidal. Although the hysteresis loss is dependent on the maximum flux density and is independent of the waveform of the flux as long as the hysteresis cycle is symmetrical and without loops, the relation between the maximum value of flux density and the effective value of the

generated electromotive force does depend upon the waveform. Thus, when expressed in terms of effective electromotive force, the hysteresis loss is correctly given by the first term of the right hand side of the Eq. 39 only when the waveform is sinusoidal.

In contrast, the second term in the core-loss expression, Eq. 39, gives the correct eddy-current loss regardless of the waveform provided the frequencies involved in the non-sinusoidal wave are not high enough to produce a considerable skin effect. When the flux wave is made up of components as discussed in previous section, each of these components induces eddy currents in the core. The eddy-current loss produced by each harmonic component in the flux is proportional to square of the same harmonic component of the electromotive force generated in the winding. Then if  $E_1$ ,  $E_5$ ,  $E_7$ ,.... are the effective values of the fundamental and harmonic components of the generated electromotive force, the total eddy-current loss is, according to the second term of Eq. 39,

$$p_e = K_2 (E_1^2 + E_2^2 + E_7^2 + \dots). \tag{40}$$

But the sum of  $E_1^2$ ,  $E_2^2$ ,  $E_3^2$ , ...... equals the square of the effective value E of the generated electromotive force. Note also that the eddy-current loss, when expressed in terms of E, is independent of frequency.

Changes in temperature such as are encountered in practice have a negligible effect on hysteresis loss. The eddy current loss decreases somewhat with increase in temperature. For a given flux variation, the eddy current loss is inversely proportional to the resistivity of the core material as indicated in Eq. 25. The resistivity increases with temperature.

Since Eqs. 33 and 34 are derived on the basis of several assumptions that in practice may not be fulfilled. Therefore, these equations are not so much for the calculation of the loss in particular cases rather they serve effectively as guides to the analysis of experimental data and also indicate the possible ways of modifying the loss. Since the validity of the assumptions depends on the condition of use of the materials, a restatement of these assumptions should be serviceable. The derivation of the hysteresis-loss term in Eq. 33 assumes that:

- (a) Each lamination is homogeneous magnetically; that is, each element of its volume has the same magnetic characteristics.
- (b) The flux density is uniform throughout each lamination; that is, the effect of the eddy currents on the flux distribution is negligible.

Furthermore, the empirical expression for the hysteresis term of Eq. 34 is subject to the additional assumptions that:

- (c) The hysteresis loop is of the normal symmetrical shape with no re-entrant loops.

  Provided this condition is satisfied, no restriction is placed on the manner in which B varies with time throughout a cycle of magnetization.
- (d) The material, the range of maximum flux density, and the manner of fluxdensity variations are such that an empirical exponent n can be used with reasonable accuracy.

The derivation of the eddy-current loss term of Eq. 33 or 34 assumes that:

(a) The material is magnetically and electrically homogeneous. In practice, this condition is not perfectly fulfilled, since such factors as grain size, the direction of the grain produced by rolling, and the relatively poorer magnetic properties of the surface layers have an appreciable effect, especially in thin laminations.

- (b) The thickness of the lamination is constant and very small compared with its other dimensions. This condition is usually realized in practice.
- (c) The flux density is uniform throughout the thickness of the lamination; that is, the eddy-current magnetomotive force is negligible compared with the magnetizing magnetomotive force acting on the core.
- (d) The volume of core involved is subjected to a uniform field so that at any instant the flux density is the same in the different laminations.
- (e) The laminations are perfectly insulated from each other. This assumption is seldom fulfilled in commercial apparatus on account of the considerable pressures under which the laminations are clamped together.
- (f) The flux density undergoes a sinusoidal time variation and is always directed parallel to the plane of the lamination. The assumption of a sinusoidal time variation is not a restriction, however, since it was shown that the factor  $(f B_{\text{max}})^2$  can be replaced by  $E^2$  times a constant, where E is the root-mean-square voltage induced in a coil linked by the alternating core flux which may have any waveform.

## 2.5 SEPARATION OF HYSTERESIS AND EDDY-CURRENT LOSSES

Any direct measurement of the power loss in the iron necessarily gives the total loss, but the division into the two components can be determined through the different ways in which the two are related to the variables. Equations 33 and 34 indicate that, when the flux density is a sinusoidal function of time, each component of loss is a different function of frequency and maximum flux density. In addition, the eddy-current loss is a function of lamination thickness and of the resistivity; but, since these quantities cannot be changed in an actual sample of material, they are not available as variables.

A method of separating the hysteresis and eddy-current components of core loss depends on the fact that the hysteresis component varies linearly and the eddy-current component varies as the square of the frequency. Stated differently, the hysteresis component of the total energy per cycle,  $P_e/f$ , is independent of frequency and the eddy-current component is a linear function of frequency. If the loss is measured at a given constant maximum flux density and the frequency is varied, then a plot of the loss per cycle as a function of the frequency, if it follows the theoretical relation

$$\frac{P_c}{f} = \int_{ldop} H \ dB + \left[ \frac{\pi^2 \tau^2 B_{\text{max}}^2}{6 \rho} \right] f \tag{41}$$

$$= k_b + k_c f ,$$

should be a straight line. The ordinate where the line intercepts the  $P_c/f$  axis at zero frequency gives the hysteresis loss per cycle  $k_h$ , and the slope of the line is the

parenthetical coefficient of f in Eq. 41, namely

$$k_e = \frac{\pi^2 \, \tau^2 \, B_{\text{max}}^2}{6 \, \rho} \ . \tag{42}$$

#### CHAPTER III

ANALYTICAL CALCULATION OF (ADDITIONAL) TRANSFORMER LOSSES
DUE TO HARMONICS

## 3.1 INTRODUCTION

The harmonics of the terminal voltage (current) introduce joule losses in the windings and iron losses in the core.

Voltage harmonics cause harmonic currents in the primary and secondary windings and, depending upon conductor size and the order of harmonic frequency v, the skin effect may cause an increase of the a.c. winding resistances  $R_{p,v}$  and  $R'_{s,v}$ .

Usually the load impedance (e.g. resistor and inductor)

$$Z_{load,v} = R_{load,v} + jv\omega L_{load,v}$$
 (43)

is dependent upon frequency. This increase of the impedance may decrease the harmonic currents significantly.

The precence of harmonics in the terminal voltage also cause additional iron losses. Some experimental results have shown that these losses are largest within the iron stack portions which are in the vicinity of the harmonic current-carrying windings and smallest in the iron portions that are farther away from such windings. Thus, the presence of harmonics result in a locally varying loss that results in a locally-varying temperature rise.[5]

In the following analytical part, average iron and copper harmonic losses will be calculated as functions of harmonic frequency and amplitude.

.

# 3.2 EQUIVALENT CIRCUIT

The harmonic losses of transformers can be calculated from the equivalent circuit shown for the vth harmonic in Figure 4,

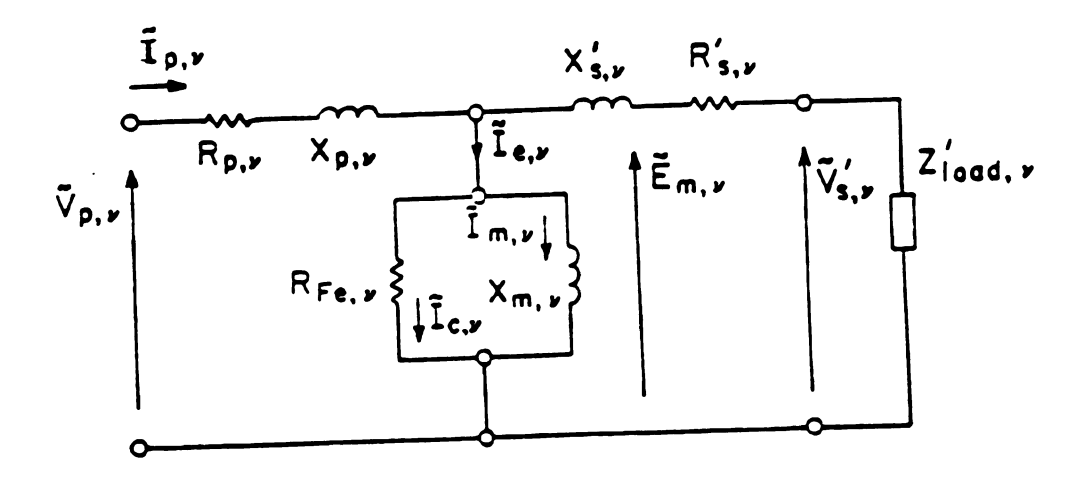


Figure 4, Equivalent circuit of a transformer for the vth harmonic

where

 $R_{p,v}$  is the resistance of primary winding for vth harmonic current,

 $R'_{s,v}$  is the resistance of secondary winding for the vth harmonic current referred to primary,

 $R_{Fe,v}$  is the core-loss resistance for vth harmonic flux density,

 $X_{p,v}$  is the leakage reactance of primary winding for vth harmonic,

 $X'_{s,v}$  is the leakage reactance of secondary winding for vth harmonic referred to primary,

 $X_{m,v}$  is the magnetizing reactance for vth harmonic

 $ilde{V}_{p, \mathbf{v}}$ ;  $ilde{I}_{p, \mathbf{n} \mathbf{u}}$  are the voltage and the current of primary winding of  $\mathbf{v} t h$  harmonic order,

 $\tilde{V}_{s,v}$ ;  $\tilde{I}_{s,nu}$  are the voltage and the current of secondary winding of vth harmonic order,

 $\tilde{E}_{m,v}$ ;  $\tilde{I}_{e,v}$  are the emf and no-load current of parallel branch of vth harmonic order, respectively,

 $\tilde{I}_{m,v}$  is the magnetizing current of vth harmonic order, and

 $\tilde{I}_{c,v}$  is the core-loss current of vth harmonic order.

For the calculation of the ohmic losses the above equivalent circuit may be simplified by neglecting the parallel branch ( see fig. 5), since the magnetizing current is negligible as compared to the load current.

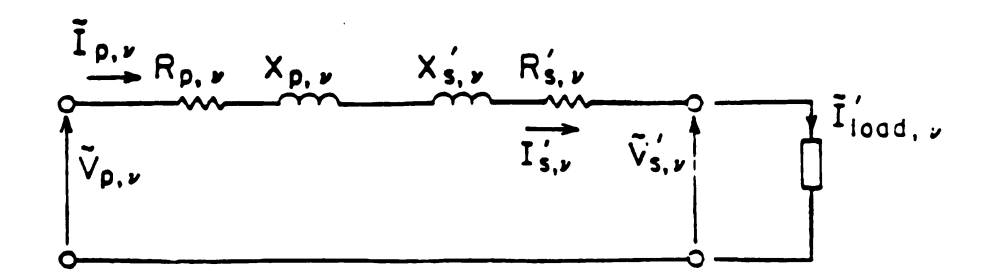


Figure 5. Approximate equivalent circuit of a transformer

Neglecting the magnetizing current, the load current can be written as:

$$|\tilde{I}_{load,v}| = |\tilde{I}_{p,v}| = \left\{ \frac{|\tilde{V}_{p,v}|}{\sqrt{(R_{p,v} + R_{s,v}' + R_{load,v}')^2 + (v\omega)^2 (L_{p,v} + L_{s,v}' + L_{load,v}')^2}} \right\}$$
(44)

 $R_{load,v}$  and  $X_{load,v} = v\omega L'_{load,v}$  represents the resistance and reactance of the load which is connected across the terminals of the secondary winding.  $\tilde{I}_{load,v}$  is the  $v^{th}$  harmonic current of the load.

## 3.3 CALCULATION OF OHMIC LOSSES DUE TO HARMONICS

The ohmic losses of a transformer are given for the vth harmonic by

$$P_{ohmic,v} = |\vec{l}_{p,v}|^2 R_{p,v} + |\vec{l}_{s,v}|^2 R'_{s,v}$$

$$= |l_{load,v}|^2 (R_{p,v} + R'_{s,v})$$
(45)

substituting the expression of  $\tilde{I}_{load,v}$  of equation 44 into equation 45 one obtains

$$P_{ohmic,v} = \frac{|\tilde{V}_{p,v}|^2 (R_{p,v} + R'_{s,v})}{(R_{p,v} + R'_{s,v} + R'_{load,v})^2 + (v\omega)^2 (L_{p,v} + L'_{s,v} + L'_{load,v})^2} . \tag{46}$$

This relationship may be used for the calculation of the ohmic losses at any angular frequency  $v\omega$ , where  $\omega = 2\pi f$  and v is an integer. However, at higher frequencies where the depth of penetration becomes comparable to the diameters of the transformer's wires of the primary and secondary, the winding resistance and reactances must be corrected.

## 3.4 CALCULATION OF IRON LOSSES DUE TO HARMONICS

The iron losses consists of eddy current losses  $(P_e)$  and hysteresis losses  $(P_h)$ . In Ref [6] these losses are given by the following relations:

$$P_{e,v} = \sigma(\frac{f_v}{100}B_{\text{max},v})^2 \qquad (Watts/kg)$$
 (47)

$$P_{h,v} = \varepsilon \frac{f_v}{100} (B_{\text{max},v})^2 \qquad (Watts/kg)$$
 (48)

where:

Constants  $\sigma$  and  $\varepsilon$  depend upon the core material [7].  $f_{\nu}$  is the frequency in Hz,  $B_{\nu}$  is the flux density in Tesla and can be calculated from the applied voltage as follows:

$$\Phi_{\text{max,v}} = \frac{\tilde{V}_{p,\text{max,v}}}{2\pi f_{\nu} N} \qquad (Weber)$$
(49)

using the effective value of applied voltage,  $B_{\text{max,v}}$  can be given by :

$$B_{\text{max,v}} = \frac{\sqrt{2}\tilde{V}_{p,v}}{2\pi f_{v}NA} \qquad (Tesla)$$
 (50)

The total iron losses per unit weight,  $P_{iron,v}$ , is given by the sum of the above relations:

$$P_{iron,v} = P_{e,v} + P_{h,v} = \left\{ \sigma(\frac{f_v}{100}B_v)^2 + \varepsilon \frac{f_v}{100}(B_v)^2 \right\}$$
 (Watts/kg) (51)

Note that this relation can be used directly for low frequencies at which the reaction of the eddy currents in the laminations can be neglected. At higher frequencies the relations for  $P_e$  and  $P_{iron}$  must be modified by coefficient  $k_m$  which takes the reaction of the eddy currents [8] into account. Thus,

$$P_{e,v}^* = \sigma(\frac{f_v}{100}B_v)^2 k_m^2 \quad (Watts/kg)$$
 (52)

and

$$P_{iron,v}^{*} = \left\{ \sigma(\frac{f_{v}}{100}B_{v})^{2}k_{m}^{2} + \varepsilon \frac{f_{v}}{100}(B_{v})^{2} \right\} \qquad (Watts/kg)$$
 (53)

The asterisk denotes that the eddy currents is taken into account;

Where

$$k_m = \frac{3}{\zeta} \left\{ \frac{\sinh \zeta - \sin \zeta}{\cosh \zeta - \cos \zeta} \right\} \le 1.0$$
 (54)

and

$$\zeta = \alpha \ \Delta \tag{55}$$

with

$$\alpha = 2\pi \sqrt{\frac{\mu_r f_v}{10^5 \rho}} \qquad (1/cm) \tag{56}$$

 $\Delta$  in *cm* the thickness of the laminations,

 $\rho$  is the resistivity in  $\Omega mm^2/m$  of the core material, and

μ, represents the relative permeability of the core material.

Since  $k_m$  is smaller than one, the modified expression for  $P_e$  indicates that at higher frequencies the eddy current iron losses are reduced in the iron regions near the conductors while it is greatly reduced in the iron regions farther away from the conductors.

# 3.5 SAMPLE CALCULATION

In this section, the copper losses of a transformer model, whose finite element analysis is done in the next chapter as well, is calculated for a six-step applied (primary) voltage.

In reference 9, the change in resistance of a cylindrical conductor is discussed; If R' is the effective resistance of a linear cylindrical conductor to sinusoidal alternating current of given frequency and R is the true resistance with continuous current, then

$$R' = K R \tag{57}$$

where K is determined from Table 4-6 of reference 9 in terms of x. The value of x is given by

$$x = 2 \pi a \sqrt{\frac{2f\mu}{\rho}} \tag{58}$$

where:

a the radius of conductor in centimeters.

f frequency in cycles per second,

μ, relative magnetic permeability of conductor,

ρ resistivity in abohm-centimeters (abohm= $10^{-9}\Omega$ ).

The relative permeability of non-magnetic materials (copper, aluminum) is 1.

The six-step applied voltage shown in Figure. 6 can be expressed in the form of equation 59 after applying the fourier series analysis.

$$v = \frac{20}{v \pi} \sum_{v=1}^{\infty} \left[ 1 + \cos \frac{v \pi}{3} \right] \sin (v \omega t)$$
 (59)

The effective and non-zero harmonics of such wave form are 1, 5, 7, 11, 13. For these harmonics, the additional copper losses is given in Table 1. In this

calculation, It is assumed that the load resistance is changing with frequency but not the load reactance. It should be noted that the leakage resistance is not changing with the frequencies whose harmonics are given above.

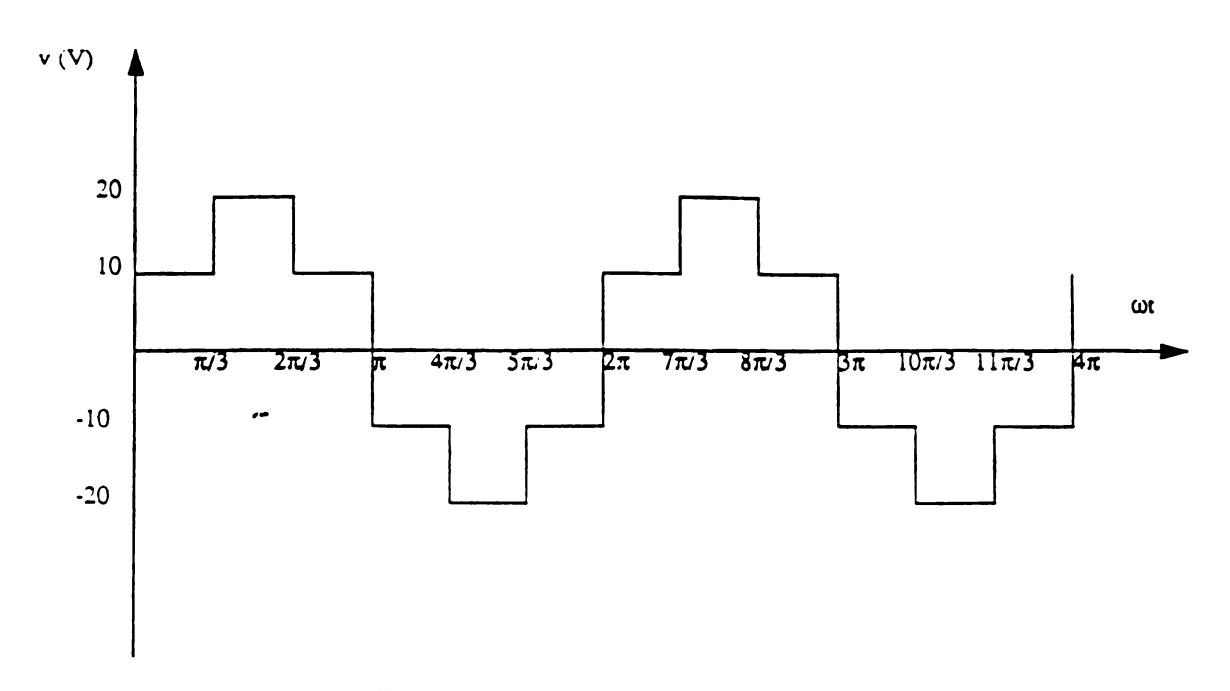


Figure 6. Six-step applied voltage

٧	V <sub>pv</sub> (V)	$R_{pv} + R_{sv} (\Omega)$	R <sub>load,v</sub> (Ω)	L <sub>load,v</sub> (H)	Pohmic,v (W)
1	6.75	0.2351	3.0	0.01	0.4
5	1.35	0.2351	3.15	0.01	162 x 10 <sup>-3</sup>
7	0.96	0.2351	3.20	0.01	0.308 x 10 <sup>-3</sup>
11	0.61	0.2351	3.23	0.01	5.109 x 10 <sup>-5</sup>
13	0.52	0.2351	3.25	0.01	2.625 x 10 <sup>-5</sup>

Table 1. The additional copper losses for six-step applied voltage.

# CHAPTER IV

NON-LINEAR TIME DEPENDENT FINITE ELEMENT METHOD ANALYSIS OF TRANSFORMERS

#### 4.1 INTRODUCTION

The standard procedure of using finite element analysis is to approximate magnetic field quantities within a fixed device or region. The user describes the problem geometry and material characteristics, sets boundary conditions, and specifies numerically all current densities, which act as the source of the magnetic field. The region of interest is then discretized in space into mesh, and the finite element field approximation equations are set up and solved. The solution consists of a set of approximations for the field at each node of the mesh.

Hovewer, such a procedure is inadequate for a large class of practical problems, for example, in the transient analysis of an electromagnetic devices which is activated by a voltage source, such as transformers, and motors.

The voltage source for such devices is time-dependent; therefore, one cannot specify a priori the numerical value of the current density in the conductive regions of the device, because skin effect and eddy currents cause the current density to vary with time and position the standard finite element procedure, however, requires current current density as a known input to the analysis.

In addition, it may be necessary to attach lumped circuit components, such as resistance or inductance, between the voltage source and the region to be modelled by finite elements. The lumped components may represent the internal impedance of the voltage source, or they may be used to approximate the effects of the parts

•

of the device which are outside the region modelled by finite elements. Proper coupling of circuit equations with the finite element field equation cannot be achived with conventional finite element analysis procedures.

Therefore, modification to the procedure must be made so that:

- (a) Only terminal voltage applied to the device is required as a known input quantity, and total terminal current is calculated as an unkown;
- (b) The external circuit equations that model electrical sources and circuit components are coupled to the finite element field equations.

Moreover, the advantages of this method to analyze the electromagnetic devices are:

- (a) Deviation from the traditional and cumbersome equivalent circuit and lumped parameter models;
- (b) Better model of the device can be achieved using this method;
- (c) Effect of the non-linearity of the iron and other parameters can be easily incorporated in the model close to the actual.

In this chapter, the field and circuit equations of a transformer are coupled giving a time dependent set of non-linear equations, the solution of which gives the magnetic vector potential at every point in the cross section of the transformer and the electric field intensity together with the primary and secondary currents at the cross section of the conductors.

#### 4.2 ANALYSIS

It is common to solve for the electric field at the cross-section of a transformer with the assumptions given below:

- 1. The problem is two dimensional, i.e., considering zero non-axial components of the current density and the magnetic vector potential.
- 2. The permeability is a function of the flux density.
- 3. No eddy currents are present in the iron.
- 4. The magnetic field is contained in the geometry.

In this case, an equation that describes the field in the transformers can be given as [10,11]:

$$-\frac{\partial}{\partial x}(\frac{1}{\mu}\frac{\partial A_z}{\partial x}) - \frac{\partial}{\partial y}(\frac{1}{\mu}\frac{\partial A_z}{\partial y}) + \sigma\frac{\partial A_z}{\partial t} - \sigma E_z = 0$$
 (60)

where  $A_z$  and  $E_z$  are the axial components respectively of the magnetic vector potential and of an "applied" electric field, such that:

$$E_z = -\frac{\partial \Phi}{\partial z} = -\frac{\Delta V}{I} \tag{61}$$

where l is the length of the model and  $\Phi$  is an electric potential.

It is the circuit equations that provide the boundary conditions at the two planes perpendicular to transformer axis that define the length of the model. The following equations are obtained from (60) using Crank-Nicolson-Galerkin method.

$$SA + K\dot{A} - NE = 0 \tag{62}$$

$$\left[ (1-\theta)\mathbf{S} + \frac{\mathbf{K}}{\Delta t} \right] \mathbf{A}^{n+1} - (1-\theta)\mathbf{N}\mathbf{E}^{n+1} = \left[ -\theta\mathbf{S} + \frac{\mathbf{K}}{\Delta t} \right] \mathbf{A}^{n} + \theta\mathbf{N}\mathbf{E}^{n}$$
 (63)

where  $1 < \theta < 0$  and S, K come from local matrices with entries;

$$S_{i,j}^{local} = \frac{1}{\mu} \int_{\Omega} ((\phi_{i,x} \phi_{j,x}) + (\phi_{i,y} \phi_{j,y})) dx dy$$
 (64)

$$\mathbf{K}_{i,j}^{local} = \sigma \int_{\Omega} (\phi_i \phi_j) dx dy \tag{65}$$

When using the same elements and shape functions for E as A, the entries of N are the same as K.

Equation (63) will be augmented with circuit equations that relate the A or E to currents and external applied voltage.

Besides (60), dropping the subscript z, we can write at every node on a coil side:

$$-\sigma(\dot{A} - E) = J \quad , \tag{66}$$

since J and  $\sigma$  are considered zero everywhere except the conductor cross-sections. One need only calculate values of E and write (66) only for these regions. There, due to many thin wires carrying the same current, one can consider J uniform.

Taking two sides of the a coil and establishing for each coil a positive direction of current, one can write for the current density in the cross-section of coil side i:

$$J_i = \frac{n_i}{\Omega_i} d_i I_{pri} \qquad d_i = \pm 1 \tag{67}$$

where the value of  $d_i$  is the reference direction of the current establishing with the help of Figure 7,  $n_i$  is the number of wires in this coil side, and  $\Omega_i$  the cross-section of this coil side.

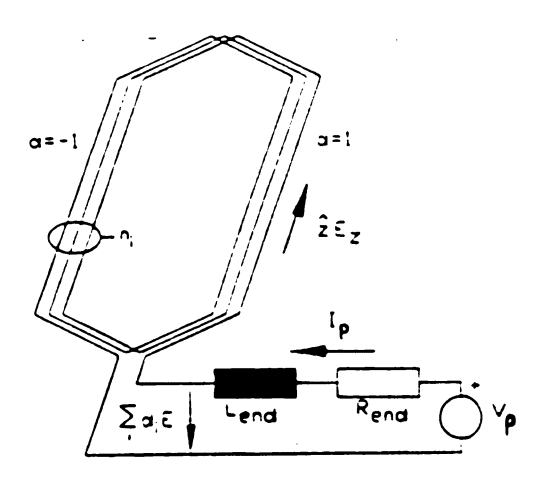


Figure 7. Reference directions and the circuit for a coil.

Writing (66) for each node of elements of conductors in primary and secondary, and premultiplying the resulting system of equation by  $N^T$  We obtain:

$$-\mathbf{N}_{\mathbf{pri}}^{\mathbf{T}}\dot{\mathbf{A}} + \mathbf{N}_{\mathbf{pri}}^{\mathbf{T}}\mathbf{E} - \frac{n}{\sigma\Omega}\mathbf{N}_{\mathbf{pri}}^{\mathbf{T}}\mathbf{d}I_{pri} = 0$$
 (68)

and as a difference equation:

$$-\mathbf{N}_{\mathbf{pri}}^{\mathbf{T}}\mathbf{A}^{n+1} + \mathbf{N}_{\mathbf{pri}}^{\mathbf{T}}\Delta t (1-\theta)\mathbf{E}^{n+1} - \frac{n}{\Omega\sigma}\Delta t \mathbf{N}_{\mathbf{pri}}^{\mathbf{T}}\mathbf{d}I_{pri}^{n+1} =$$

$$-\mathbf{N}_{\mathbf{pri}}^{\mathbf{T}}\mathbf{A}^{n} - \mathbf{N}_{\mathbf{pri}}^{\mathbf{T}}\Delta t \theta \mathbf{E}^{n} + \frac{n}{\Omega\sigma}\Delta t \mathbf{N}_{\mathbf{pri}}^{\mathbf{T}}\mathbf{d}I_{pri}^{n}$$
(69)

From Kirchoff equations, one can write for primary and secondary:

$$\sum_{pri} d_i \left[ \sum_{\Omega_i} lE_j \right] + RI_{pri} + L \frac{dI_{pri}}{dt} = V_{ext}$$
 (70)

where the inner sum extends over all the wires of the coil side i and the outer sum over all the coil sides in the primary. In this equation it is recognized that the electric field is not necessary uniform over a winding cross-section, while the current is. R and L can be written as follows:

$$R = R_{ext} + R_{end-turn}$$

$$L = L_{ext} + L_{end-turn}$$

where

 $R_{ext}$  is the external resistance with the coil.

 $L_{ext}$  is the external inductance with the coil.

 $R_{end-turn}$  is the winding resistance.

 $L_{end-turn}$  is the winding inductance.

Replacing the inner sum with an integral (70) takes the form;

$$l\frac{n}{\Omega\sigma}N_{pri}\mathbf{d}^{\mathrm{T}}\mathbf{E} + RI_{pri} + L\dot{I}_{pri} = V_{ext,pri}$$
(71)

which becomes a difference equation:

$$\frac{n}{\Omega\sigma} \Delta t (1-\theta) \mathbf{N}_{pri} \, \mathbf{d}^{\mathsf{T}} \mathbf{E}^{n+1} + \frac{1}{l} \left[ \Delta t (1-\theta)R + L \right] I_{pri}^{n+1} = \frac{\Delta t}{l} V_{ext} - \frac{n}{\Omega\sigma} \Delta t \, \theta \mathbf{N}_{pri} \, \mathbf{d}^{\mathsf{T}} \mathbf{E}^{n} - \frac{1}{l} \left[ \Delta t \, \theta R - L \right] I_{pri}^{n}$$
(72)

Combining (63),(69),(72) for single phase transformer one obtains an equation system in the following form:

$$\begin{bmatrix} C_0 & C_{2pri} & C_{2sec} \\ C_{2pri}^T & C_{4pri} & C_{5pri} \\ & -C_{5pri}^T & C_{6pri} \\ C_{2sec}^T & & C_{4sec} & C_{5sec} \\ & & -C_{5sec}^T & C_{6sec} \end{bmatrix} \begin{bmatrix} A^{n+1} \\ E_{pri}^{n+1} \\ I_{pri}^{n+1} \\ E_{sec}^{n+1} \\ I_{sec}^{n+1} \end{bmatrix} =$$

$$-\begin{bmatrix} C_{0}^{'} & C_{2pri} & C_{2sec} \\ -C_{2pri}^{T} & C_{4pri} & C_{5pri} \\ & -C_{5pri}^{T} & C_{6pri}^{'} \\ -C_{2sec}^{T} & C_{6pri}^{'} \end{bmatrix} \begin{bmatrix} A^{n} \\ E_{pri}^{n} \\ I_{pri}^{n} \\ E_{sec}^{n} \end{bmatrix} + \begin{bmatrix} F \\ 0 \\ F_{pri} \\ 0 \\ F_{sec} \end{bmatrix}$$
(73)

### 4.3 TIME DEPENDENCE AND SOLUTION METHOD

Besides  $V_{ext}$ , the matrices  $C_0$  and  $C_0'$  depend on time through the nonlinearity of permeability of transformer. To account for nonlinearity, Newton's Method[12] was utilized at every time step to provide the values of the permeability in the iron. Iterations at every step and time stepping require the repeated solution of systems with slightly non-symmetric coefficient matrices, where neither the coefficient matrices nor the solution change much in time.

### 4.4 CALCULATION OF IRON LOSSES

### 4.4.1 CALCULATION OF EDDY-CURRENT LOSSES

The use of triangular first order elements allows only one value of the flux density and one value of the iron loss density in each element. The eddy current iron loss density is often known as a function of maximum flux density and the resistivity as well as the thickness of laminations for a given type of magnetic steel as mentioned in the previous section. The effect of the frequency is included in this function when skin effect is taken into account. Generally, Eddy-current loss density can be written for a harmonic of frequency  $f_i$  as[13]:

$$p_e = \sum_{i} f_i^2 k_e (B_{\text{max},i})$$
 (74)

where i varies over the number of harmonics of the flux, and  $k_e$  is a function obtained in the previous chapter.

### 4.4.2 CALCULATION OF HYSTERESIS LOSSES

The hysteresis loss density when there are no minor loops in the B-H curve can be found as [13]:

$$p_h = f \ k_h(B_{\text{max}}) \tag{75}$$

where again  $k_h$  is obtained as described previous chapter in the section of the separation of losses and f is the frequency.

The calculation of eddy-current losses in iron requires the analysis of the flux density in each element in harmonics, while the calculation of the hysteresis is performed using a simple algorithm.

### CHAPTER V

### **APPLICATIONS**

### 5.1 INTRODUCTION

In this chapter, the results of the current and the flux density analysis of a single-phase transformer are presented. The analysis done by two different methods which are:

- (1) combining the non-linear field and the current equation by the finite element method and solving them by Newton's Method as introduced in chapter IV for a single-phase transformer,
- (2) solving the same field and current equations but in the simplified forms, so that can be coded in the ASCL (Advanced Continuous Simulation Language) for the same transformer. ACSL is a language designed for modeling and evaluating the performance of continuous systems described by time dependent, non-linear differential equations.

Besides the current and the flux density, the equipotential lines and the variables like voltages induced in primary and secondary windings are included in the analysis done by the finite element method.

In this chapter, different applied voltages and load conditions are assumed and the results of analysis of each case are introduced in separate subsections.

#### 5.2 THE MODEL.

The model chosen for the analysis is a small-size single-phase transformer which is very similar to the ones which are widely used in radio sets and home appliances. Figure 8 shows the cross section of the model and figure 9 shows a simple grid of the model for the finite element method analysis.

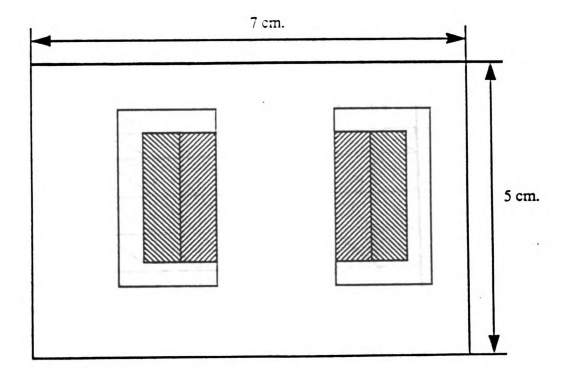
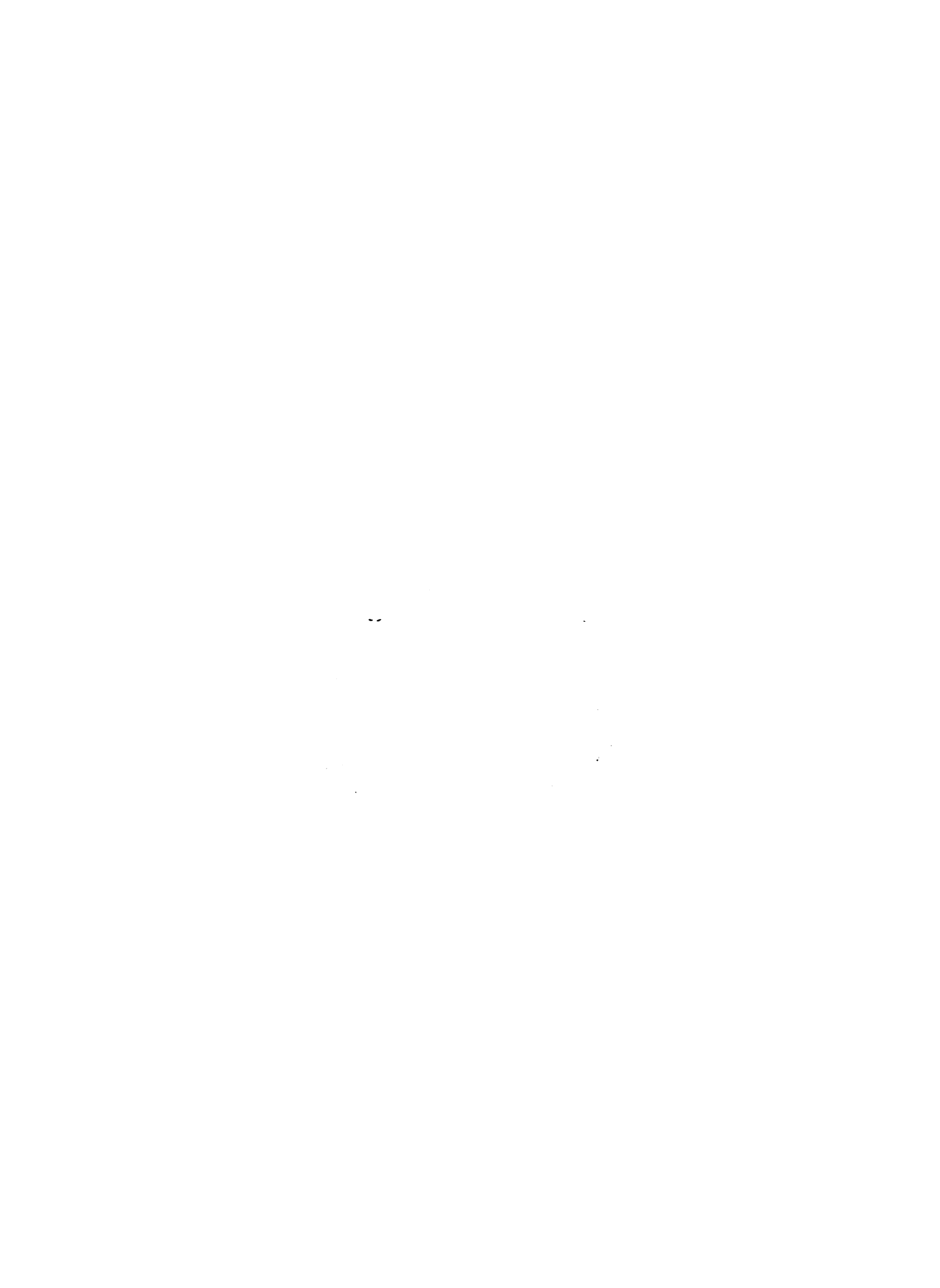


Figure 8. Cross-section of the transformer model



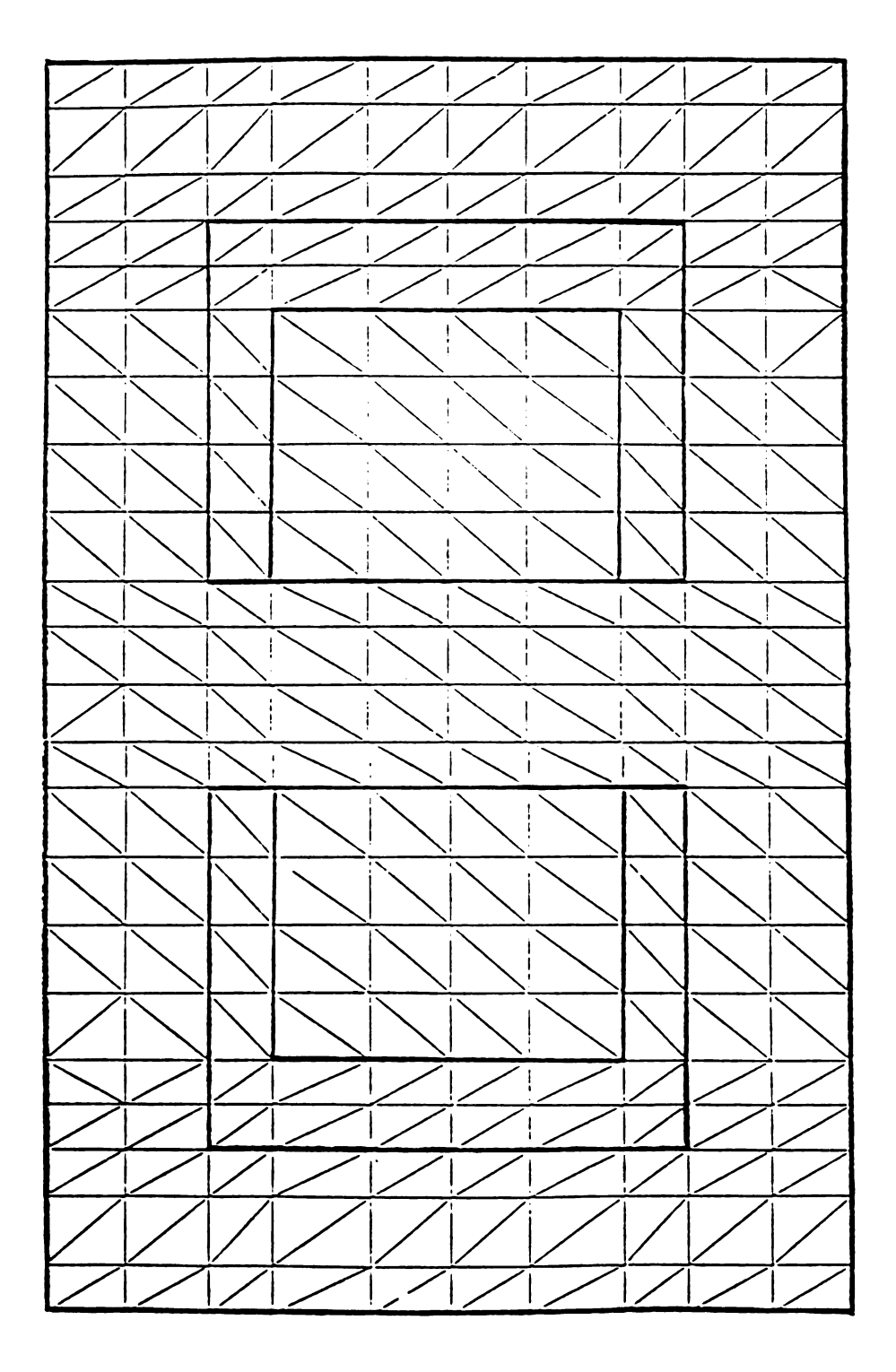


Figure 9. A simple gridding of the model for the finite element method.

### 5.3 TRANSIENT FIELD ANALYSIS

The change of the geometries of the equipotential lines (magnetic vector potential) of the model is analyzed by the time change using the finite element method.

Figure 10 shows the equipotential lines of model at 1 msec after the sinusoidal input was applied and figure 11 shows the equipotential lines at 10 msec. for the same input.

it is can easily be observed from Figure 10 that the equipotential lines of the magnetic vector potential is starting from the windings which is source and penetrating to the iron thru the windows. Later on, the equipotential lines are seen in the iron core because of the low resistivity of the core compared with the air.

# 5.4 THE RESULTS OF NON-LINEAR TIME-DEPENDENT CURRENT, FLUX DENSITY AND VOLTAGE ANALYSIS

The current, the flux density, and induced voltage analysis of the model, whose equivalent curcuit is given in figure 12, is done by both the finite element method and the ACSL for the cases given below.

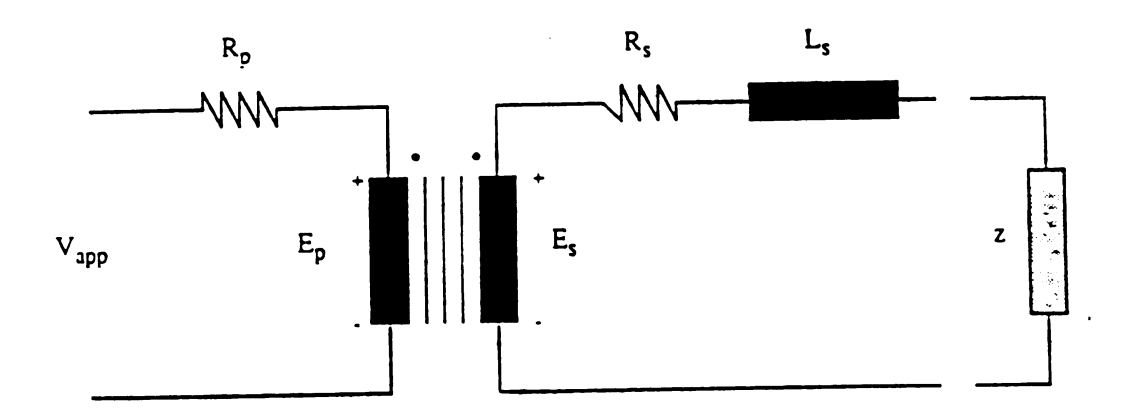


Figure 12. Equivalent circuit of the model

### 5.4.1 CASE 1: SINUSOIDAL INPUT AND RESISTIVE LOAD

In this case, a resistive load of 3  $\Omega$  is connected to the secondary and 0.3  $\Omega$  resistance is connected in serial to the primary winding. The maximum value of the applied voltage to the primary is 5 volts and the frequency is 60 Hz. The results of both the finite element method and the ACSL analysis are given below.

### 5.4.1.1 THE RESULTS OF THE FINITE ELEMENT METHOD FOR CASE 1.

In this subsection, the plots of the primary and secondary current of the model are given in figure 14 and 15 respectively in response of the applied voltage shown in figure 13 for the load condition stated above. The absolute flux density for each element is calculated in the finite element method. Therefore, the plot of the flux density of the 166th element is given in figure 16. The plots of the induced voltages of the primary and secondary together with the reluctivity of the 166 th element are given in figure 17, figure 18 and figure 19 respectively. The difference between the induced voltages is the voltage drop because of the leakage inductances and the resistances of the windings.

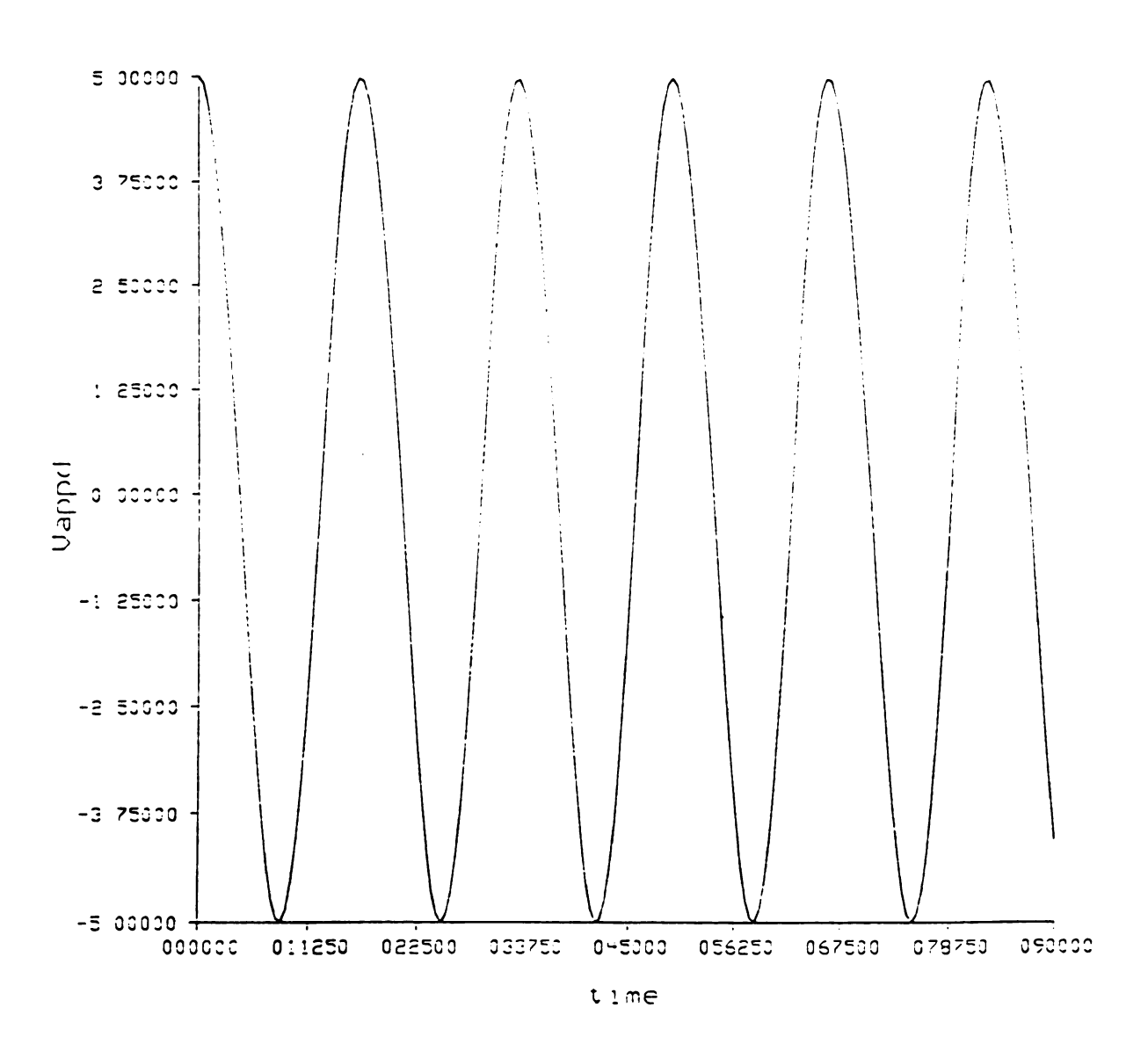


Figure 13. Applied voltage for the first case.

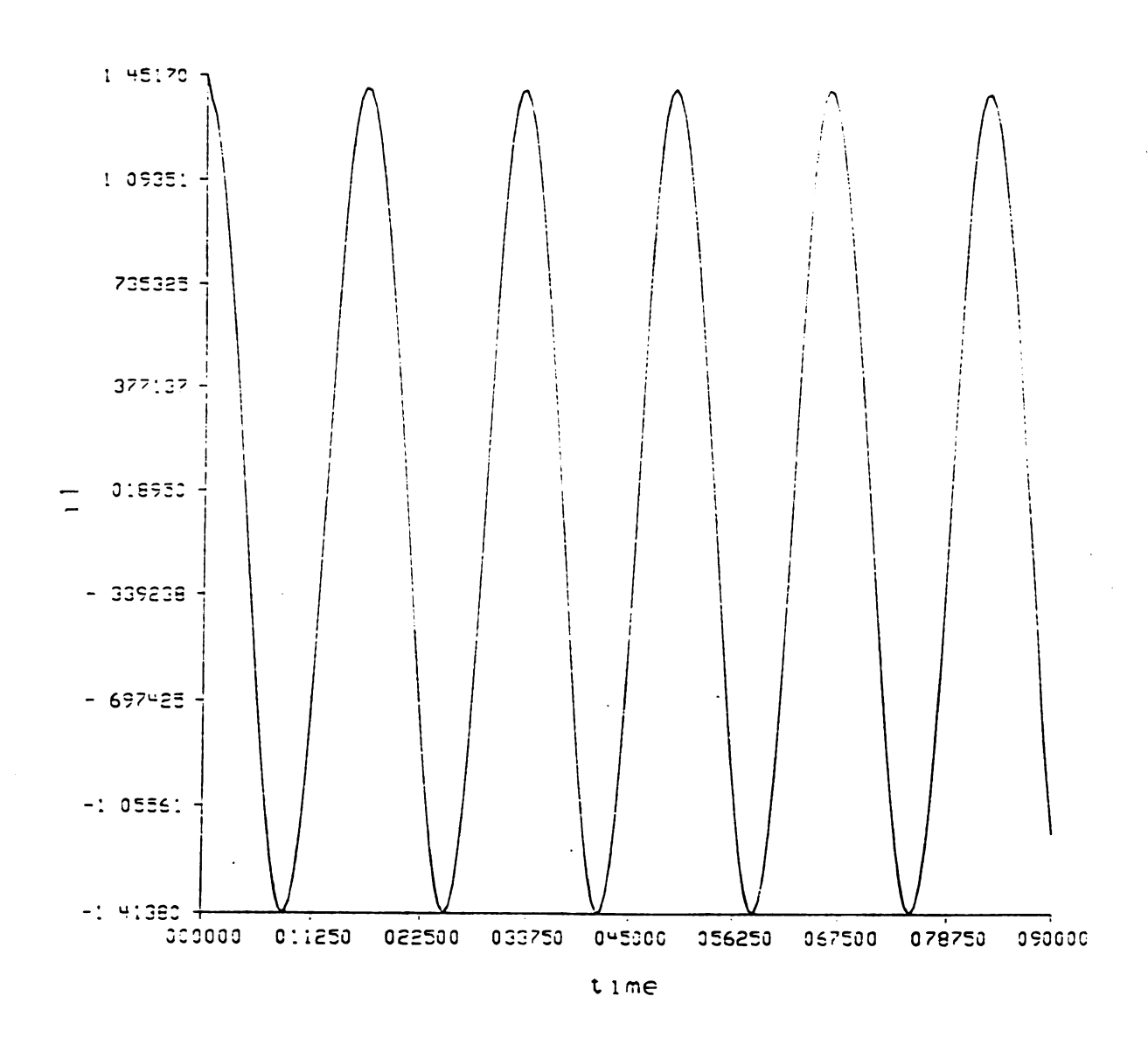


Figure 14. Primary current of the model connected to resistive load.

`

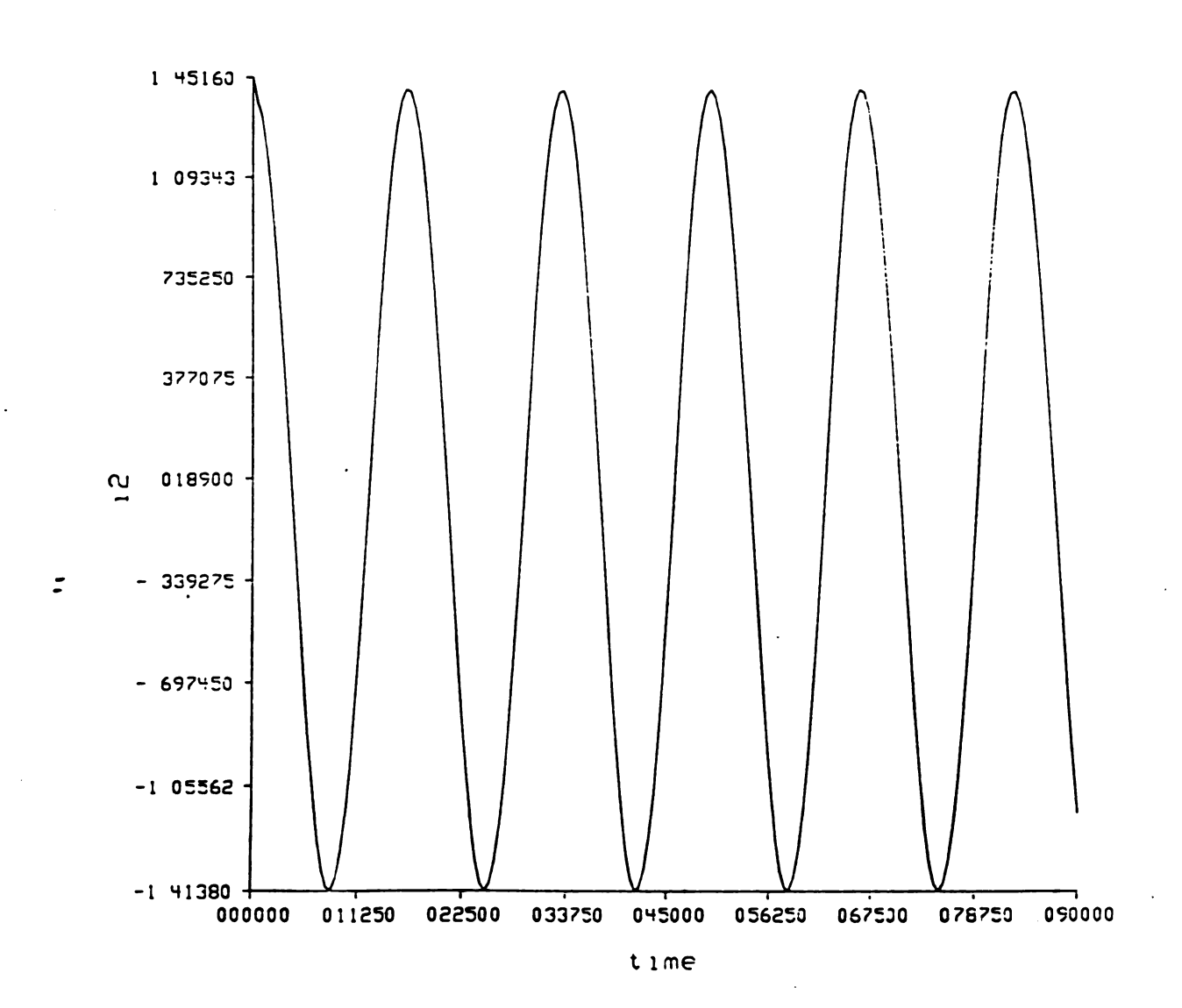


Figure 15. Secondary current of the model connected to resistive load.

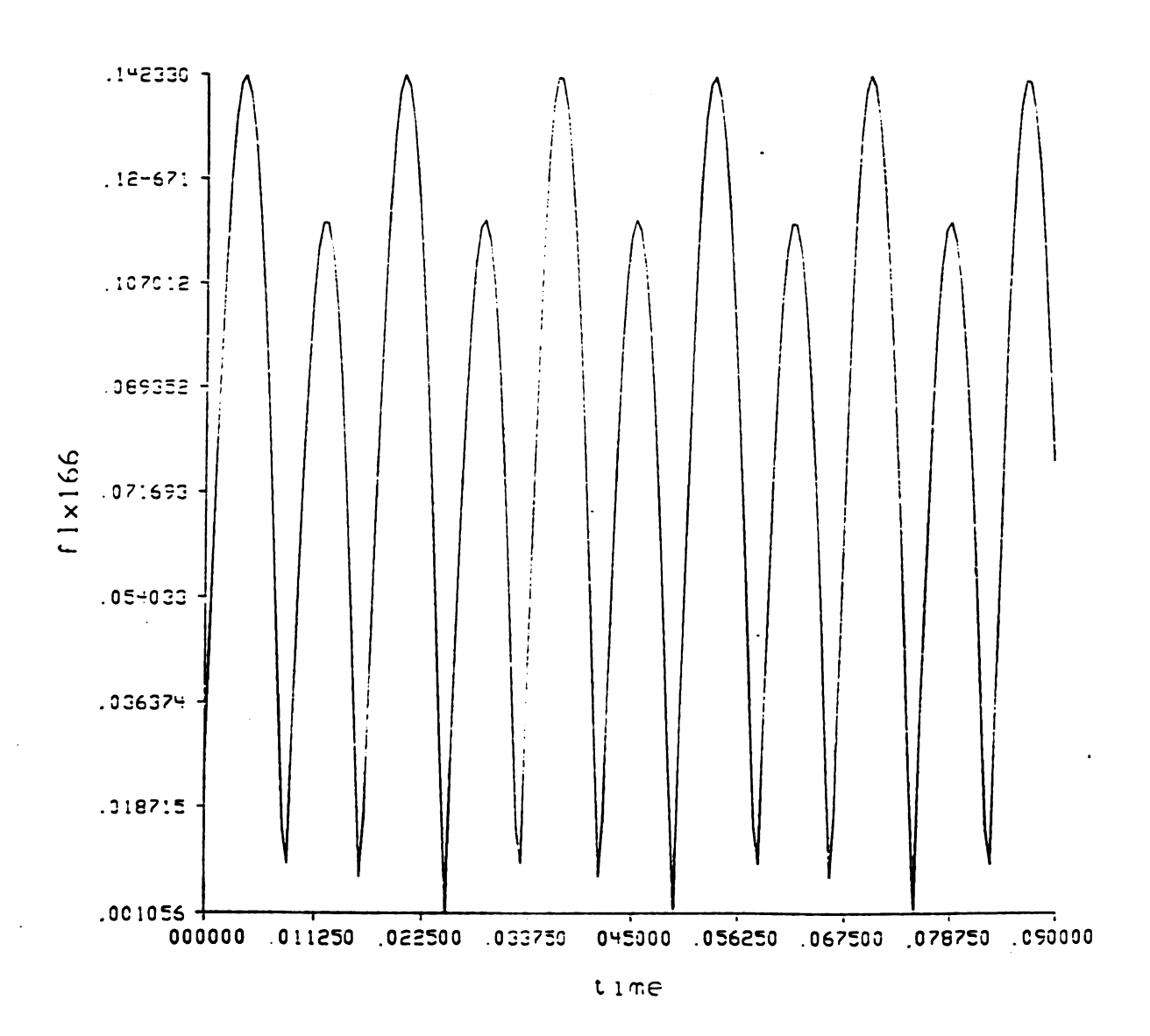


Figure 16. Flux density of the 166th element for case 1.

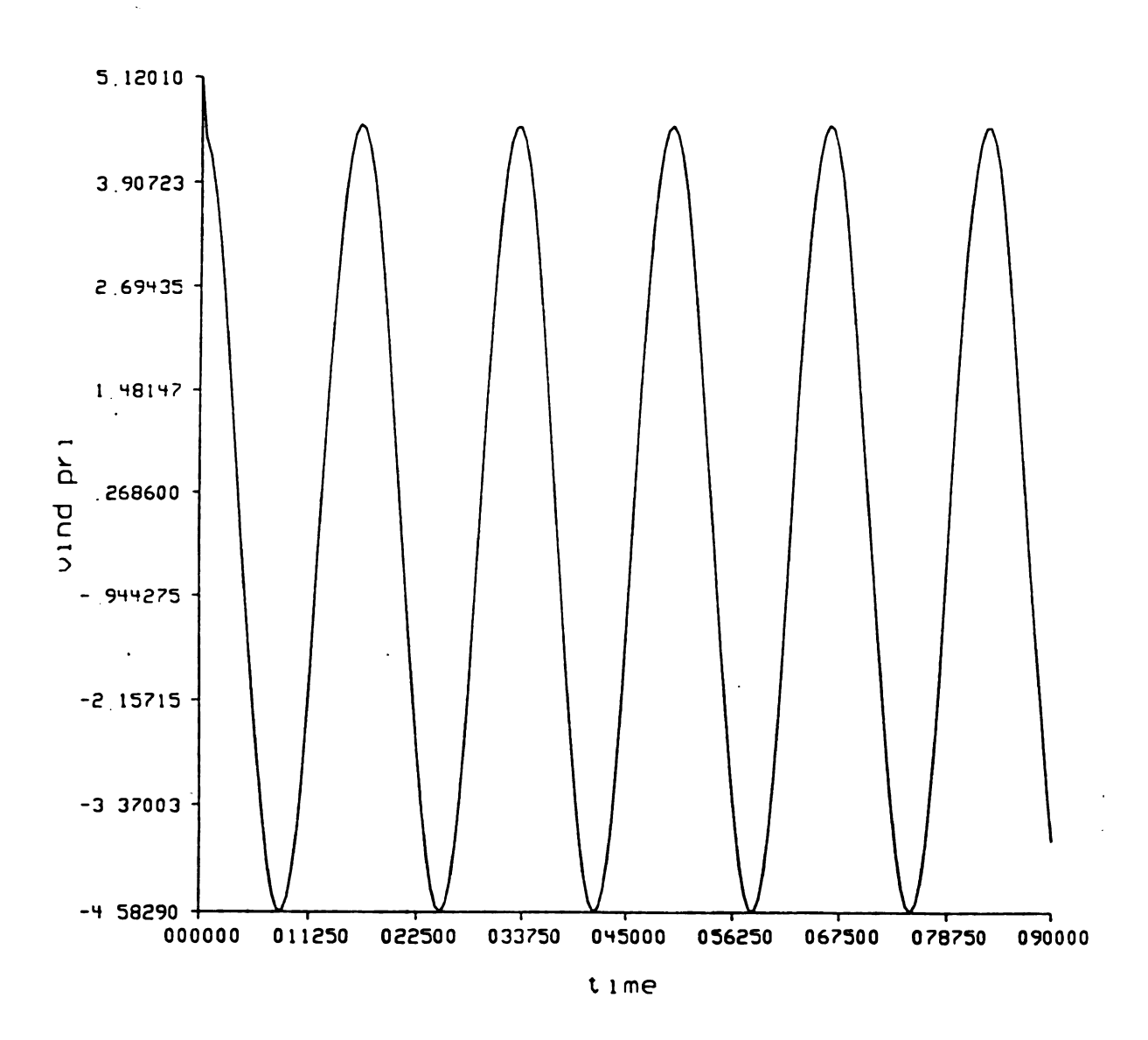


Figure 17. Induced voltage in the primary windings for case 1.

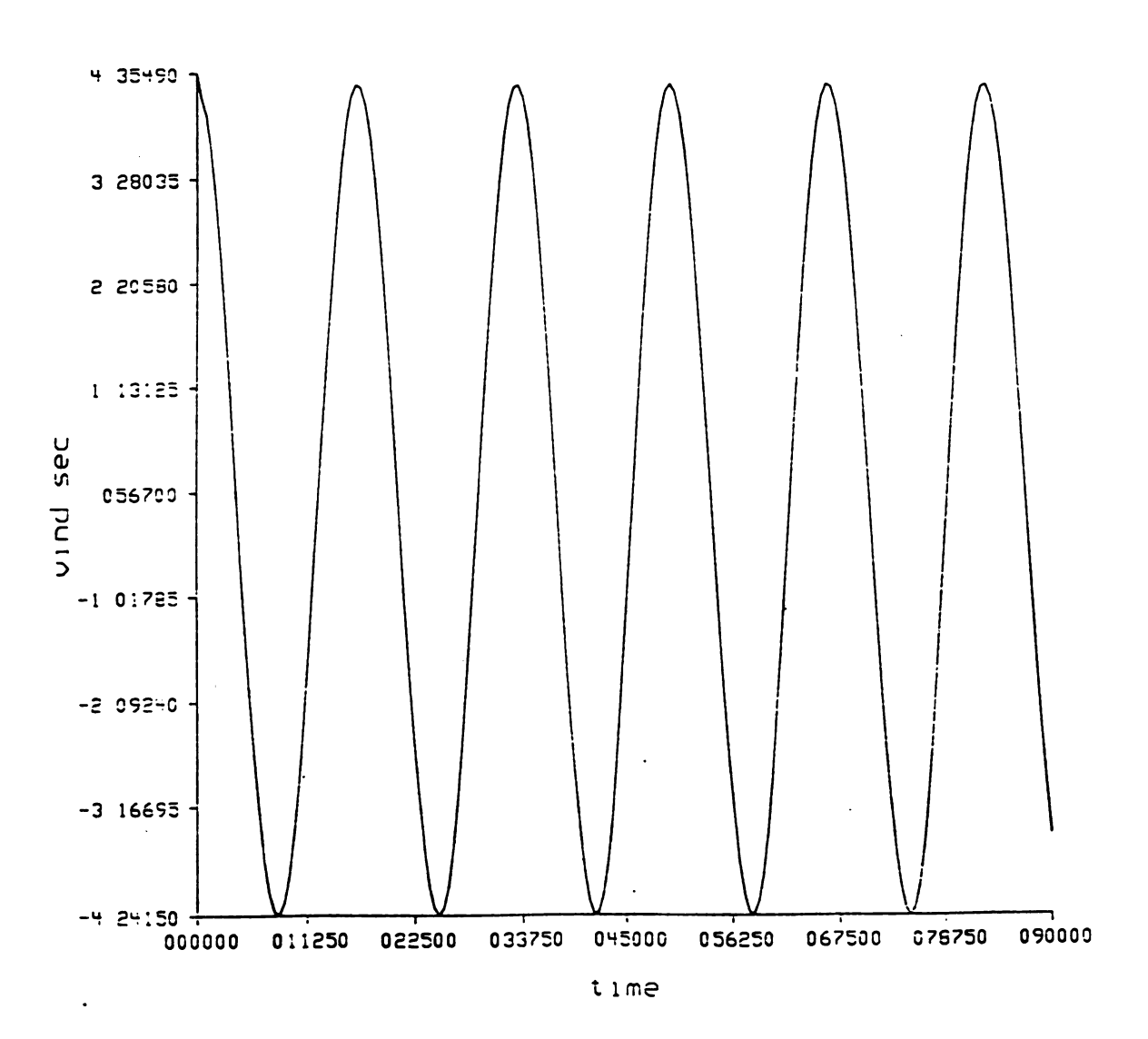


Figure 18. Induced voltage in the secondary windings for case 1.

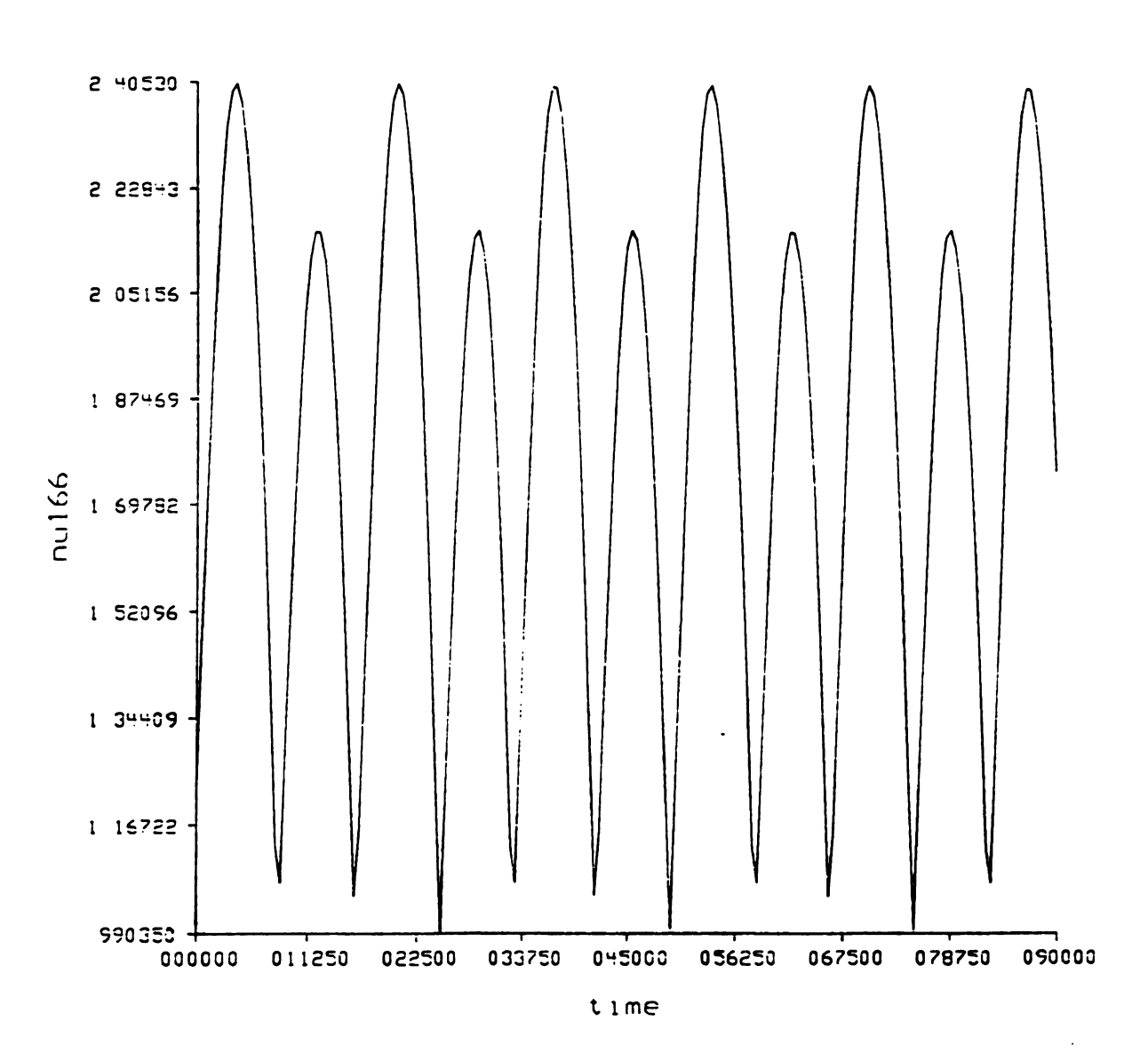


Figure 19. The reluctivity (inverse of the permeability) of the 166th element for case 1.

## 5.4.1.2 THE RESULTS OF THE ACSL FOR CASE 1

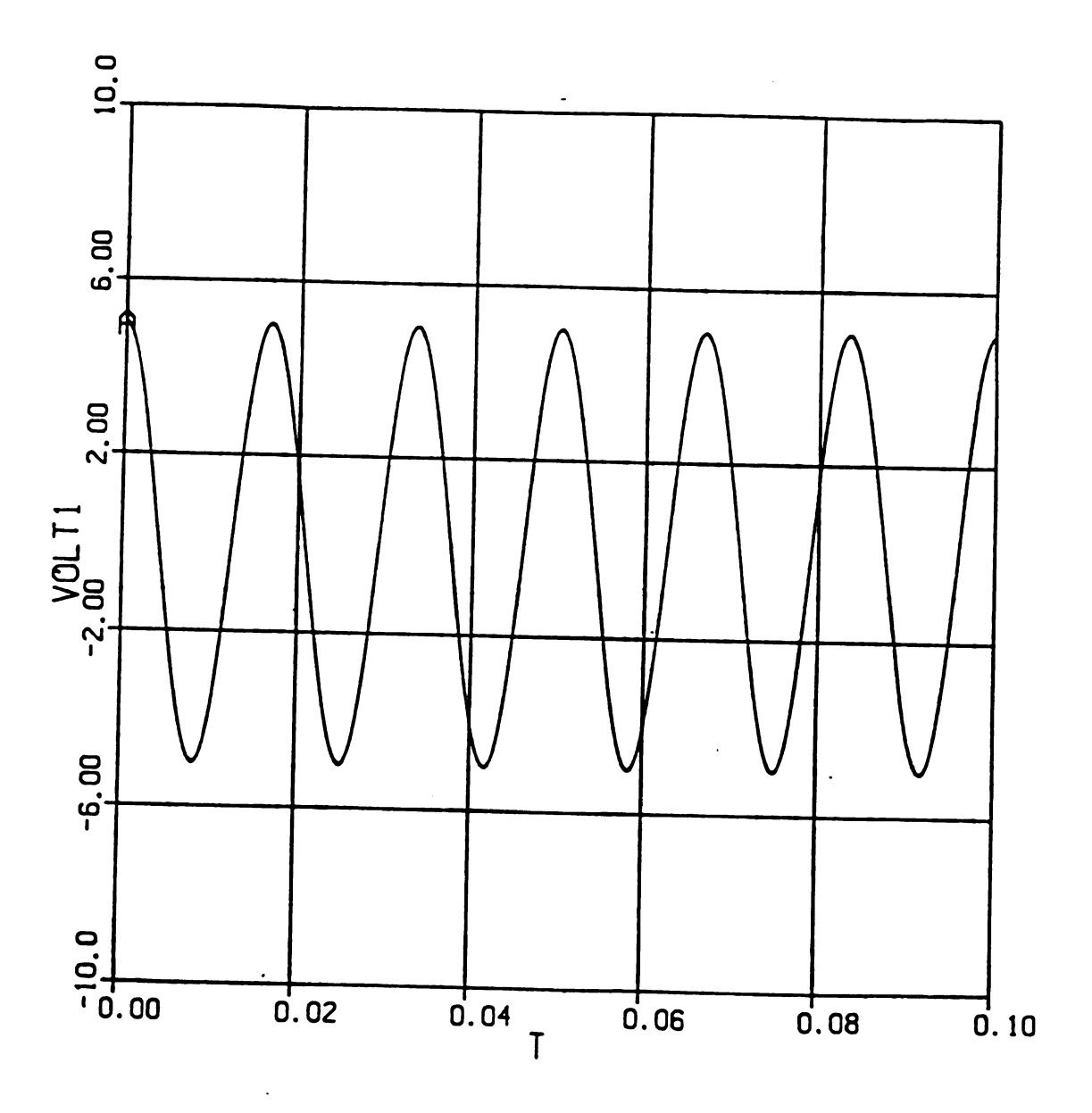


Figure 20. Applied Voltage

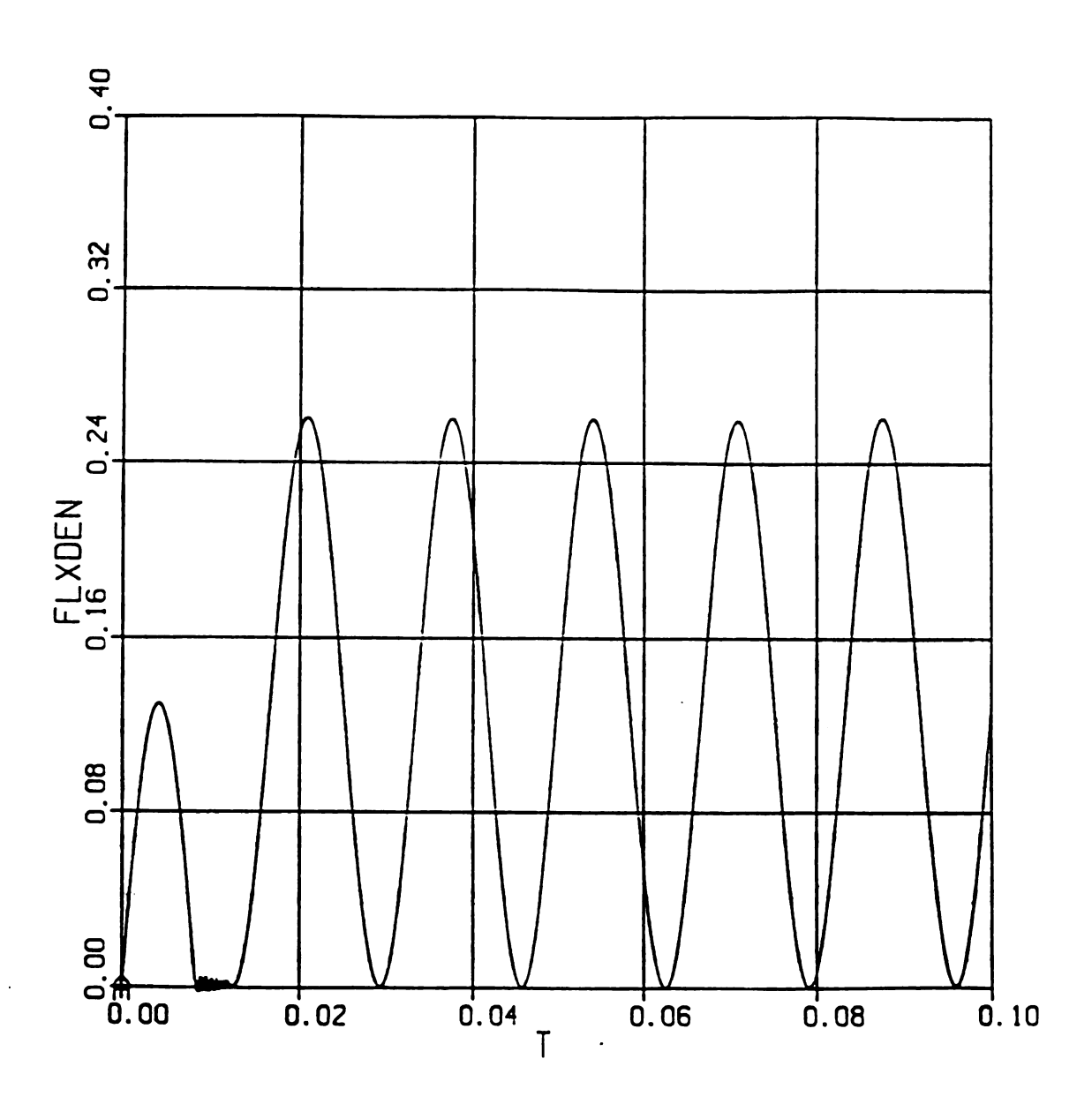


Figure 23. Flux density of the model for case 1.

·			
		•	

### 5.4.2 CASE 2: SINUSOIDAL INPUT AND INDUCTIVE LOAD

In this case, the model is connected to an inductive load. The value of the inductance of the load is 0.01 H., and of the resistance is 3  $\Omega$ . A 0.3  $\Omega$  resistance is connected to to the primary winding resistance in series. The maximum value of the applied voltage to the primary is 5 volts with 60 Hz. frequency. The results of the finite element method and the ACSL are given below.

### 5.4.2.1 THE RESULTS OF THE FINITE ELEMENT METHOD FOR CASE 2.

In this subsection, the plots of the primary current and secondary current of the model are given in figure 25 and figure 26 in response of the applied voltage shown in figure 24 for the load condition stated above. The essence of this experiment would be that the external inductances together with the derivative of the currents can be included in the finite element method. The absolute flux density for each element is calculated in the finite element method. Therefore, the plot of the flux density of the 166th element is given in figure 27. The induced voltage of the primary and secondary plots together with the reluctivity of the 166 th element are given in figure 28 and 29 and figure 30. The difference between these induced voltages is the voltage drop because of the leakage inductances and the resistances of the windings.

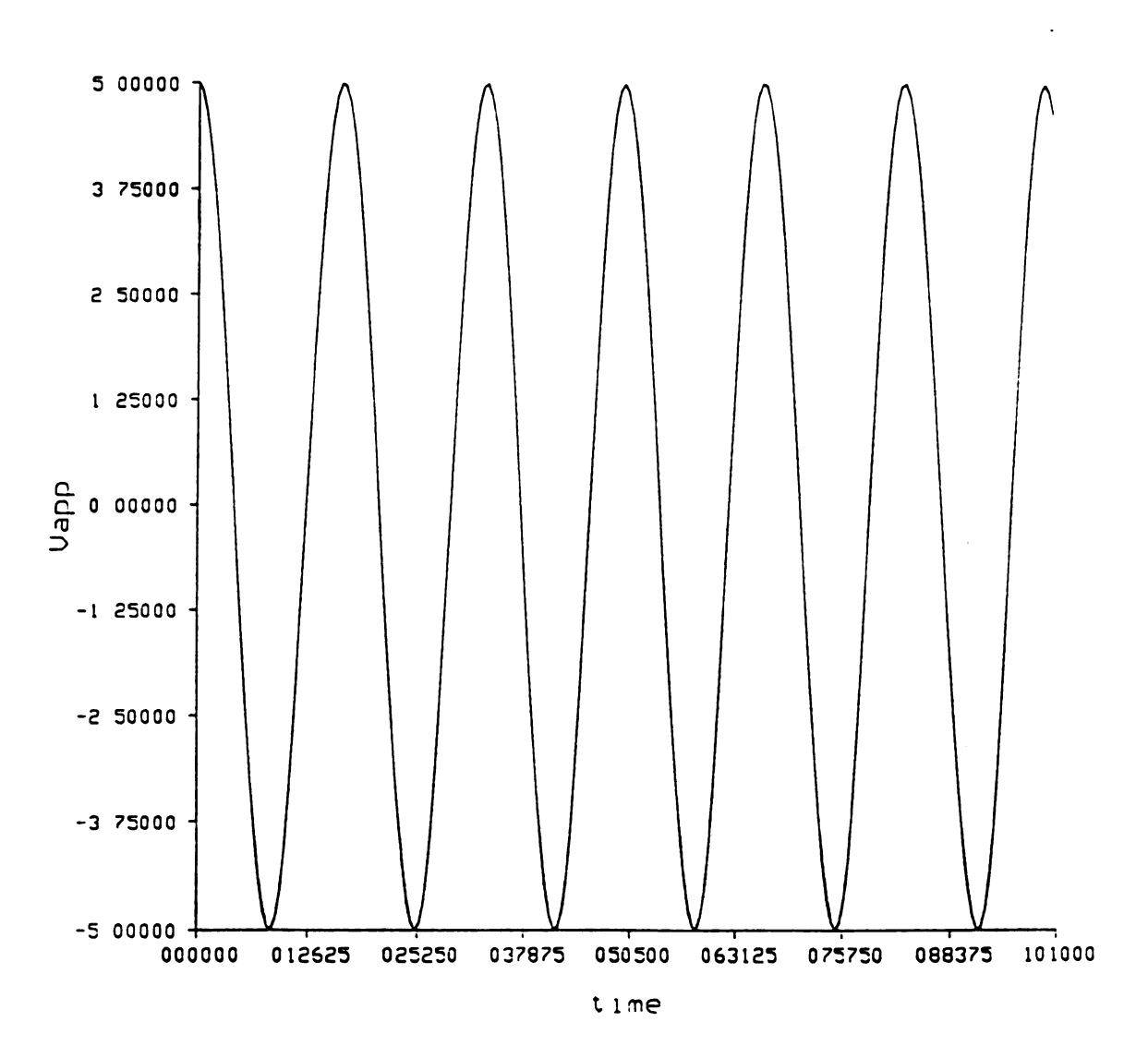


Figure 24. Applied voltage for the second case.

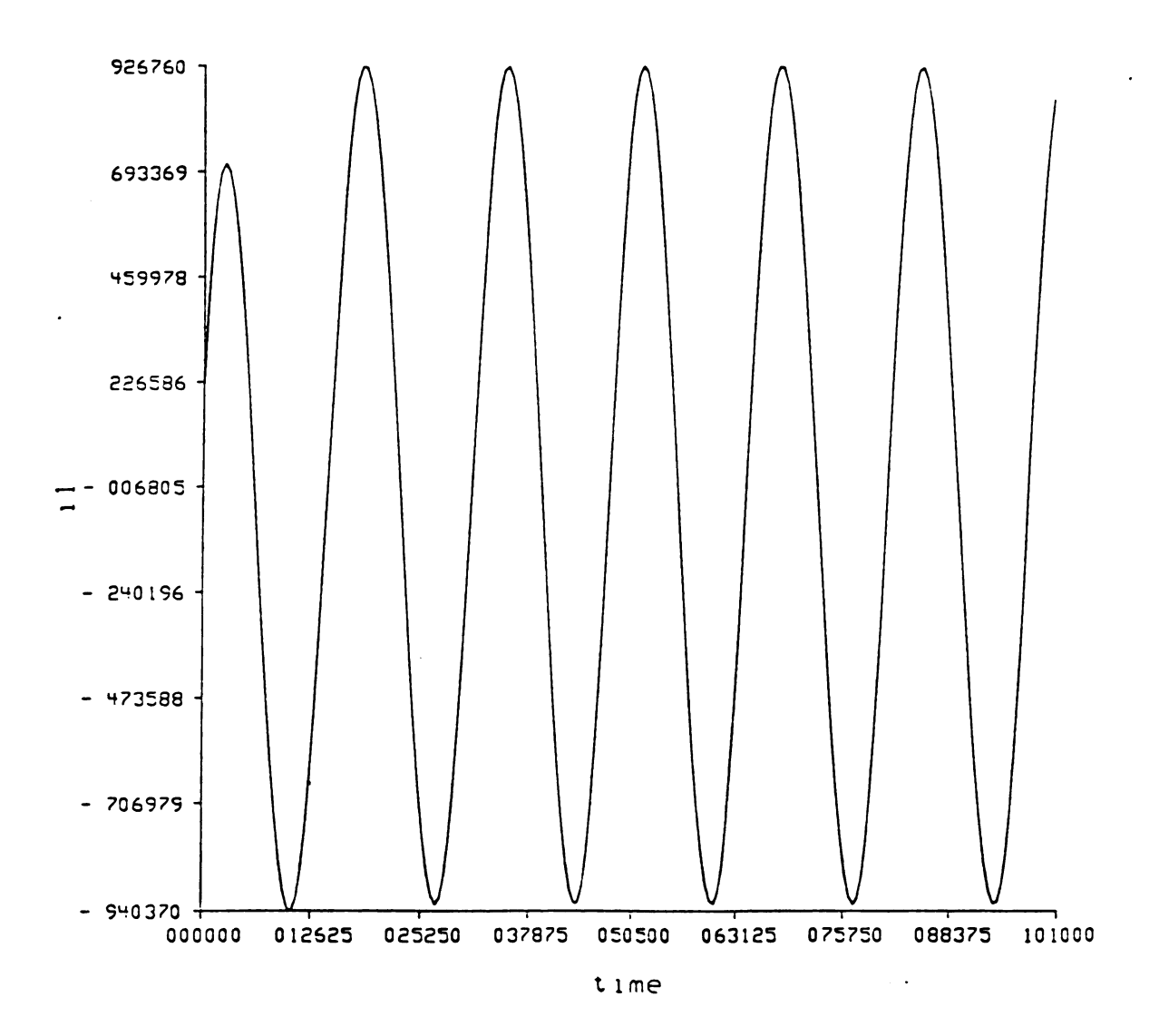


Figure 25. Primary current of the model connected to inductive load.

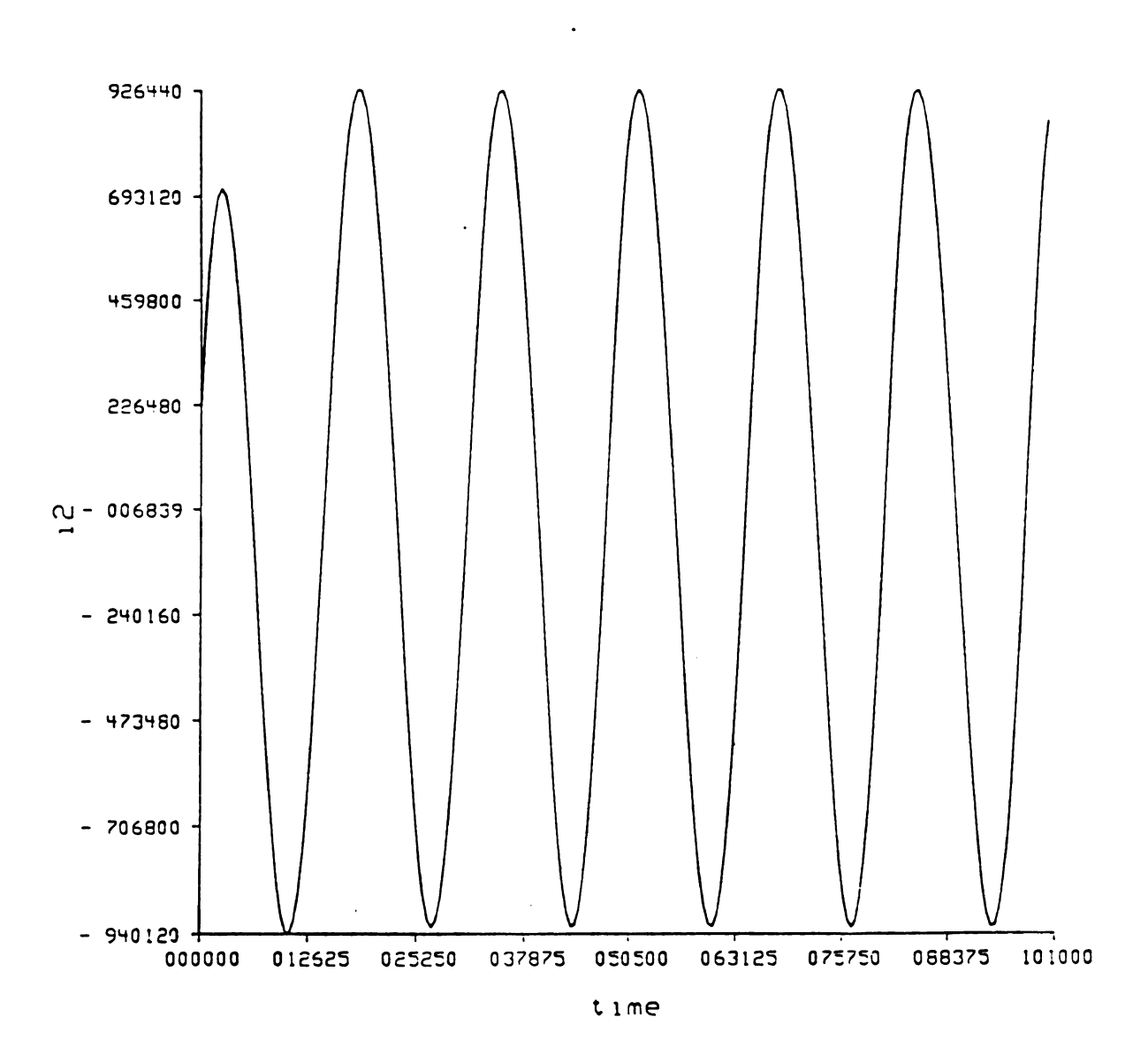


Figure 26. Secondary current of the model connected to inductive load.

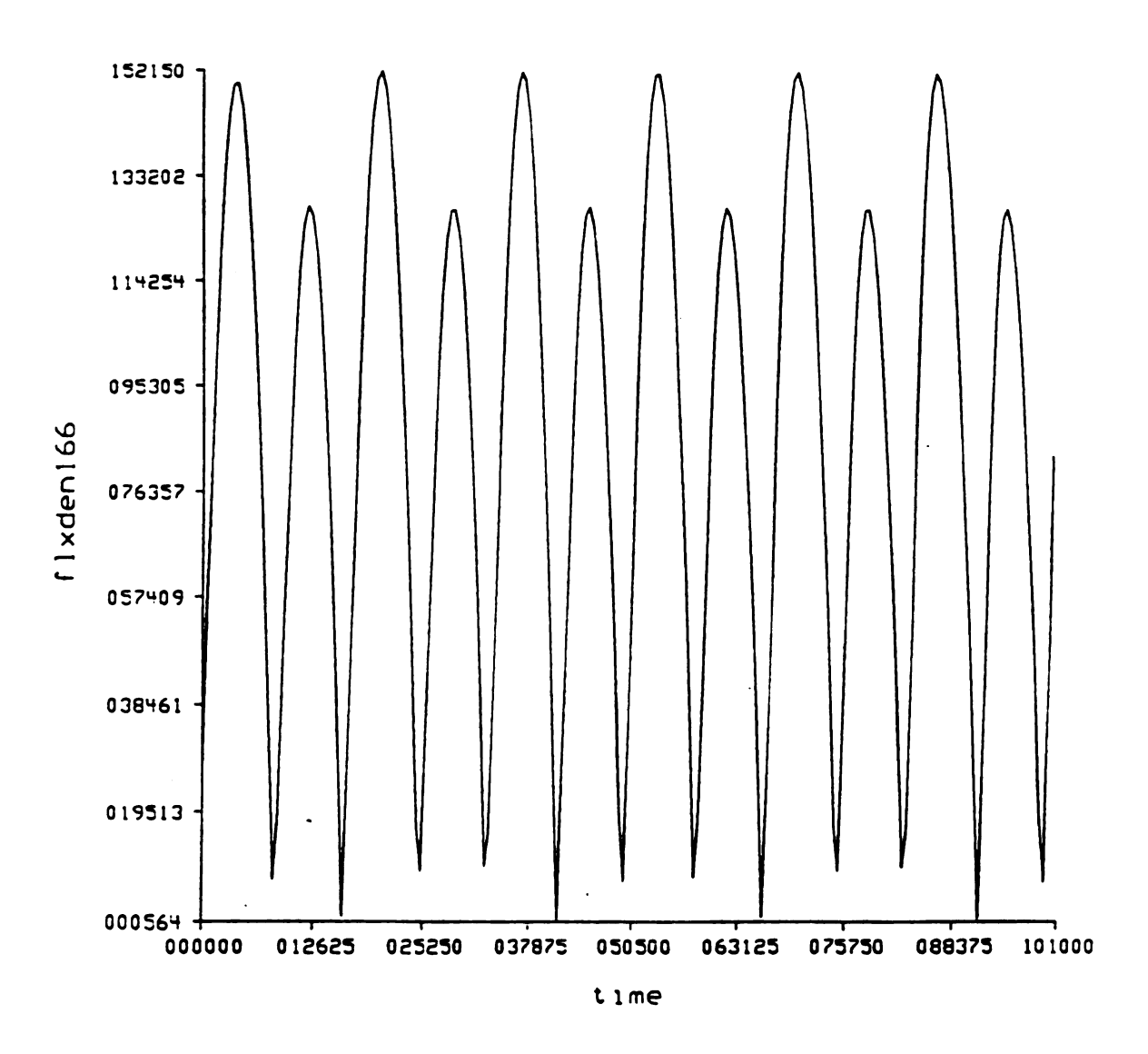


Figure 27. Flux density of the 166th element for case 2.

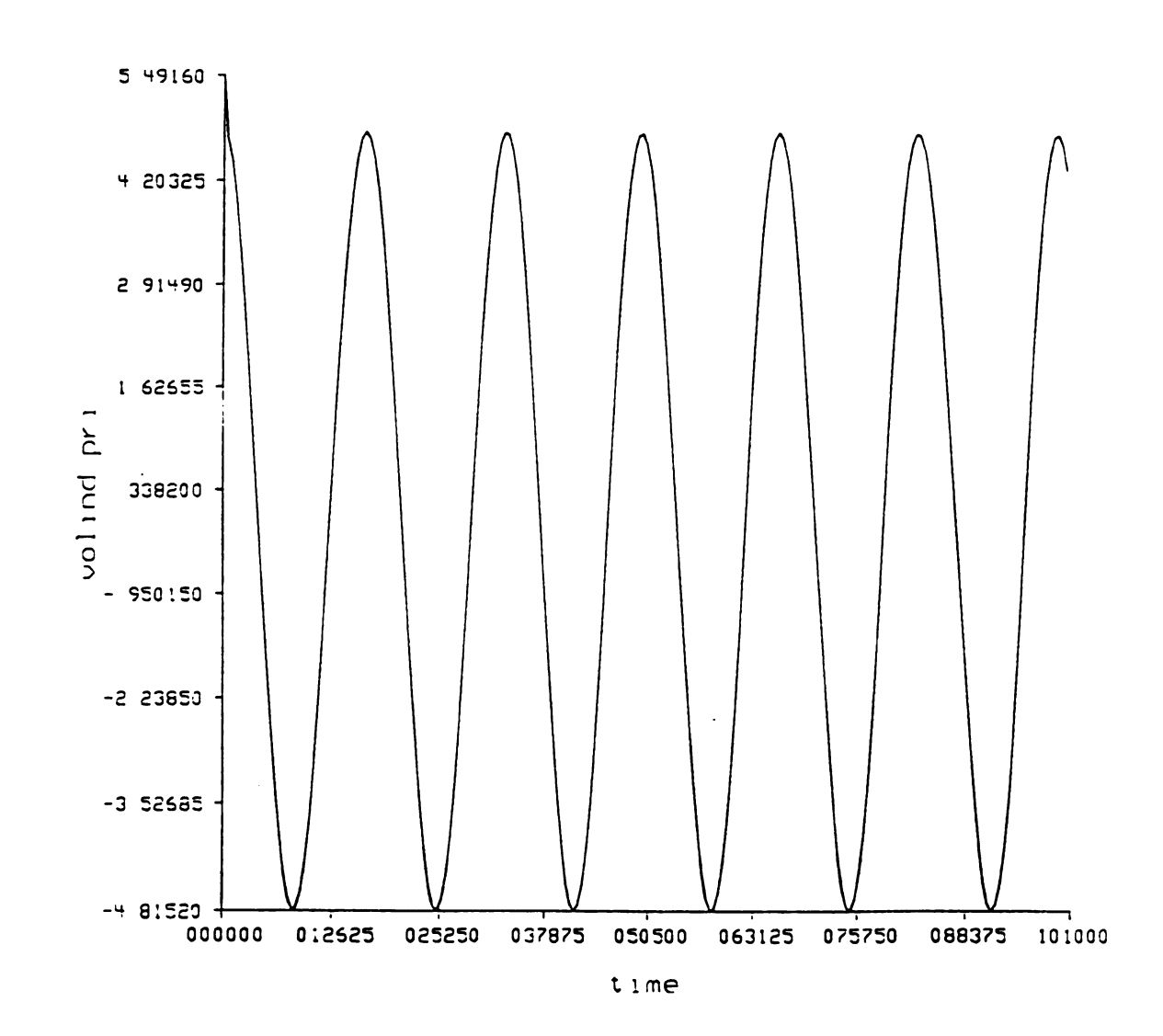


Figure 28. Induced voltage in the primary windings for case 2.

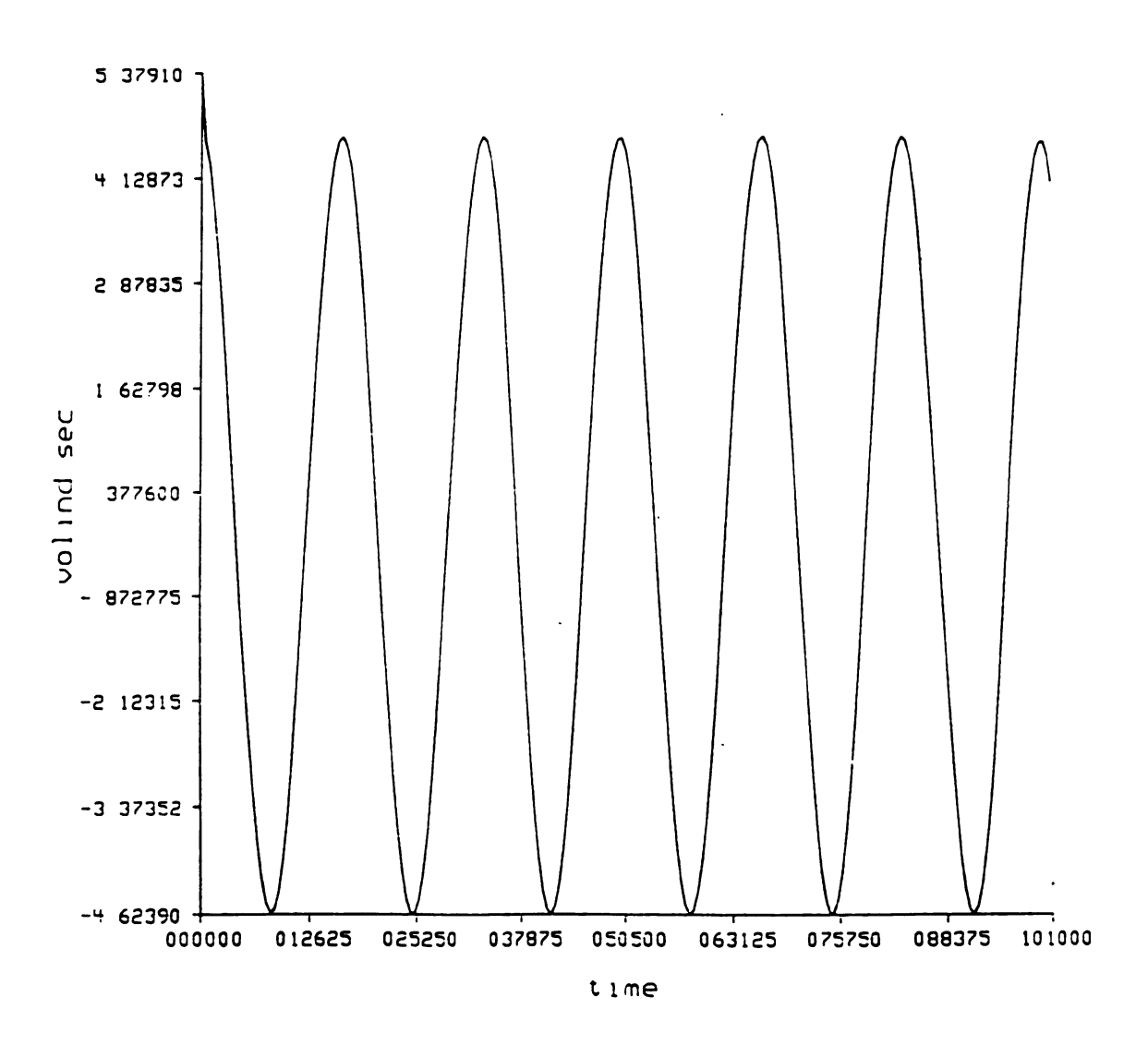


Figure 29. Induced voltage in the secondary windings for case 2.

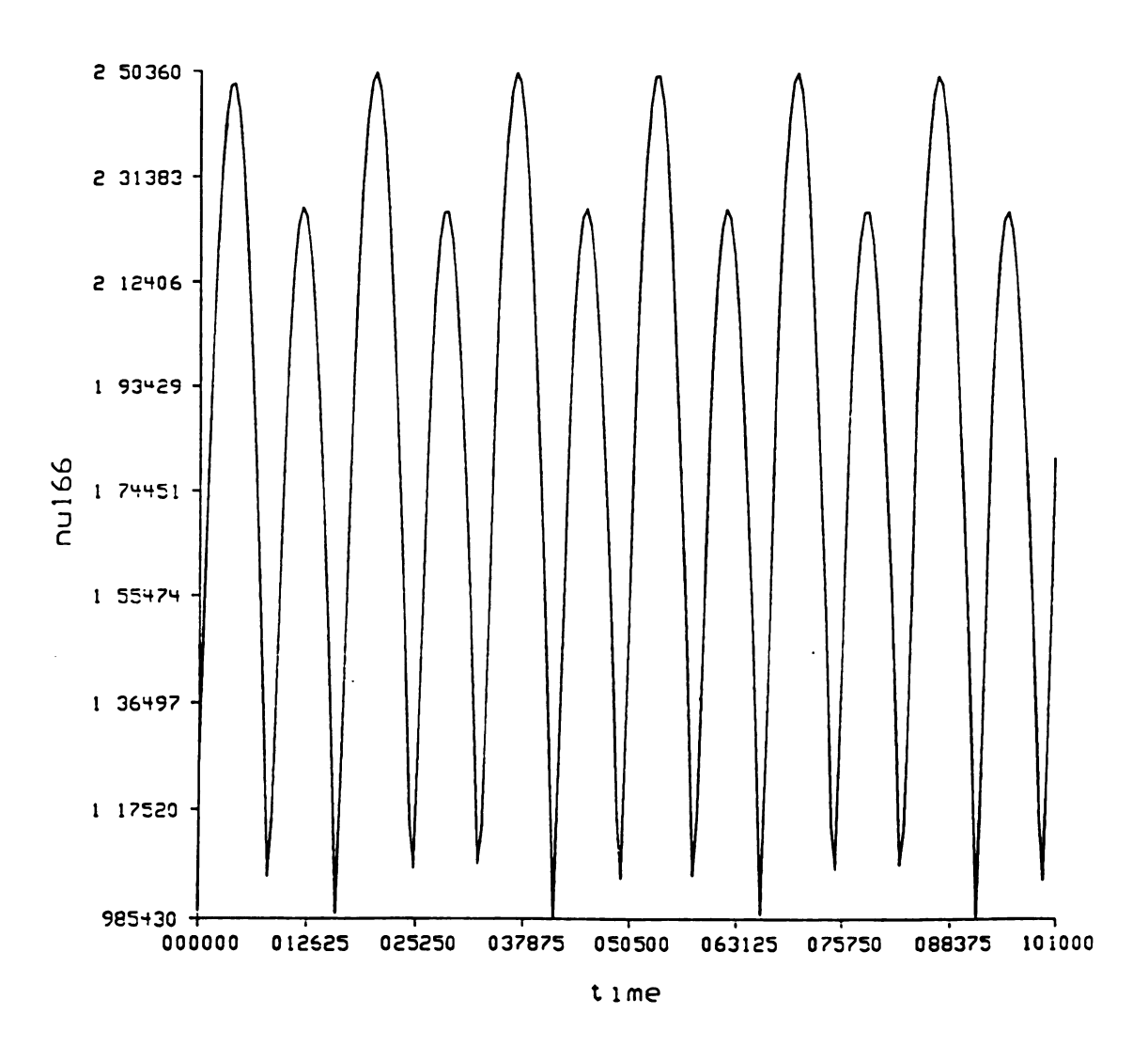


Figure 30. The reluctivity (inverse of the permeability) of the 166th element for case 2.

### 5.4.2.2 THE RESULTS OF THE ACSL FOR CASE 2

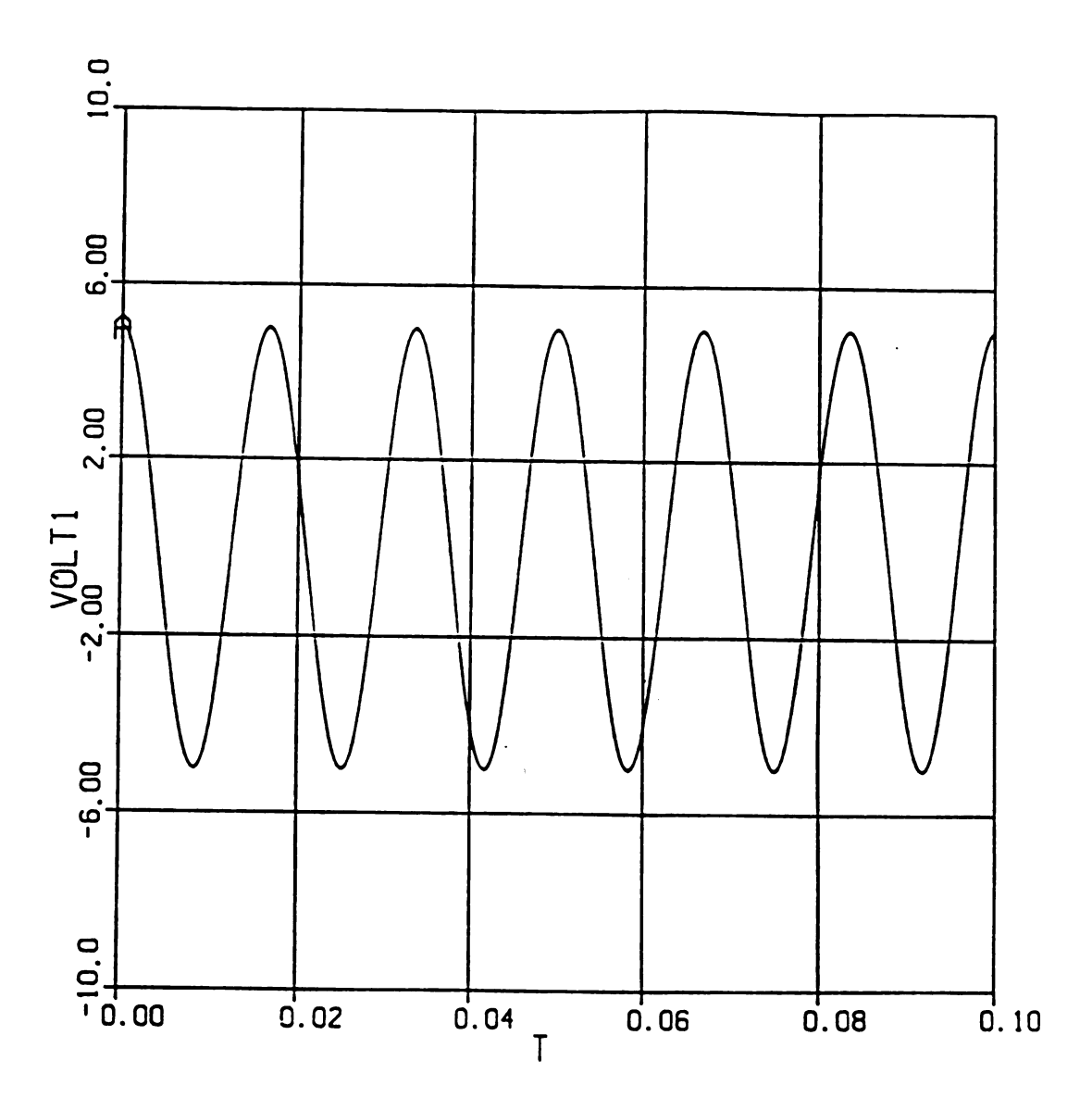


Figure 31. Applied Voltage for case 2.

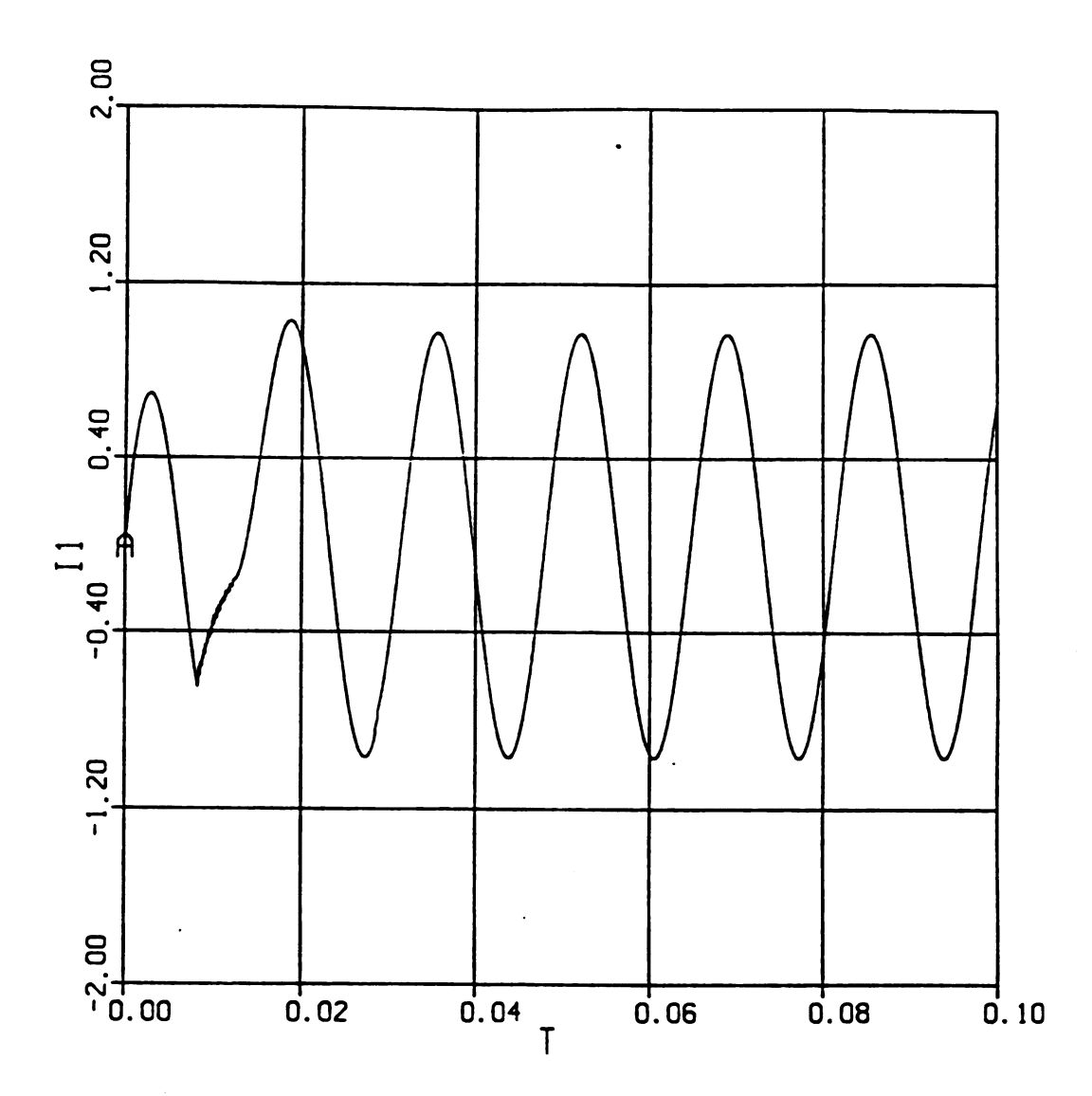


Figure 32. Primary current of the model connected to inductive load.

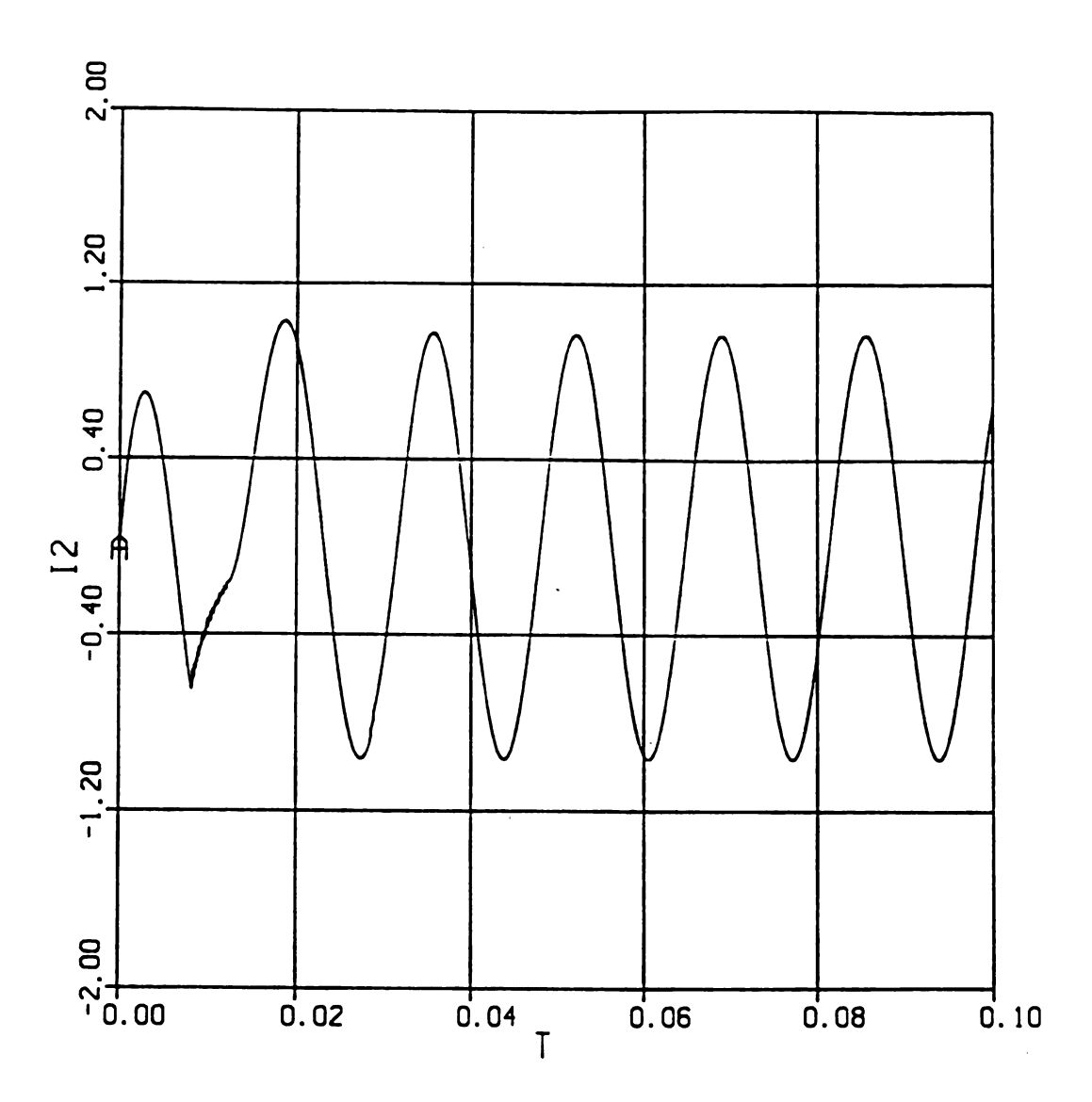


Figure 33. Secondary current of the model connected to inductive load.

## 5.4.3 CASE 3: SINUSOIDAL INPUT AND RESISTIVE LOAD WITH A ONE-WAY RECTIFIER CIRCUIT

In this case, the model is connected to a one-way rectifier circuit together with a resistive load of is 3  $\Omega$ . At the same time, 0.3  $\Omega$  resistance is connected to the primary winding resistance in series. The maximum value of the applied voltage to the primary is 5 volts with 60 Hz. frequency.

#### 5.4.3.1 THE RESULTS OF THE FINITE ELEMENT METHOD FOR CASE 3.

In this subsection, the plots of the primary and secondary current of the model are given in figure 36 and figure 37 in response of the applied voltage shown in figure 35 for the load conditions stated above. It should be noted in the current plots that the currents do not go to zero directly when a diode is connected to the secondary because of the inductances in the windings. The absolute flux density for each elements is calculated in the finite element method. Therefore, the plot of the flux density of the 166th element is given in figure 38. The steady flux increase of this experiment is because saturation is not included well into the finite element method. It should be stated that the flux density increase of the finite element method is in the cases where the average flux density do not sum up the zero. The plots of the induced voltage of the primary and secondary plots together with the reluctivity are given in figure 39, figure 40 and figure 41. The difference between the induced voltages is the voltage drop because of the leakage inductances and the resistances of the windings.

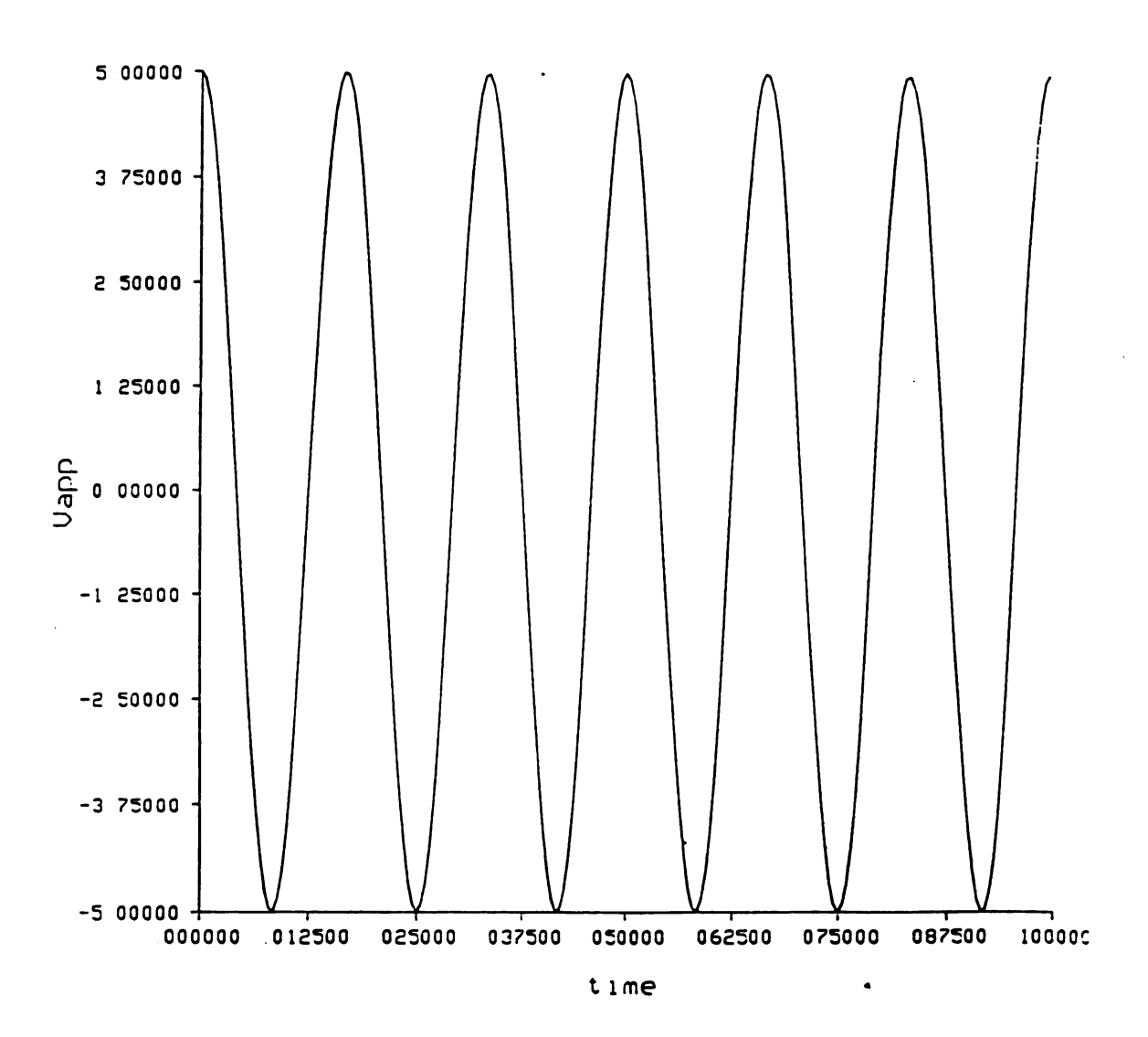


Figure 35. Applied voltage for the third case.

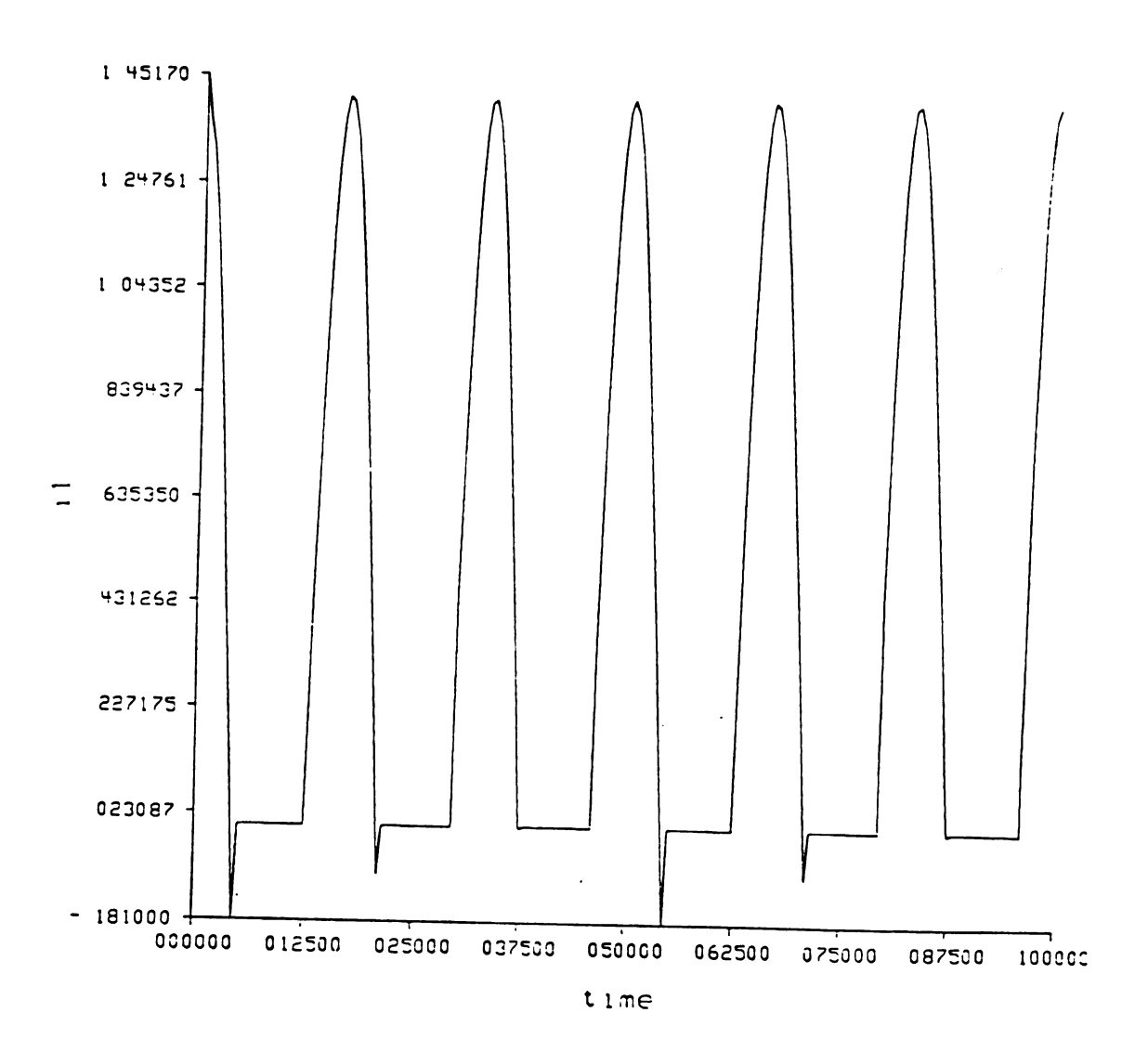


Figure 36. Primary current of the model connected to a one-way rectifier circuit together with a resistive load.

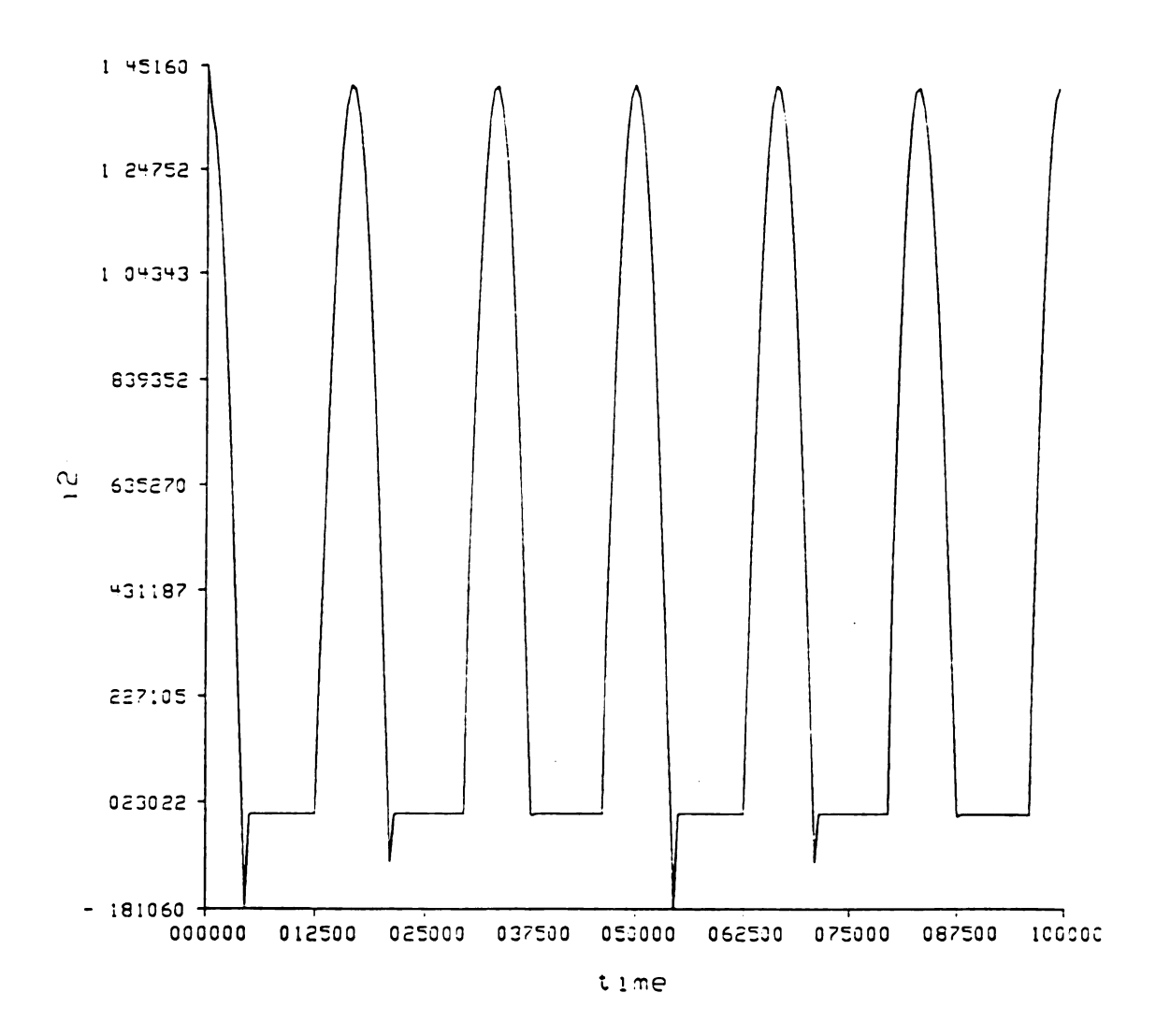


Figure 37. Secondary current of the model connected to a one-way rectifier circuit together with resistive load.

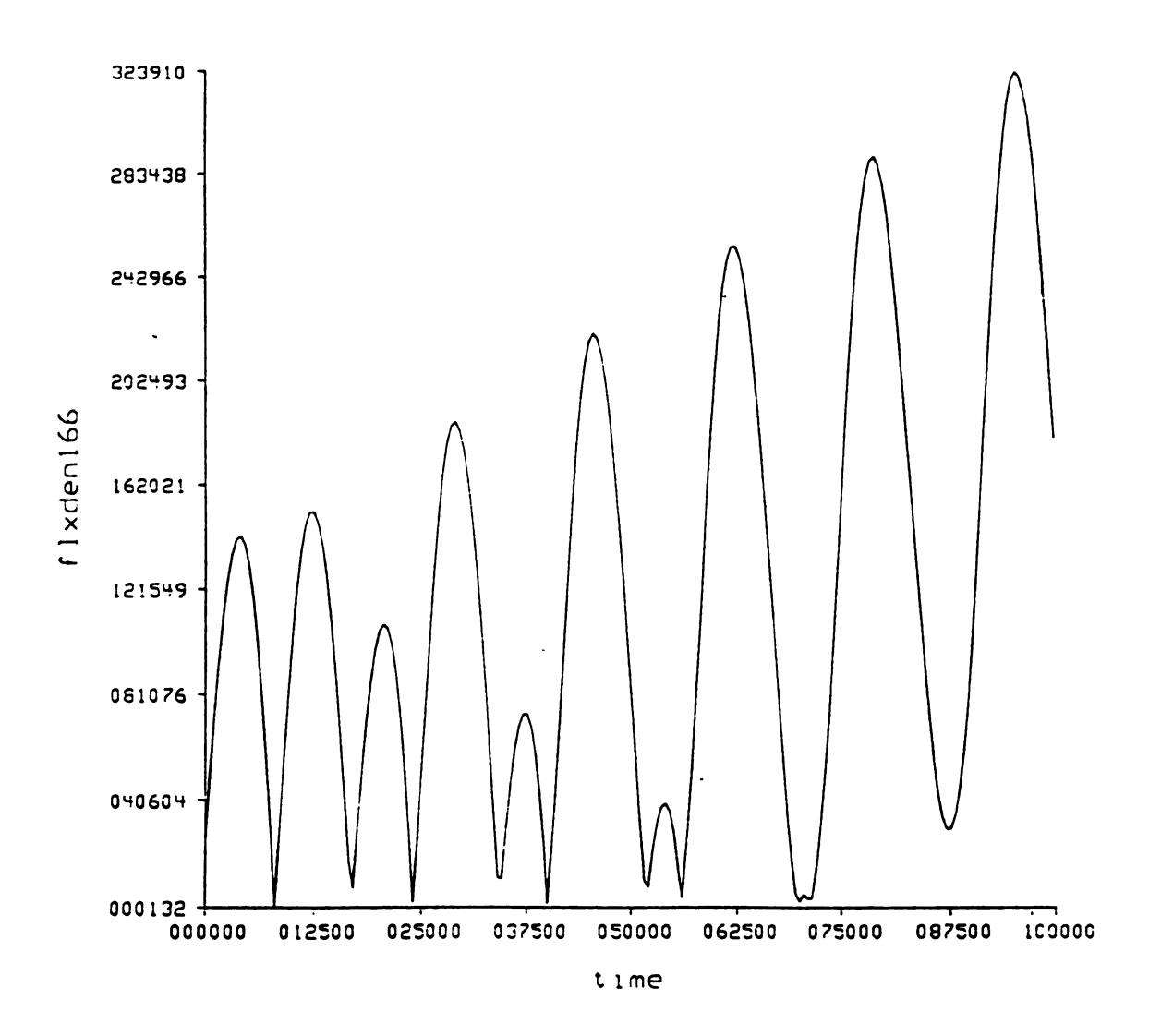


Figure 38. Flux density of the 166th element for case 3.

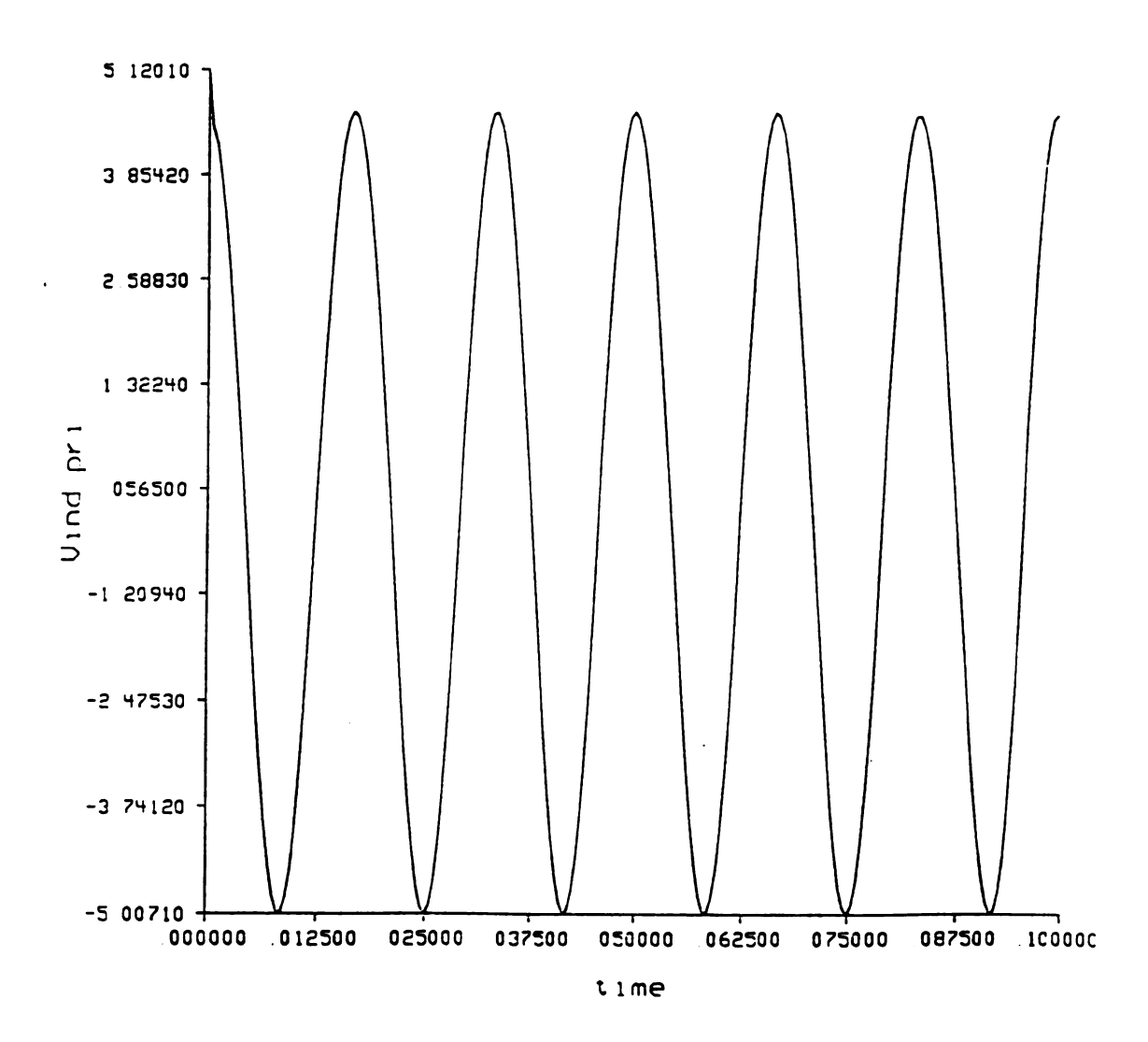


Figure 39. Induced voltage in the primary windings for case 3.

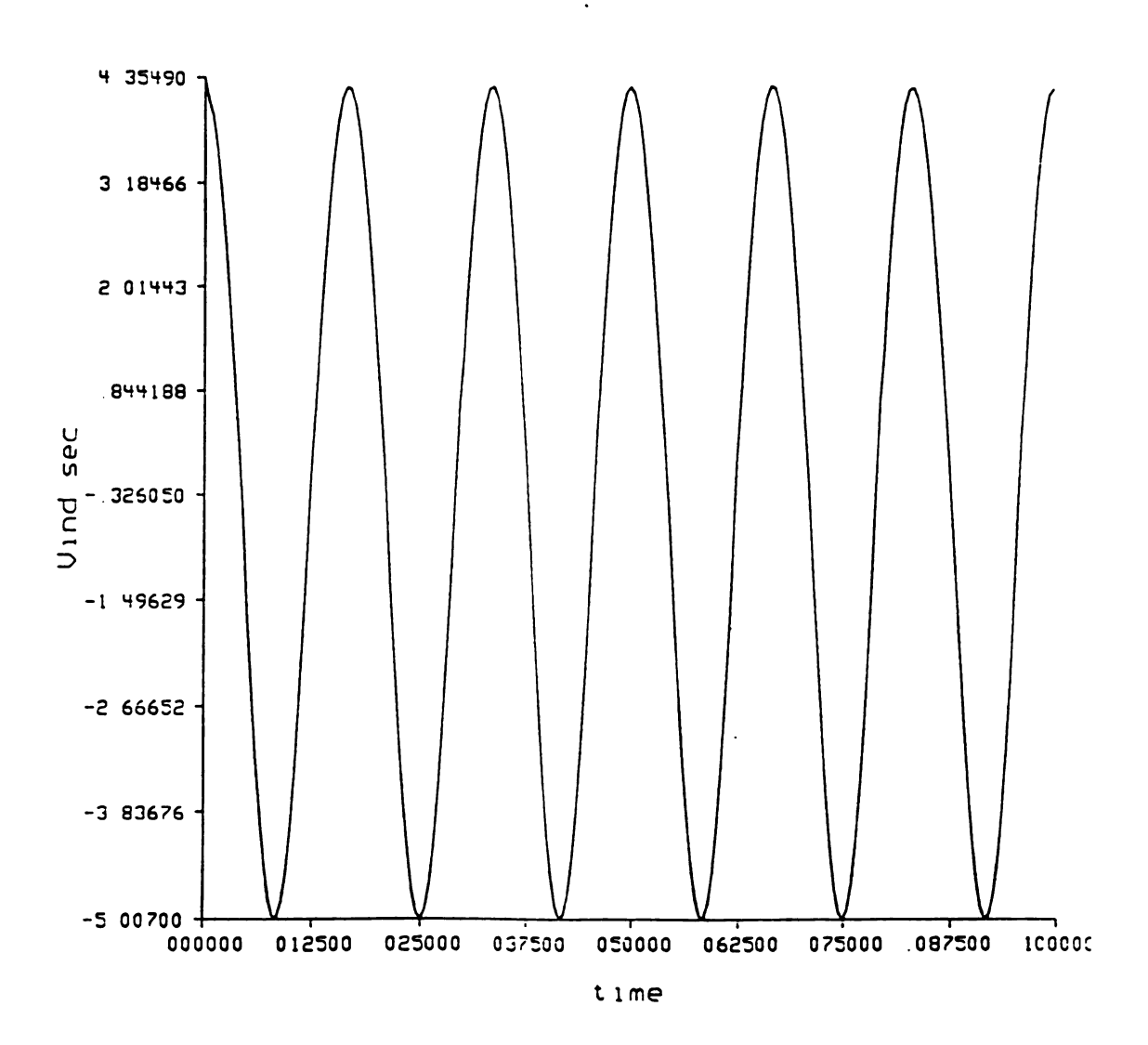


Figure 40. Induced voltage in the secondary windings for case 3.

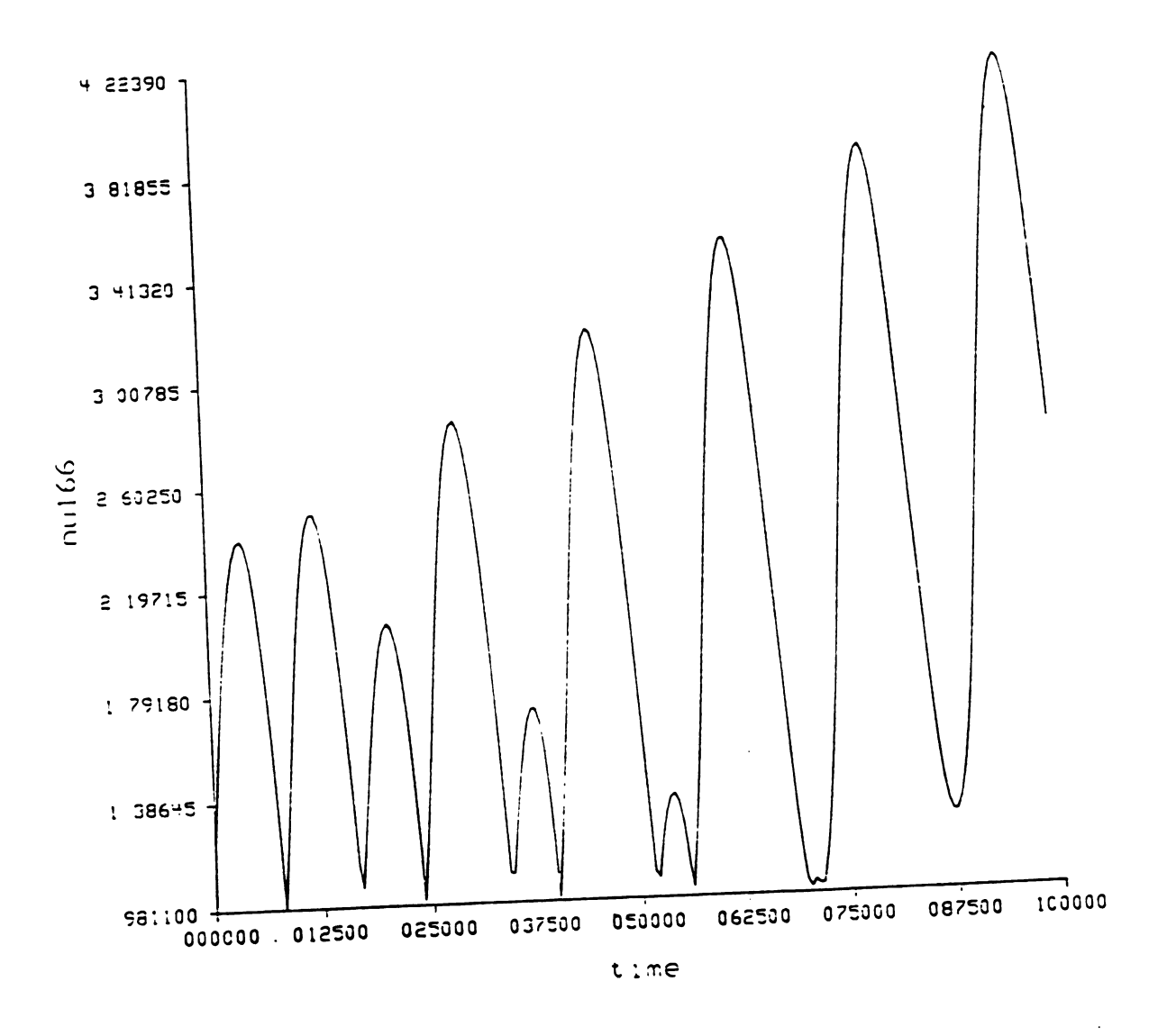


Figure 41. The reluctivity (inverse of the permeability) of the 166th element for case 3.

## 5.4.3.2 THE RESULTS OF THE ACSL FOR CASE 3

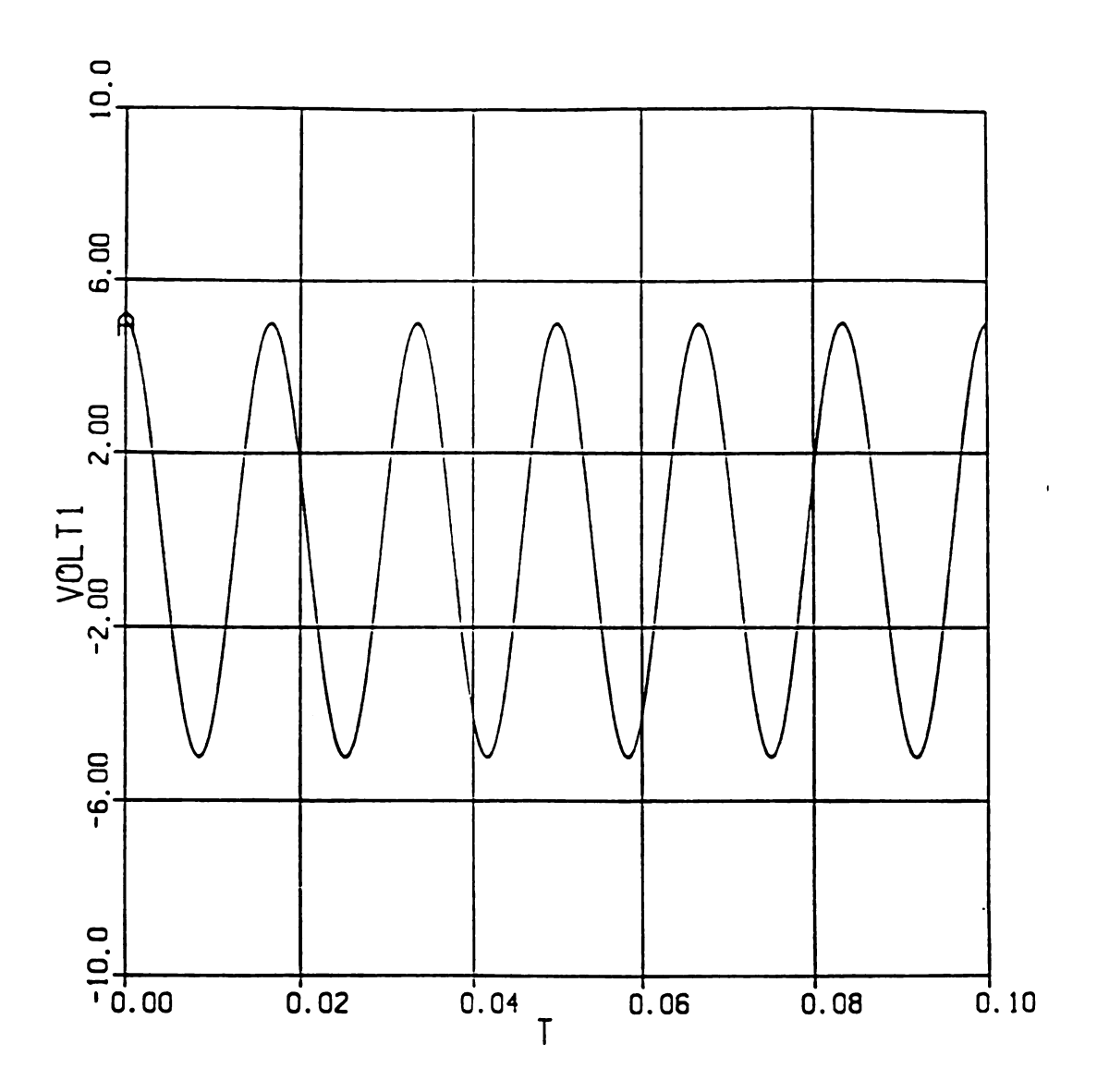


Figure 42. Applied Voltage for case 3.

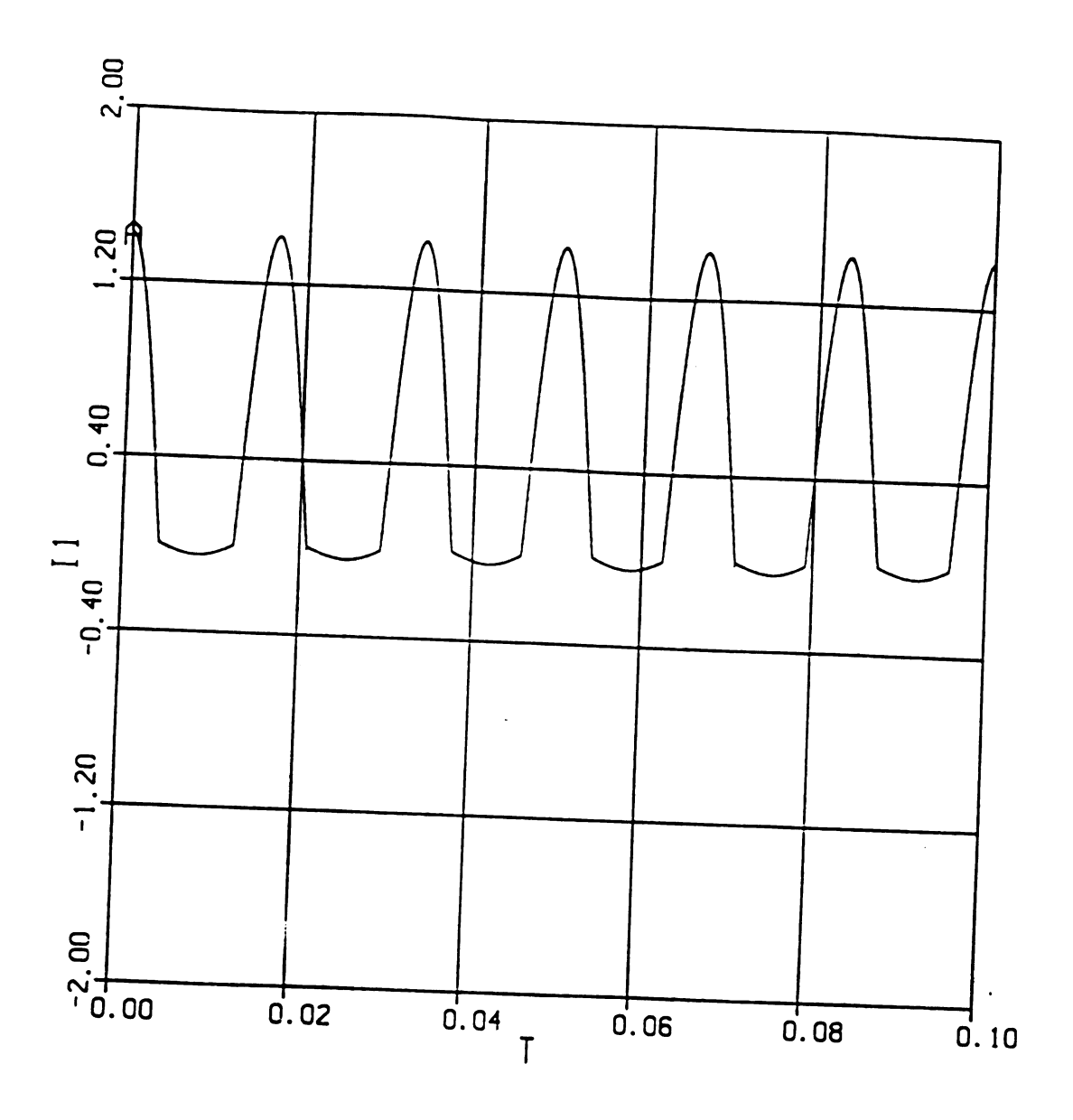


Figure 43. Primary current of the model connected to a one-way rectifier circuit together with a resistive load.

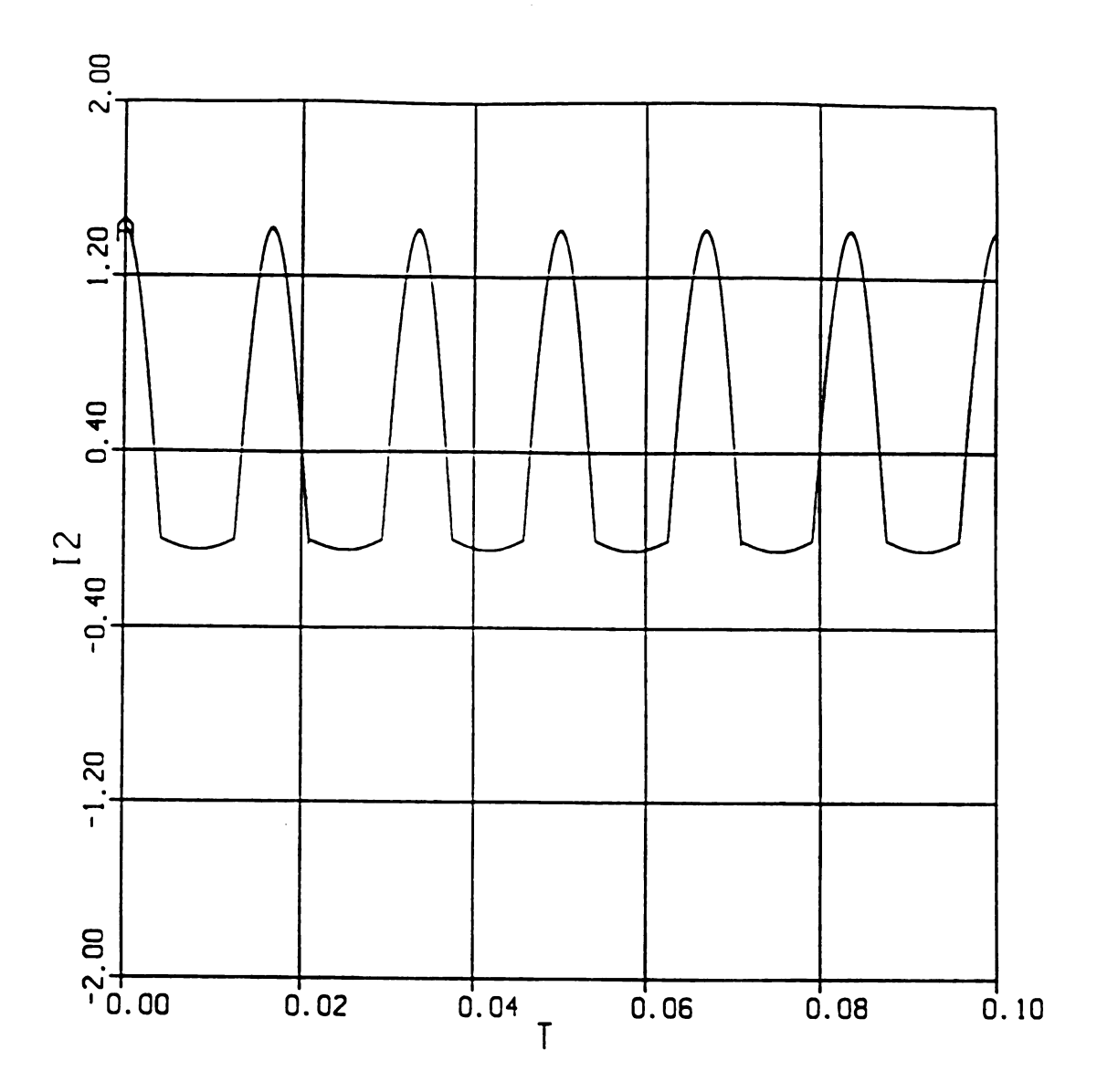


Figure 44. Secondary current of the model connected to a one-way rectifier circuit together with a resistive load.

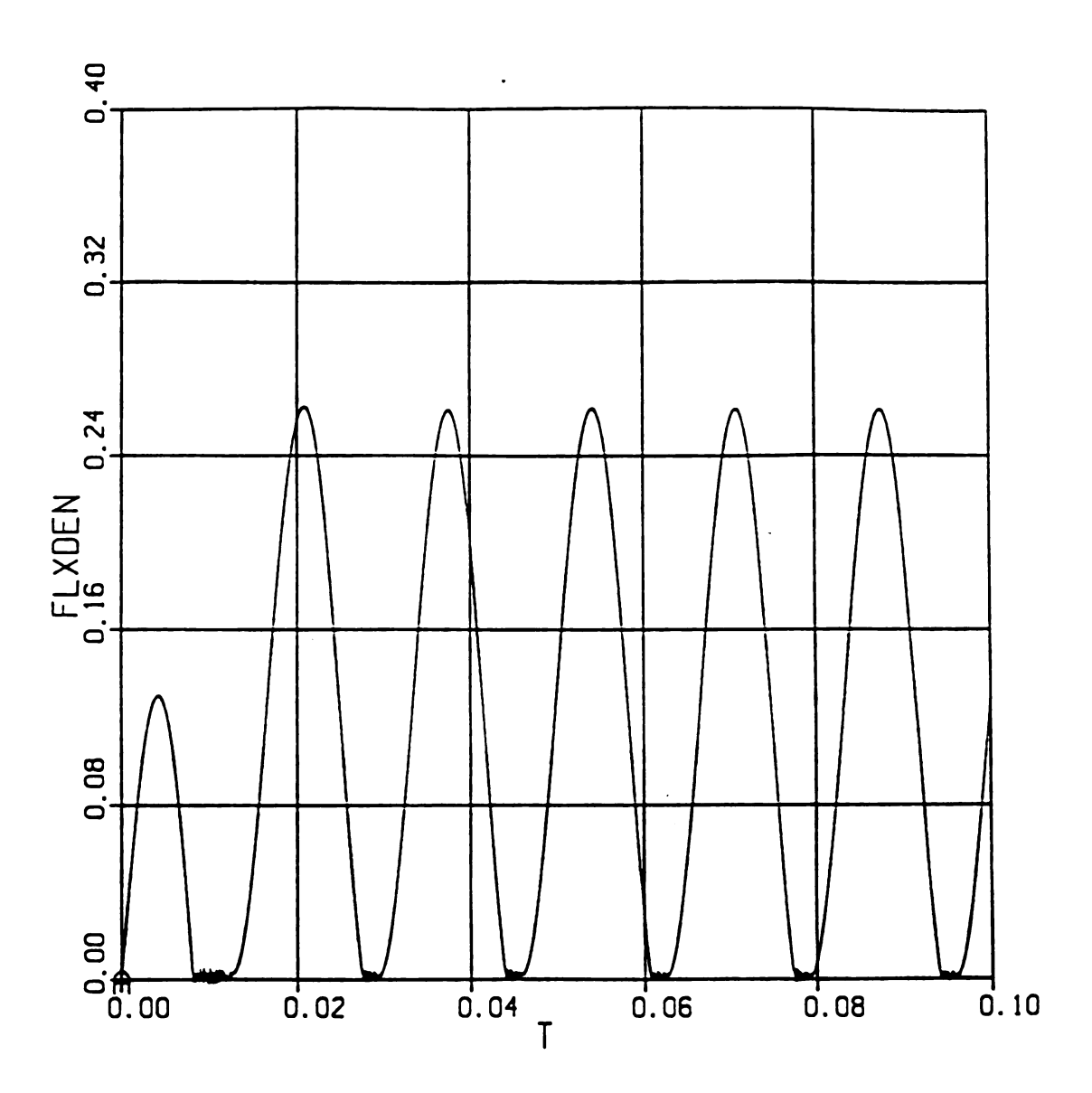


Figure 45. Flux density of the model for case 3.

# 5.4.4 CASE 4: SINUSOIDAL INPUT AND INDUCTIVE LOAD IN SERIES WITH A ONE-WAY RECTIFIER CIRCUIT

In this case, the model is connected to a one-way rectifier circuit together with an inductive load which has an inductance of 0.01 H. and a resistance of 3.0  $\Omega$ . At the same time, 0.3  $\Omega$  resistance is connected to to the primary winding resistance in series. The maximum value of the applied voltage to the primary is 5 volts with 60 Hz. frequency.

### 5.4.4.1 THE RESULTS OF THE FINITE ELEMENT METHOD FOR CASE 4.

In this subsection, the plots of the primary and secondary current of the model are given in figure 47 and 48 respectively in response of the applied voltage shown in figure 46 for the load conditions stated above. It should be noted in the current plots that the currents do not go to zero directly when a diode is connected to the secondary because of the inductances in the windings and the load. The absolute flux density for each element is calculated in this method. Therefore, the plot of the absolute flux density of the 166th element is given in figure 49. The steady flux increase of this experiment is because saturation is not included well into the finite element method. It should be stated that the flux density increase of the finite element method is in the cases where the average flux density do not sum up to zero. The plots of the induced voltage of the primary and secondary together with the reluctivity are given in figure 50, figure 51 and figure 52 respectively. The difference between these induced voltages is the voltage drop because of the leakage inductances and the resistances of the windings.

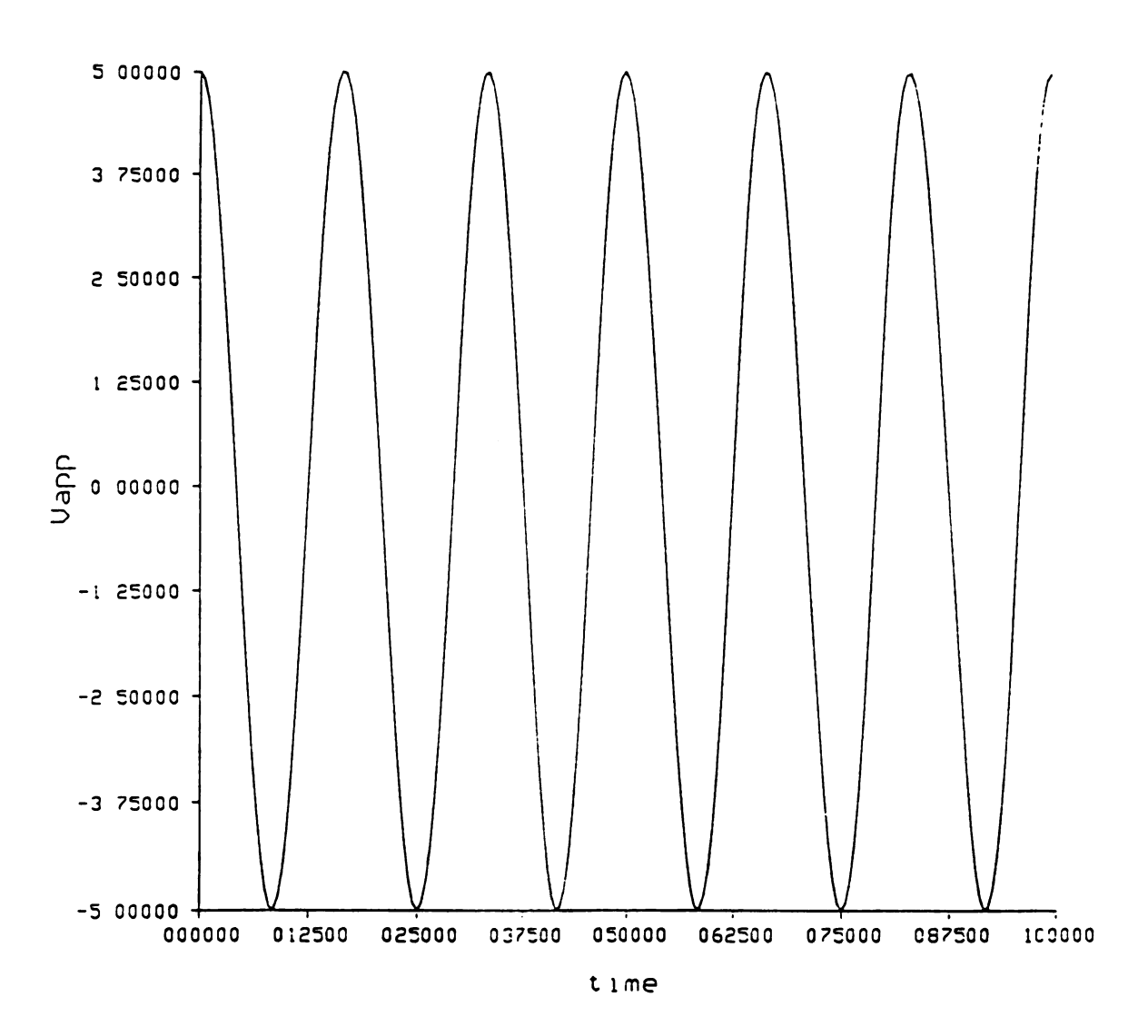


Figure 46. Applied voltage for the fourth case.

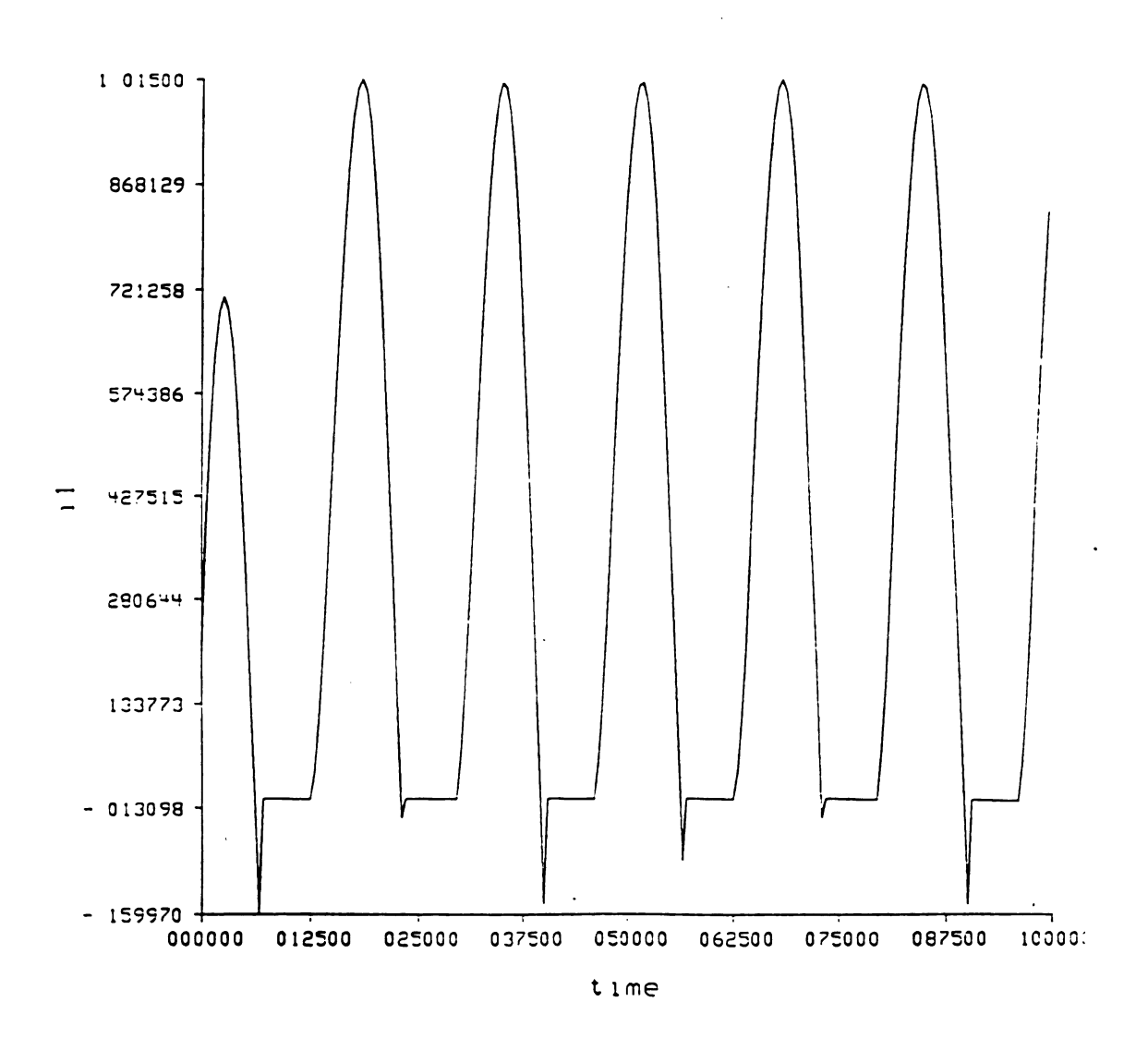


Figure 47. Primary current of the model connected to a one-way rectifier circuit together with inductive load.

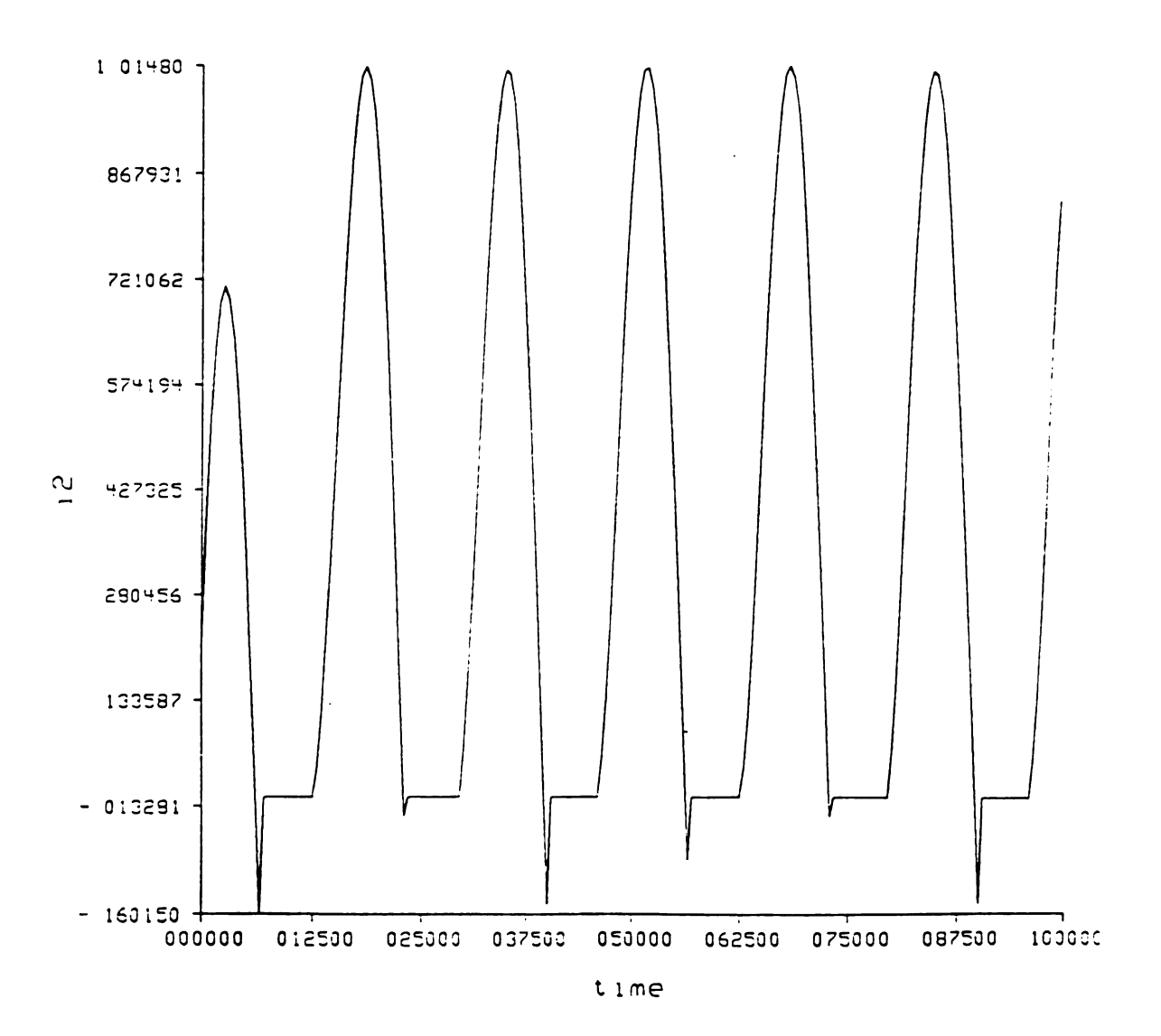


Figure 48. Secondary current of the model connected to a one-way rectifier circuit together with inductive load.

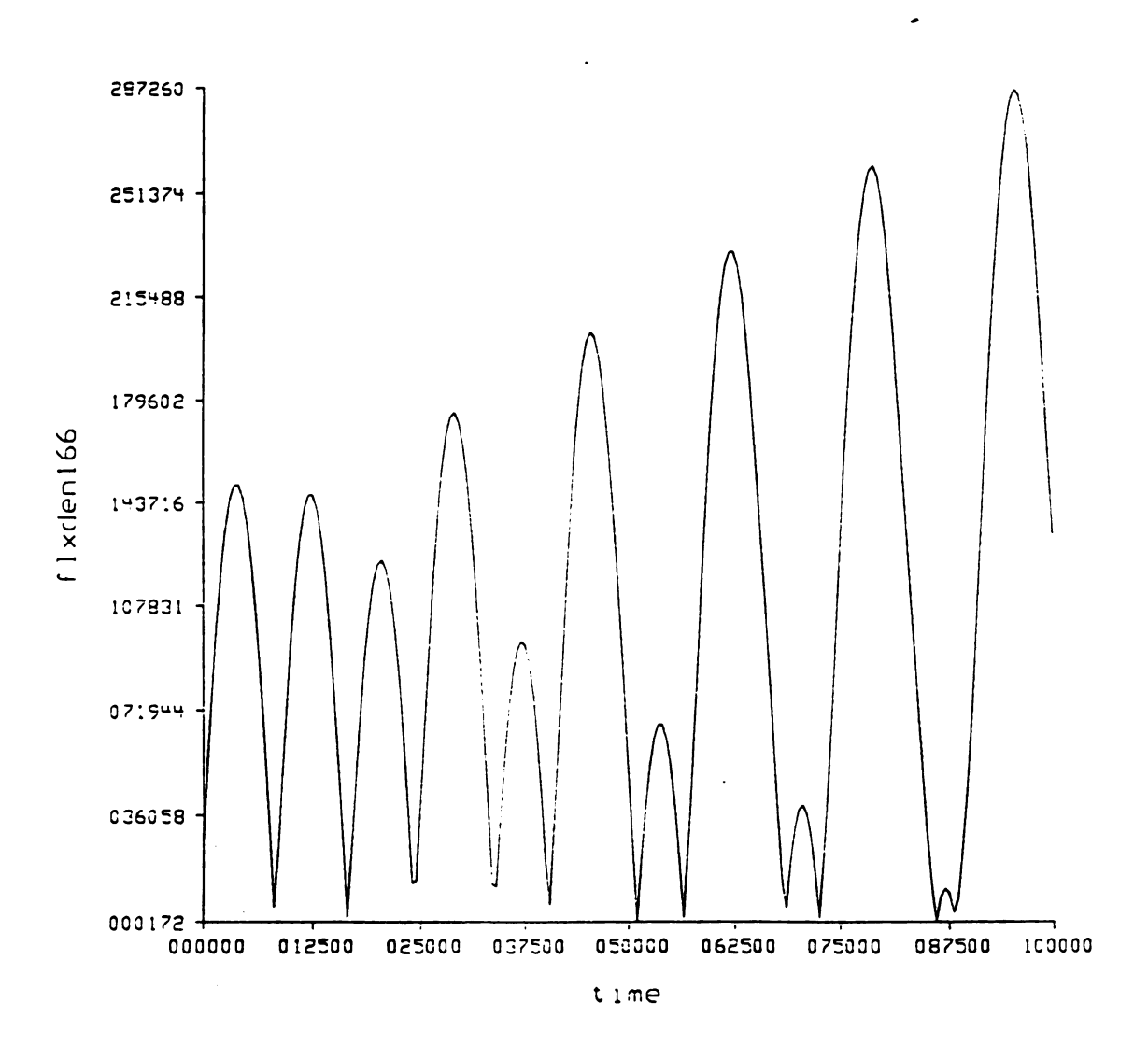


Figure 49. Flux density of the 166th element for case 4.

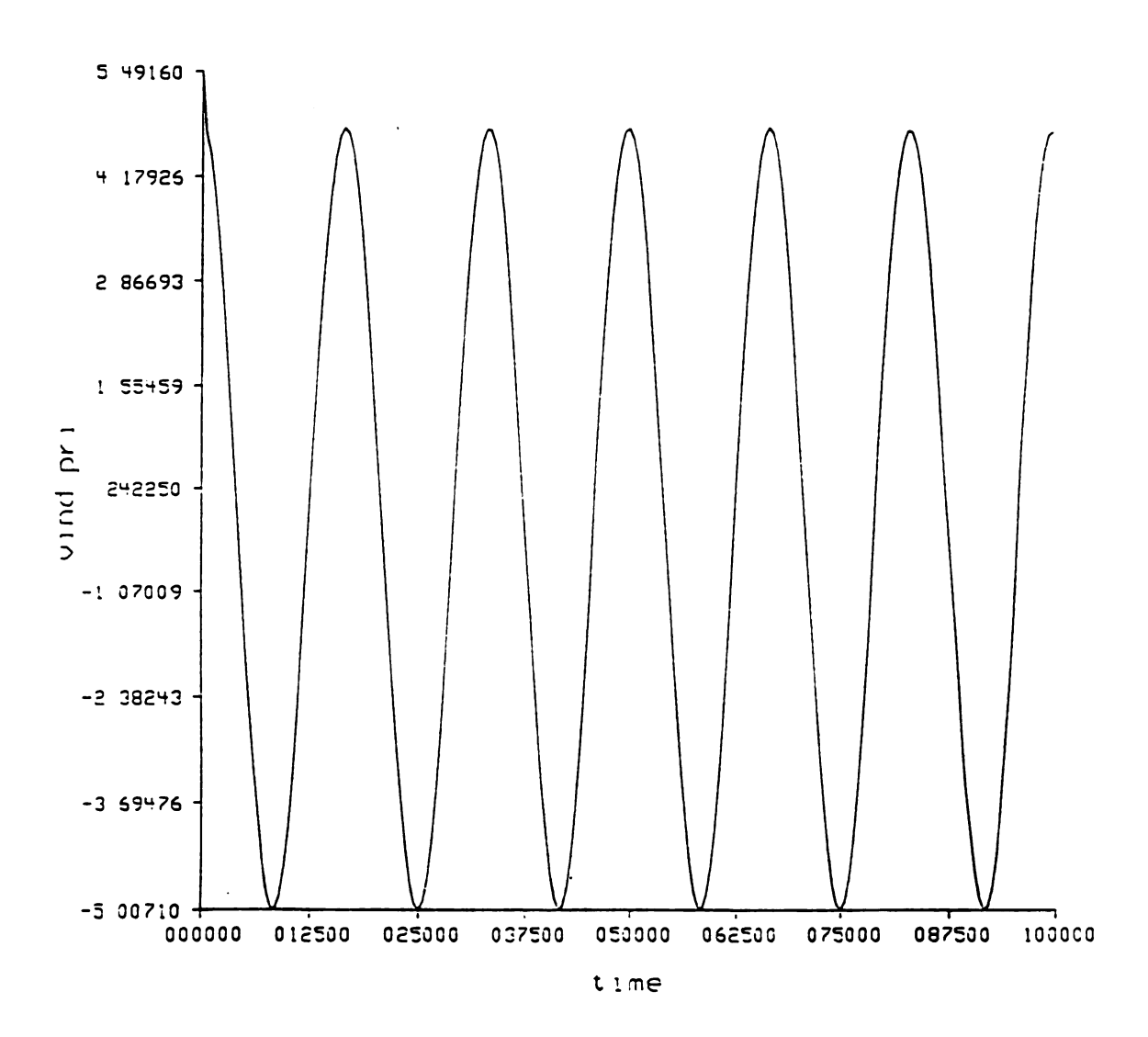


Figure 50. Induced voltage in the primary windings for case 4.

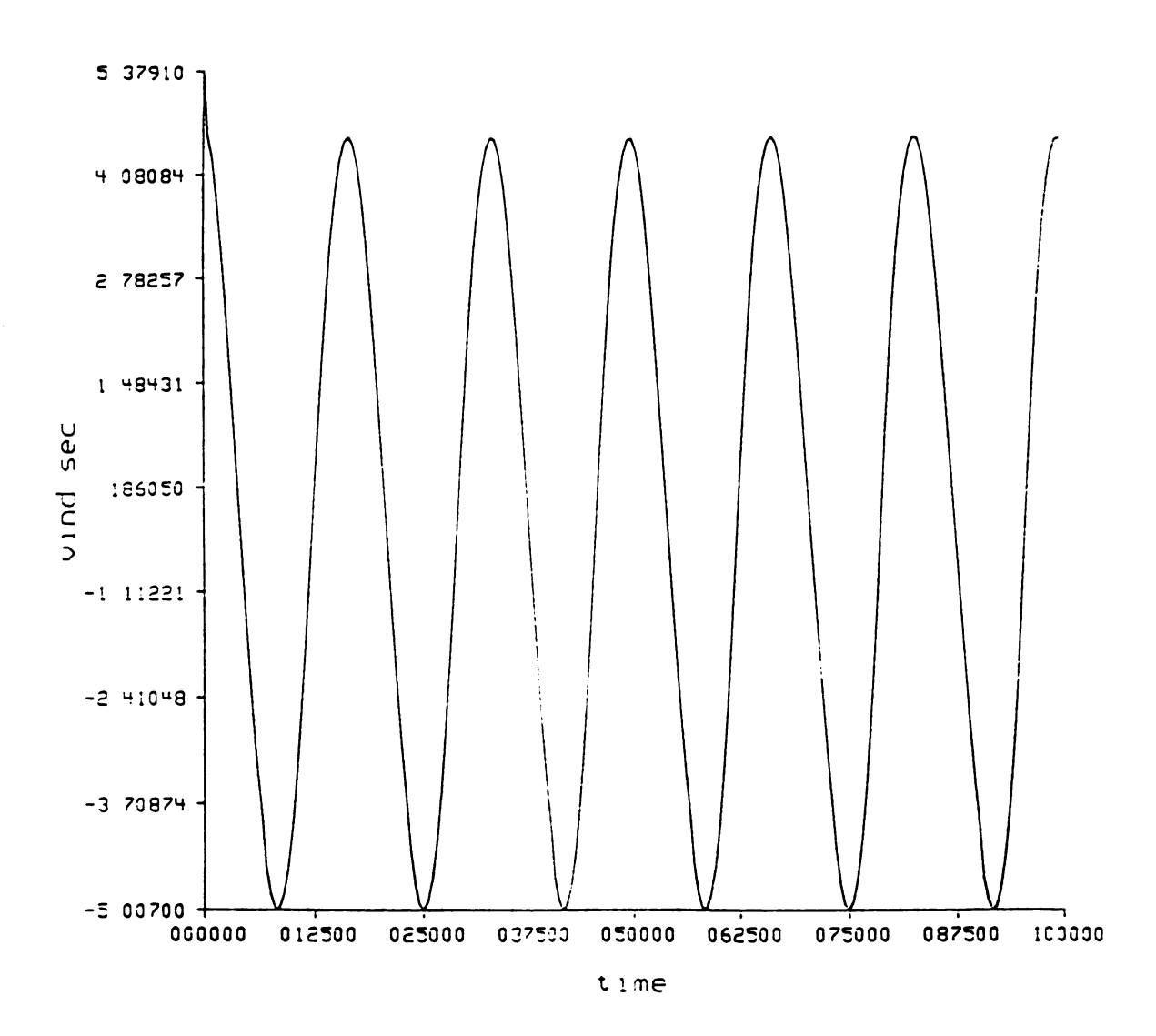


Figure 51. Induced voltage in the secondary windings for case 4.

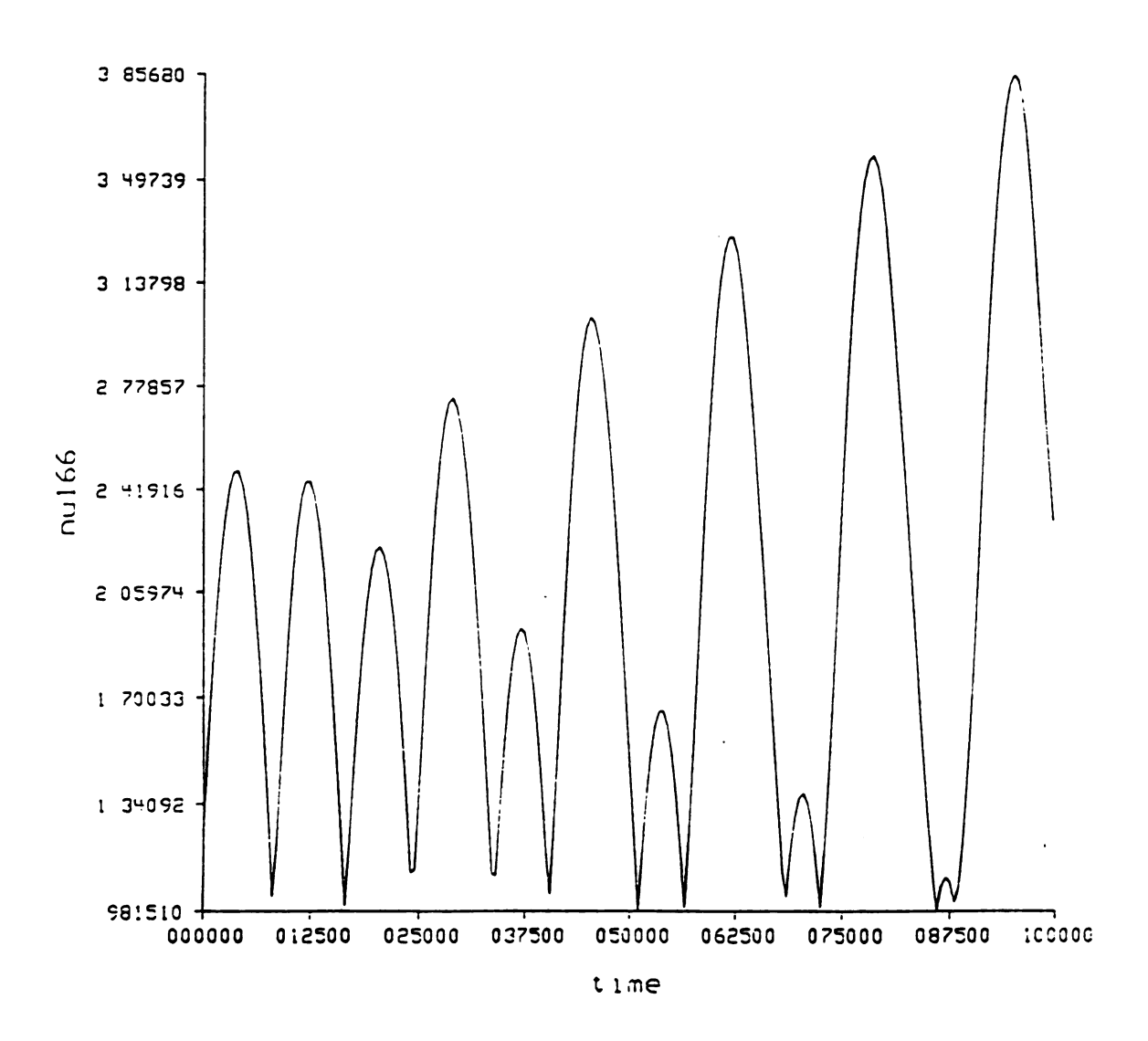


Figure 52. The reluctivity (inverse of the permeability) of the 166th element for case 4

## 5.4.4.2 THE RESULTS OF THE ACSL FOR CASE 4

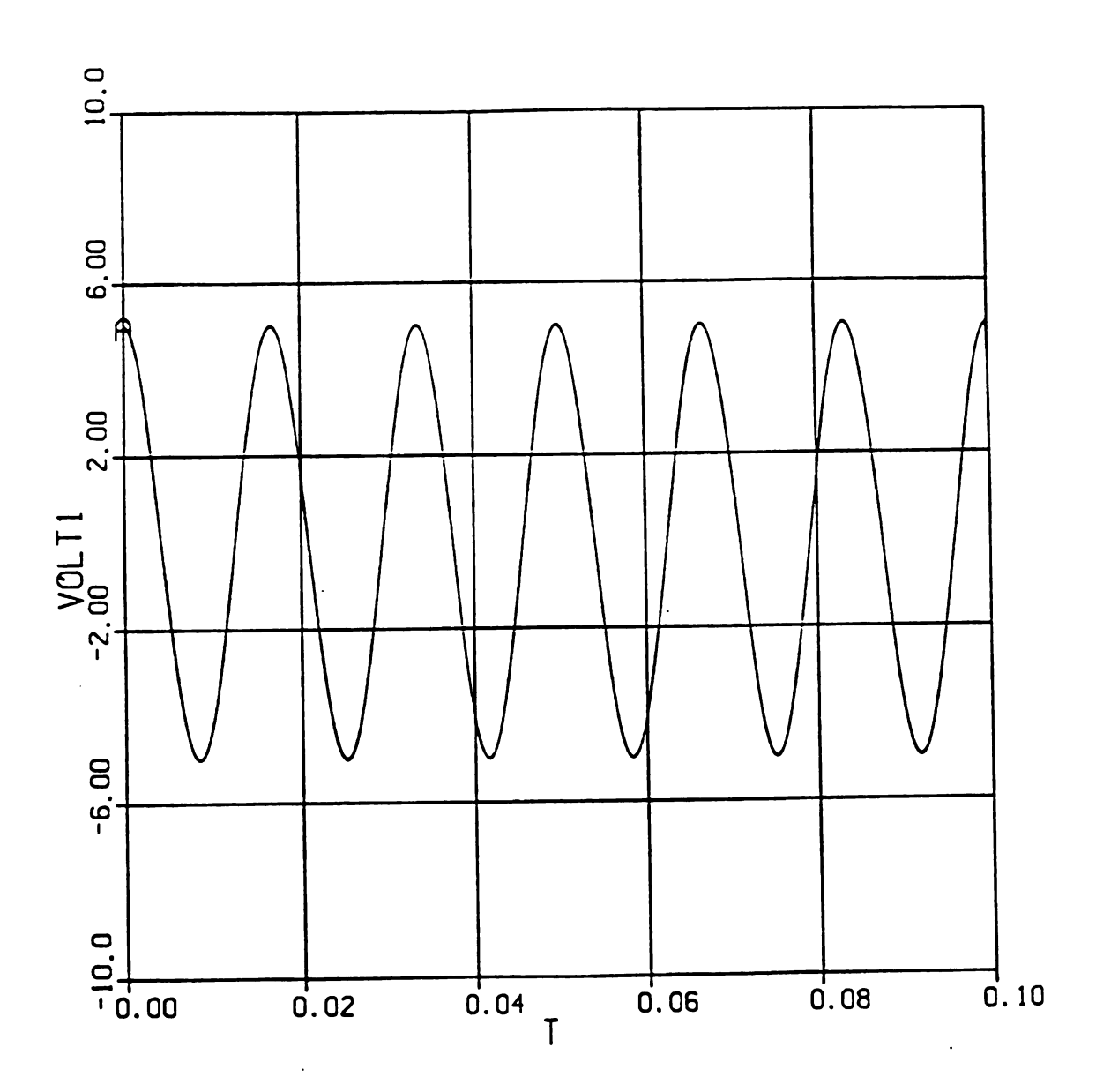


Figure 53. Applied Voltage for case 4.

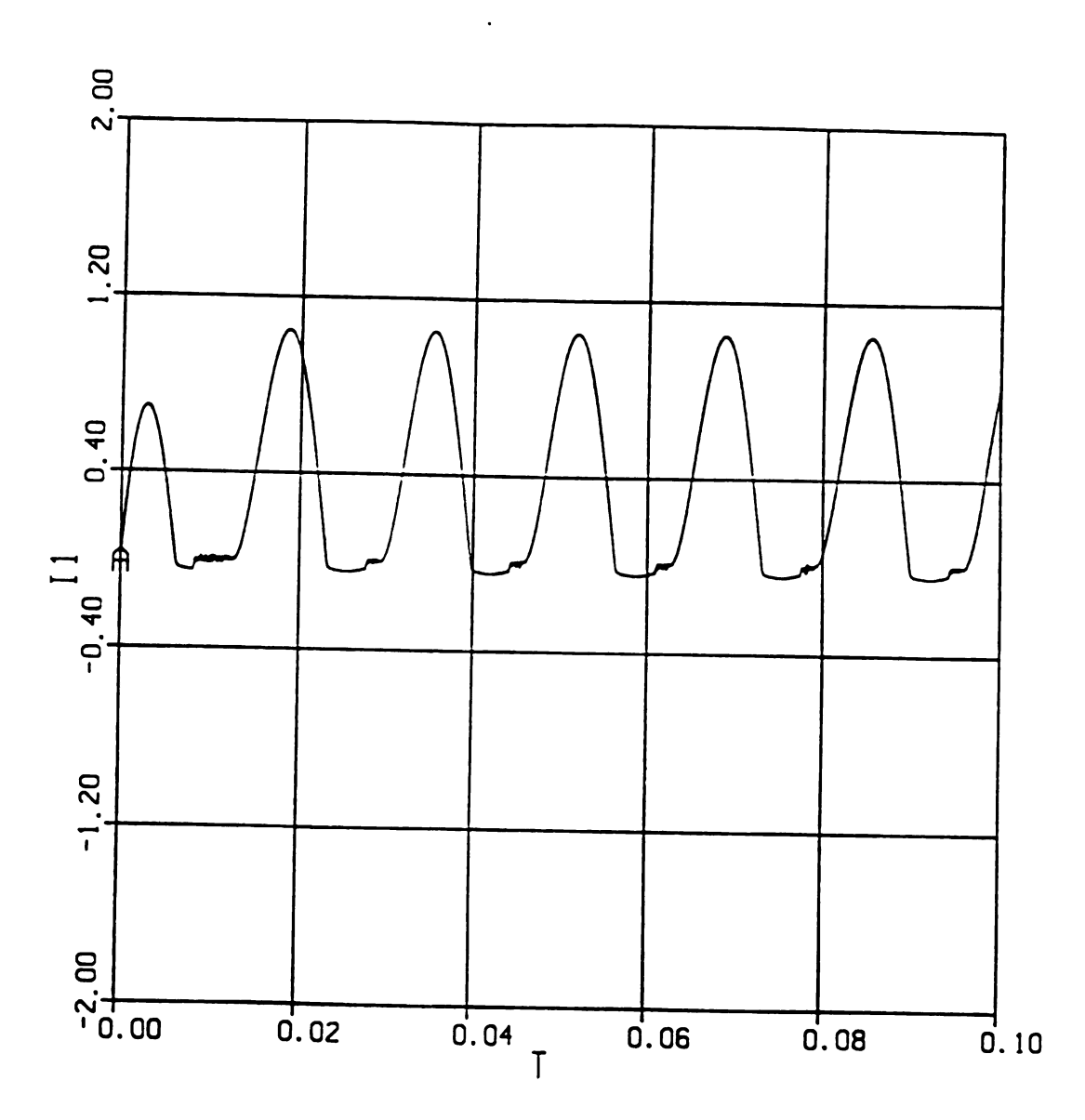


Figure 54. Primary current of the model connected to a one-way rectifier circuit together with a inductive load.

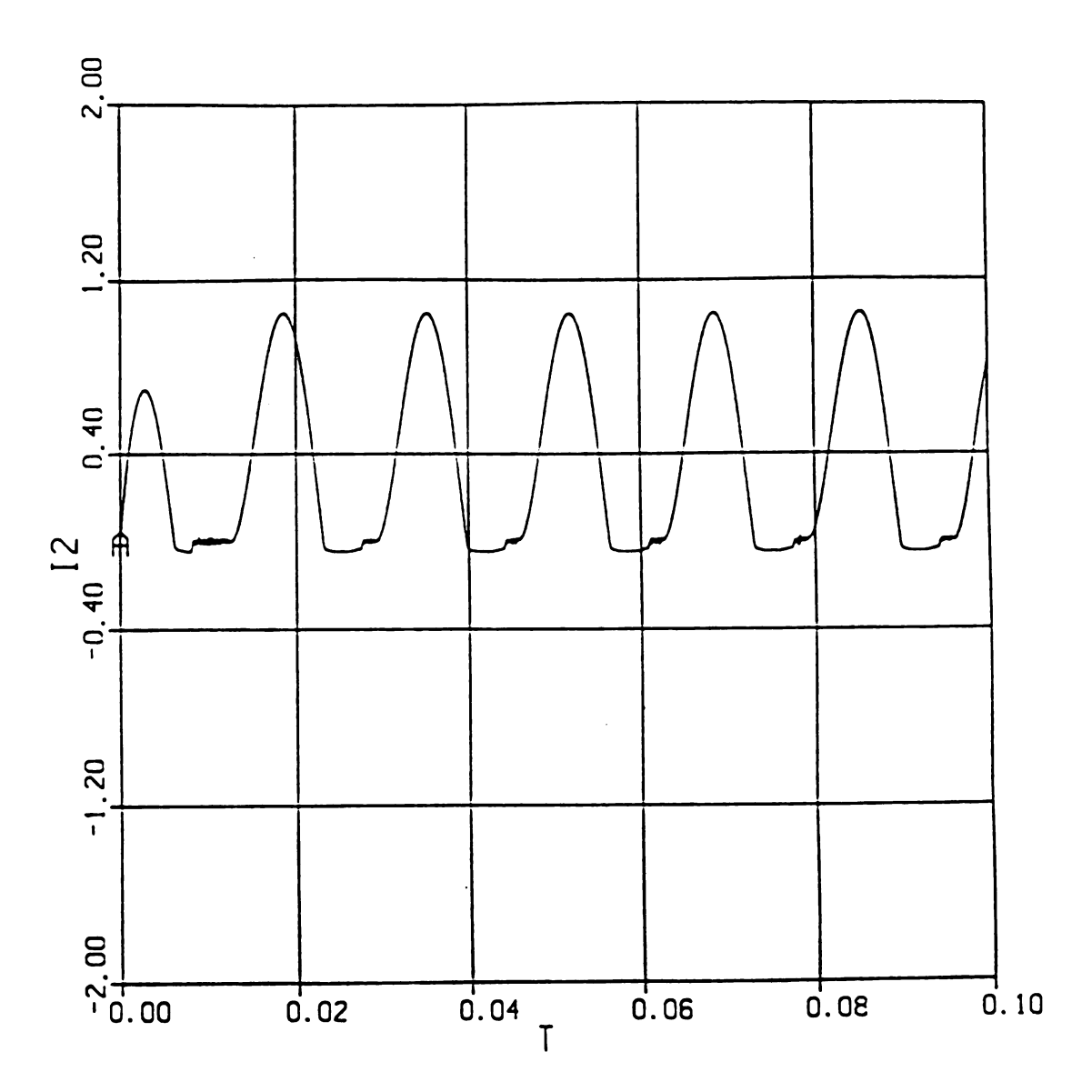


Figure 55. Secondary current of the model connected to a one-way rectifier circuit together with inductive load.

# 5.4.5 CASE 5: SIX-STEP VOLTAGE INPUT (INVERTER) AND AN INDUCTIVE LOAD

In this case, the model fed is by a six-step voltage source which could be an inverter, and is connected to an inductive load which has a inductance of 0.01 H. and a resistance of 3.0  $\Omega$ . At the same time, 0.3  $\Omega$  resistance is connected to to the primary winding resistance in series.

### 5.4.5.1 THE RESULTS OF THE FINITE ELEMENT METHOD FOR CASE 5.

In this subsection, the plots of the primary and secondary current of the model are given in figure 58 and 59 respectively in response of the applied voltage shown in figure 57 for the load conditions stated above. The notice should be taken in the current plots that the currents do not change at the step points as suddenly as voltage because of the inductance in the primary and secondary circuits. The absolute flux density the 166th element is given in figure 60. The plots of the induced voltages of the primary and secondary together with the reluctivity of the 166 th are given in figure 61, figure 62 and figure 63 respectively. The difference between these induced voltages is the voltage drop because of the leakage inductances and the resistance of the windings.

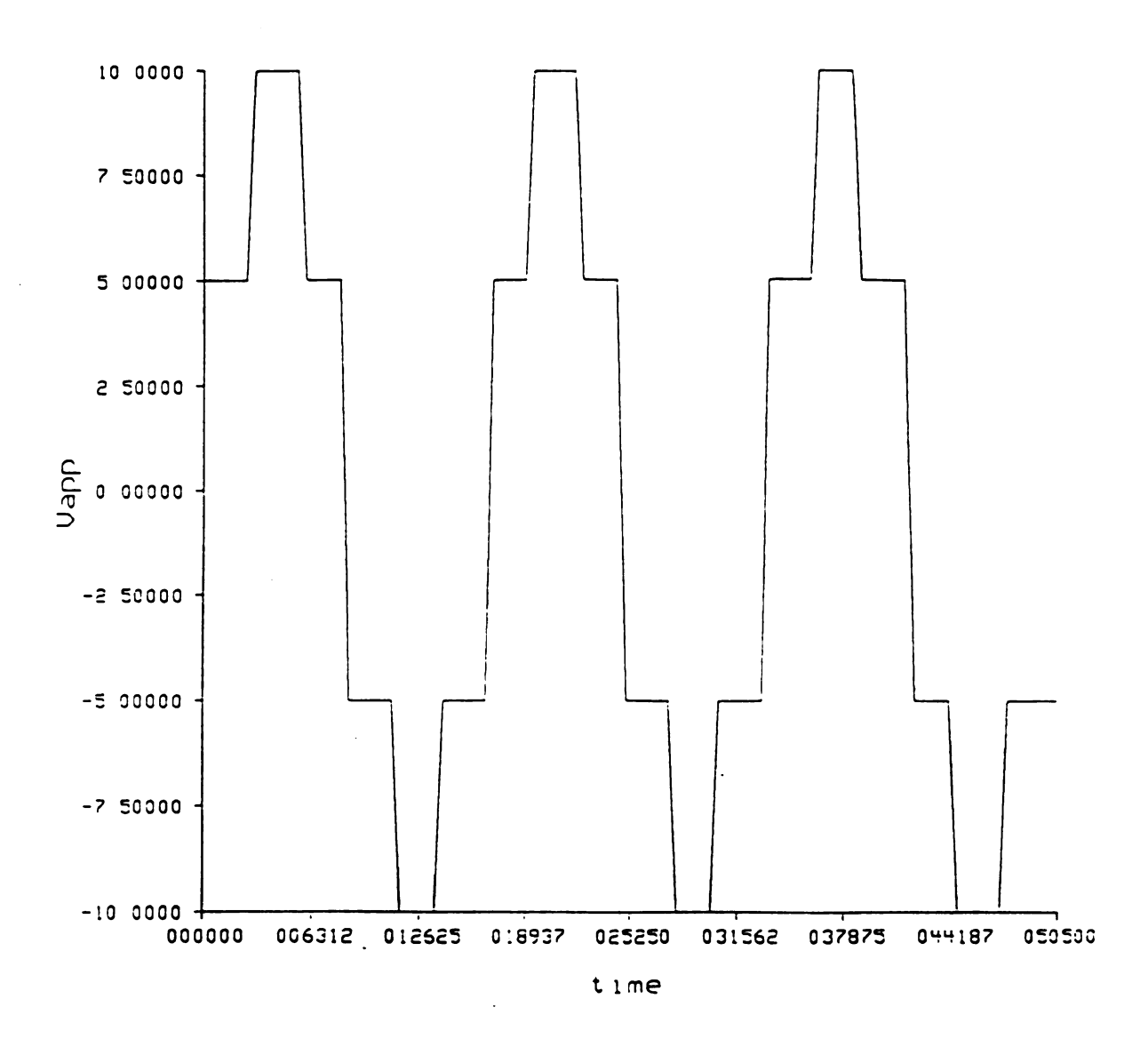


Figure 57. Applied voltage for the fifth case.

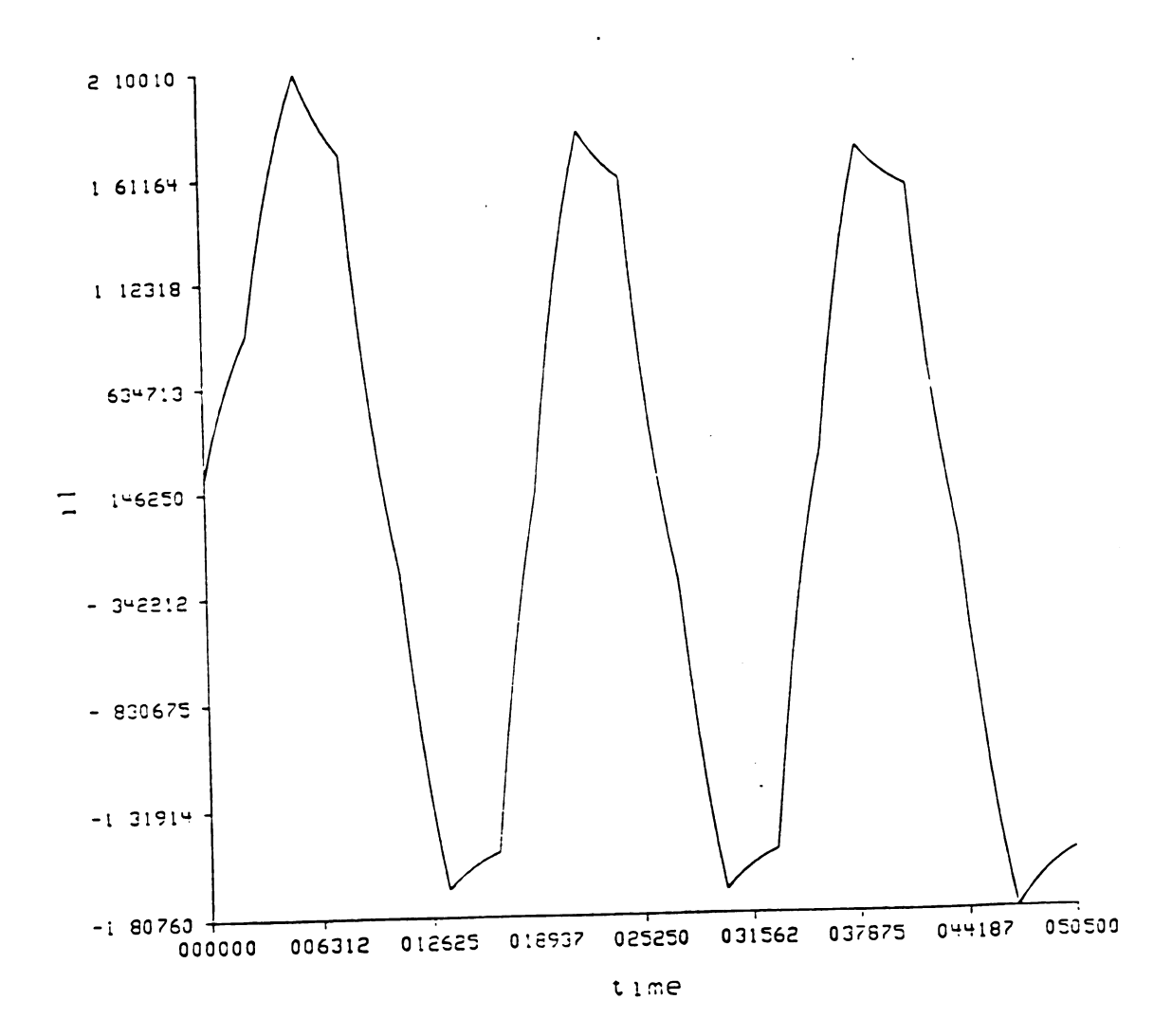


Figure 58. Primary current of the model connected to inductive load and fed by the six-step voltage.

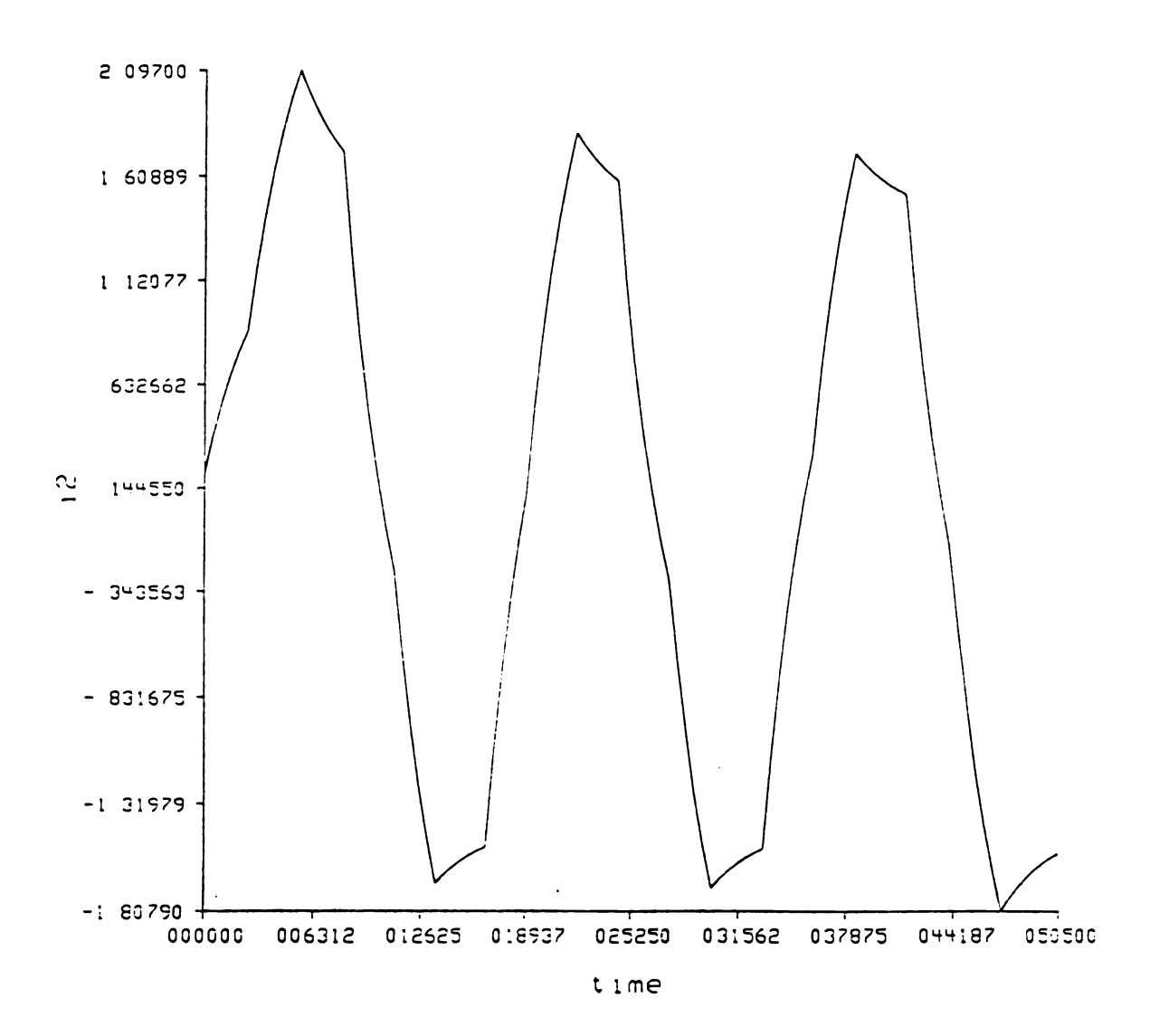


Figure 59. Secondary current of the model connected to inductive load and fed by six-step voltage.

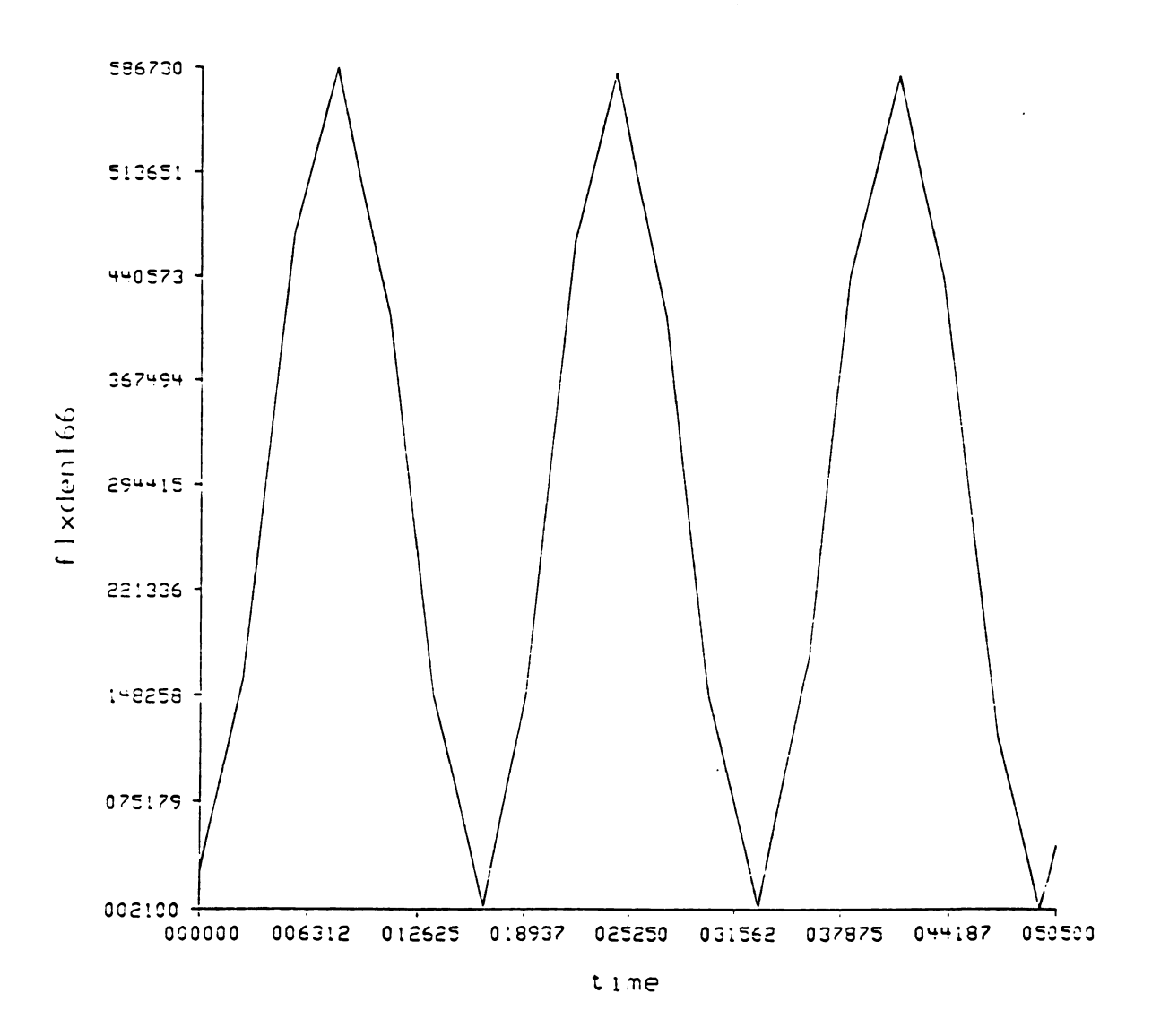


Figure 60. Flux density of the 166th element for case 5.

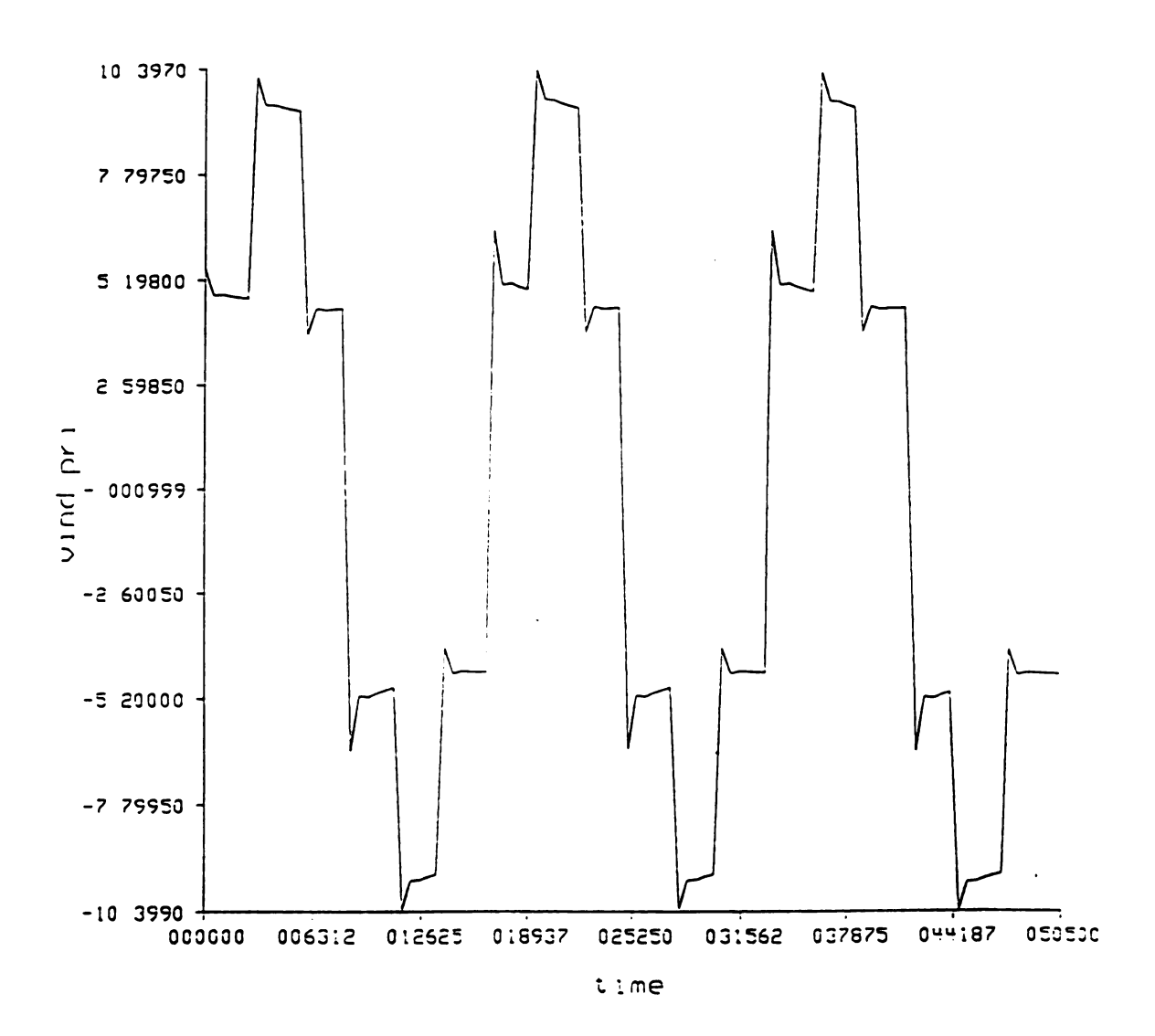


Figure 61. Induced voltage in the primary windings for case 5.

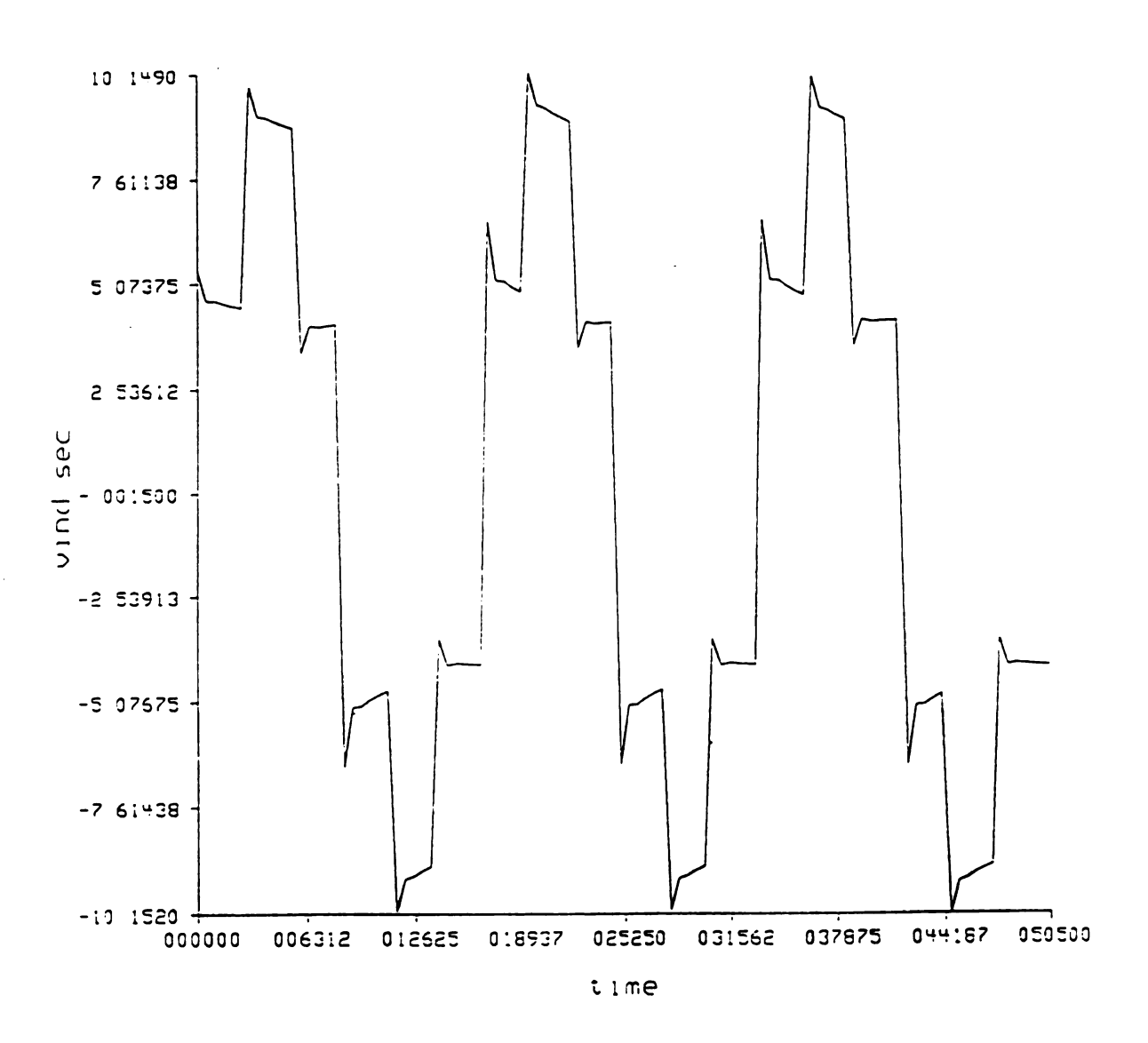


Figure 62. Induced voltage in the secondary windings for case 5.

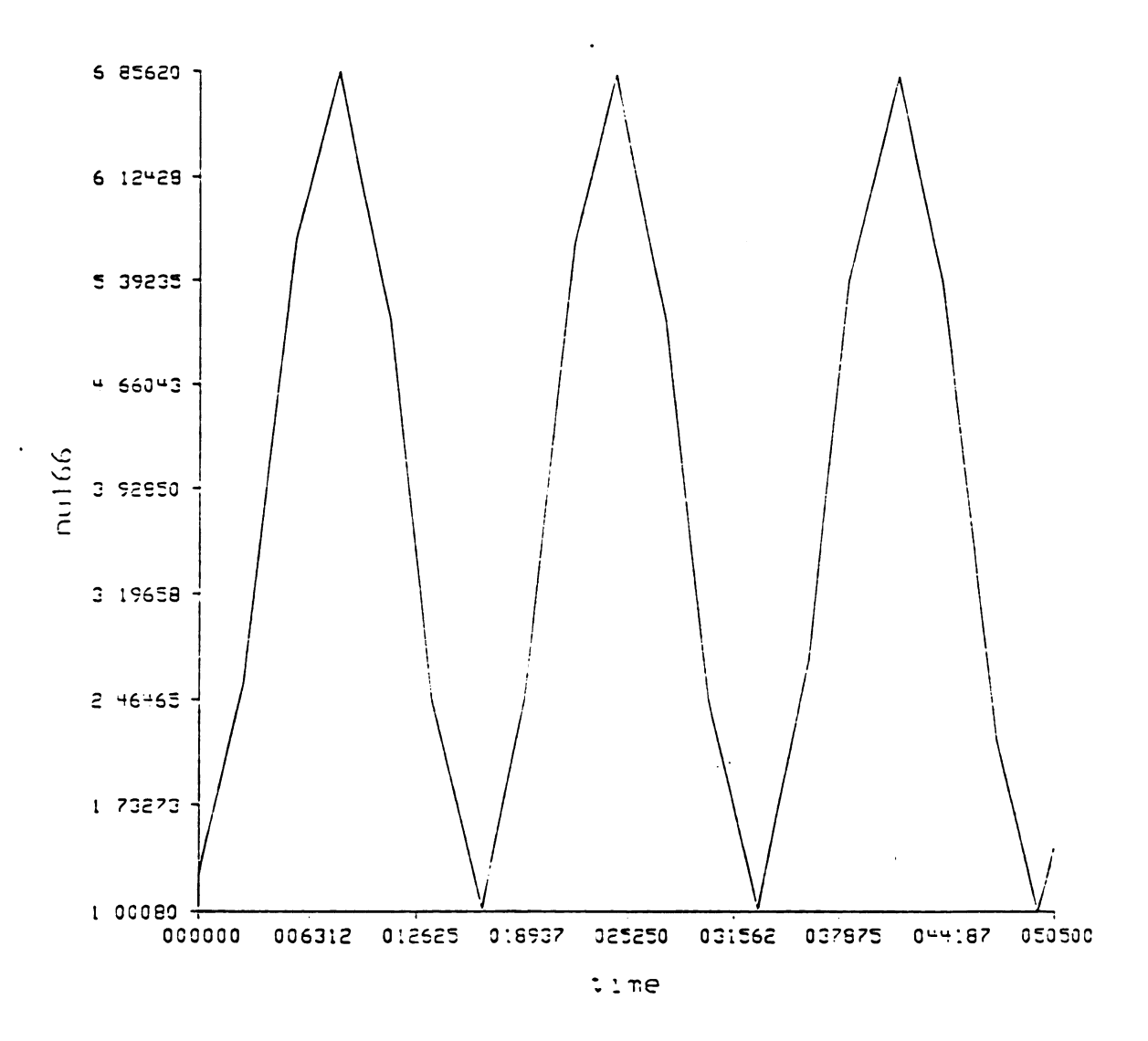


Figure 63. The reluctivity (inverse of the permeability) of the 166th element for case 5.

#### CHAPTER VI

#### CONCLUSIONS

In this thesis the copper and the iron losses in a transformer are analyzed considering all the harmonics of the currents in the conductors and the flux density in the iron core of a single-phase transformer.

In the analysis of the current and the flux density, two different methods are used. The first is coupling the non-linear time-dependent field and the circuit equations and solve them by the finite element method, and the second the solution of a system of differential equations derived from lumped parameter model of the transformer by ACSL, which is a language designed for modeling and evaluating the performance of continuous systems described by time dependent, non-linear differential equations.

In the analysis of the copper losses, a method to calculate the additional copper losses due to the harmonics in the current is presented and a sample calculation is given for a single-phase small size transformer fed by an inverter.

In the iron losses analysis, first the derivation of loss related iron parameters is introduced and then a simple method to separate the total iron losses into hysteresis and the eddy current losses from the experimental data is given. The experimental coefficients of the hysteresis and the eddy current loss parameters are obtained from the separation of the iron losses for the use of the iron loss calculations.

The eddy current losses are calculated by analyzing of the flux density in harmonics in the iron core, whereas the calculation of the hysteresis losses is performed using a simple, non-recursive algorithm.

The results of the primary and secondary current values, needed for the calculation of copper losses, using the finite element method and ACSL are closely matching both, for the linear and non-linear load conditions. Whereas, the results of the flux density values, used for the iron-loss calculation of the finite element method and the ACSL are differing from each other for the cases where the non-linear loads are connected to the secondary circuit. The explanation of this situation would be the finite element method does not allow easily for the saturation in the iron.

Relating these losses with the design parameters of a transformer has been left for future work.

### LIST OF REFERENCES

- [1] F. C. Connelly, Transformers: Their Principles and Design, Sir Isaac & Sons, First Ed., 1950.
- [2] C. P. Steinmetz, "On The Law of Hysteresis", A.I.E.E. Trans., Vol. 9, 1892, pp. 3-51.
- [3] P. G. Agnew, "A Study of The Current Transformer With Particular Reference to Iron Loss", A.I.E.E. Trans., 1911, pp. 423-433.
- [4] F. Brailsford, "Hysteresis Loss in Electrical Sheet Steel", I.E.E.J., Vol 83, 1938, pp. 566-575.
- [5] E. F. Fuchs, D. J. Roesler, F. S. Alashhab, "Sensitivity of Electrical Appliances to Harmonics and Fractional Harmonics of The Power System's voltage. Part1: Transformers and Induction Machines", IEEE Trans. on Power Delivery, Vol. PWRD-2, No. 2, April 1987, p. 437.
- [6] E. F. Fuchs, D. J. Roesler, K. P. Kovacs, "Aging of Electrical Appliances Due to Harmonics of The Power System's Voltage", IEEE Trans. on Power Delivery, Vol. PWRD-1, No. 3, July 1986.

- [7] R. Richter, Elektrische Maschinen, Vol. 1, Julius Spinger Verlag, Berlin, 1924.
- [8] Sensitivity of Transformer and Induction Motor Operation to Power System's Harmonics, Topical Report, April 1983.
- [9] D. E. Fink, H. W. Beaty, Standard Handbook For Electrical Engineers, Beaty, 12th Edition.
- [10] E. G. Strangas, K. R. Theis, "Shaded Pole Motor Design And Evaluation Using Coupled Field on Circuit Equations", IEEE Trans. on Magnetics, Vol. Mag21, No. 5, Sep. 1985.
- [11] E. G. Strangas, "Coupling The Circuit Equations to The Non-Linear Time Dependent Field Solution in Inverter Drives Induction Motors.", IEEE Trans. on Magnetics Vol. MAG-21, No. 6, November 1985. pp
- [12] P. P. Silvester, P. L. Ferrari, "Finite Elements For Electrical Engineers", Cambridge Univ. Press, 1983.
- [13] E. G. Strangas, T. Ray, "Combining Field And Circuit Equations For Analysis of Permanent Magnet AC Motor Drives". IEEE, IAS-88.

MICHIGAN STATE UNIV. LIBRARIES
31293007841285